

May 2022

Advanced UK Instrumentation Training 2022

Diamond Detectors

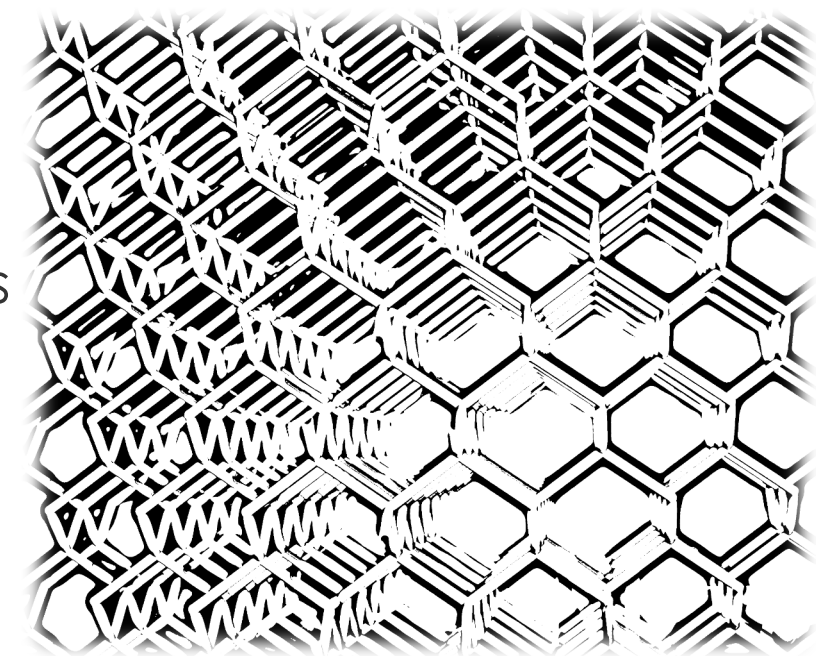
Alexander Oh
University of Manchester

Outline

Part 1

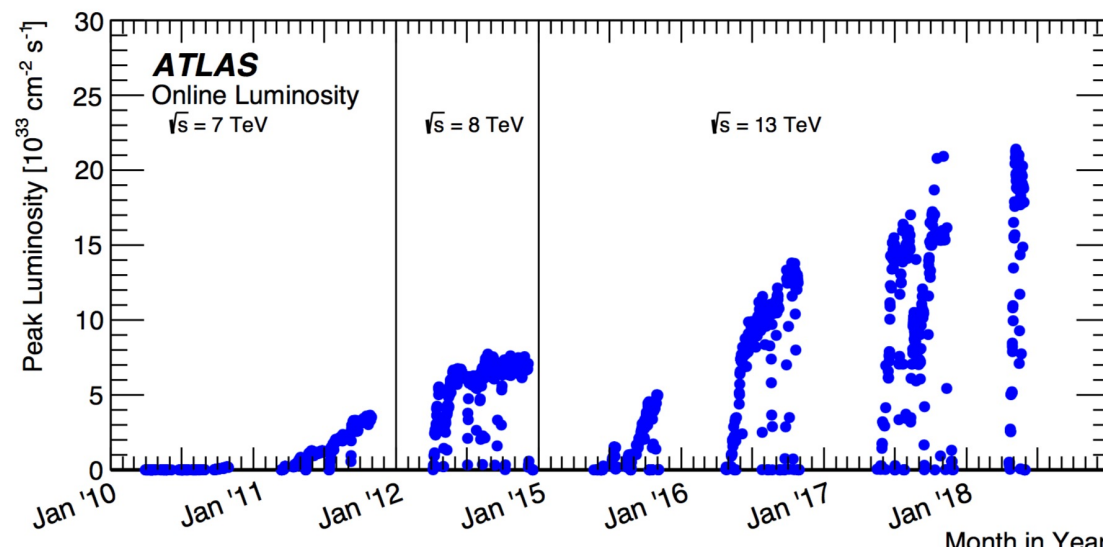
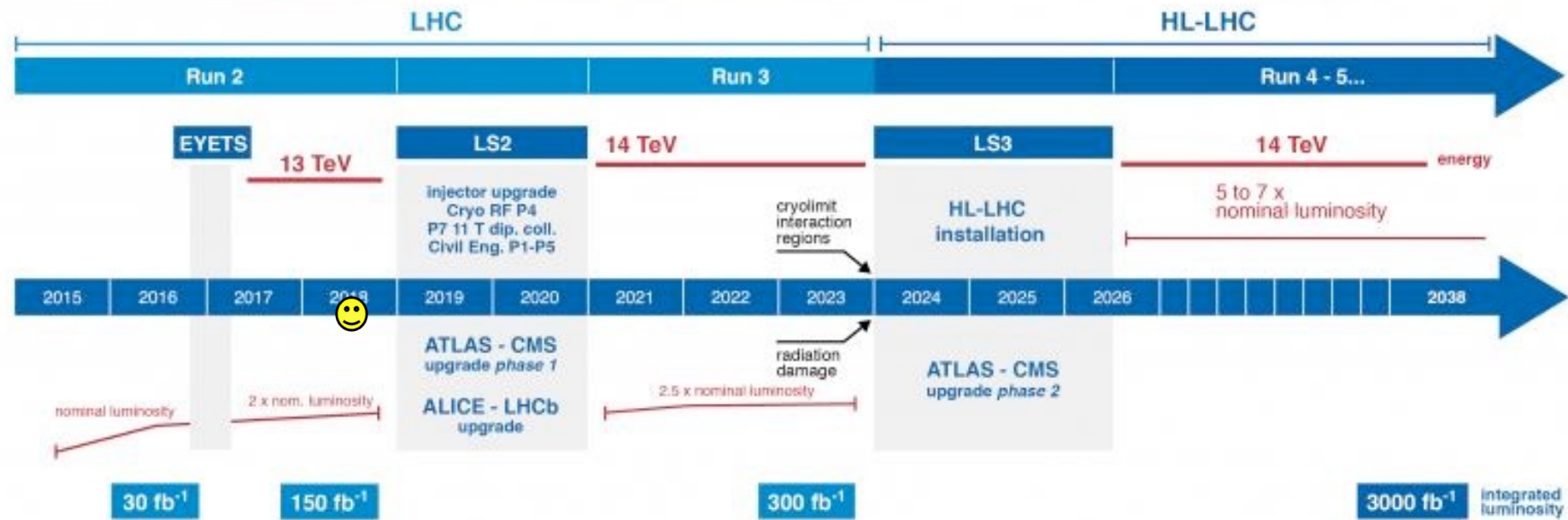
Part 2

- Diamond basics and detector principle
- Diamond strip and pixel detectors
- Radiation Hardness
- 3D Diamond detectors
- Current and future diamond detector installations



Thanks for the material from the RD42 and ADAMAS collaborations!

Challenges Ahead

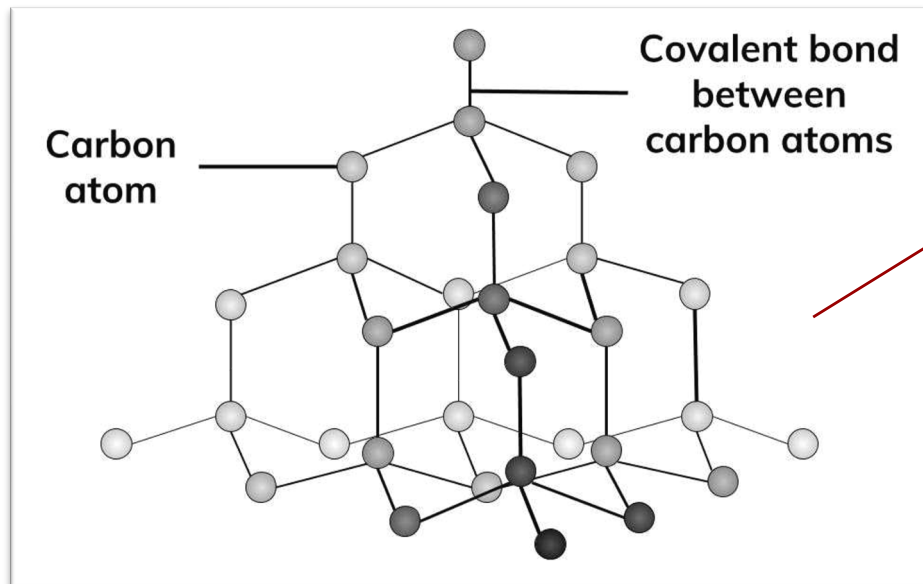
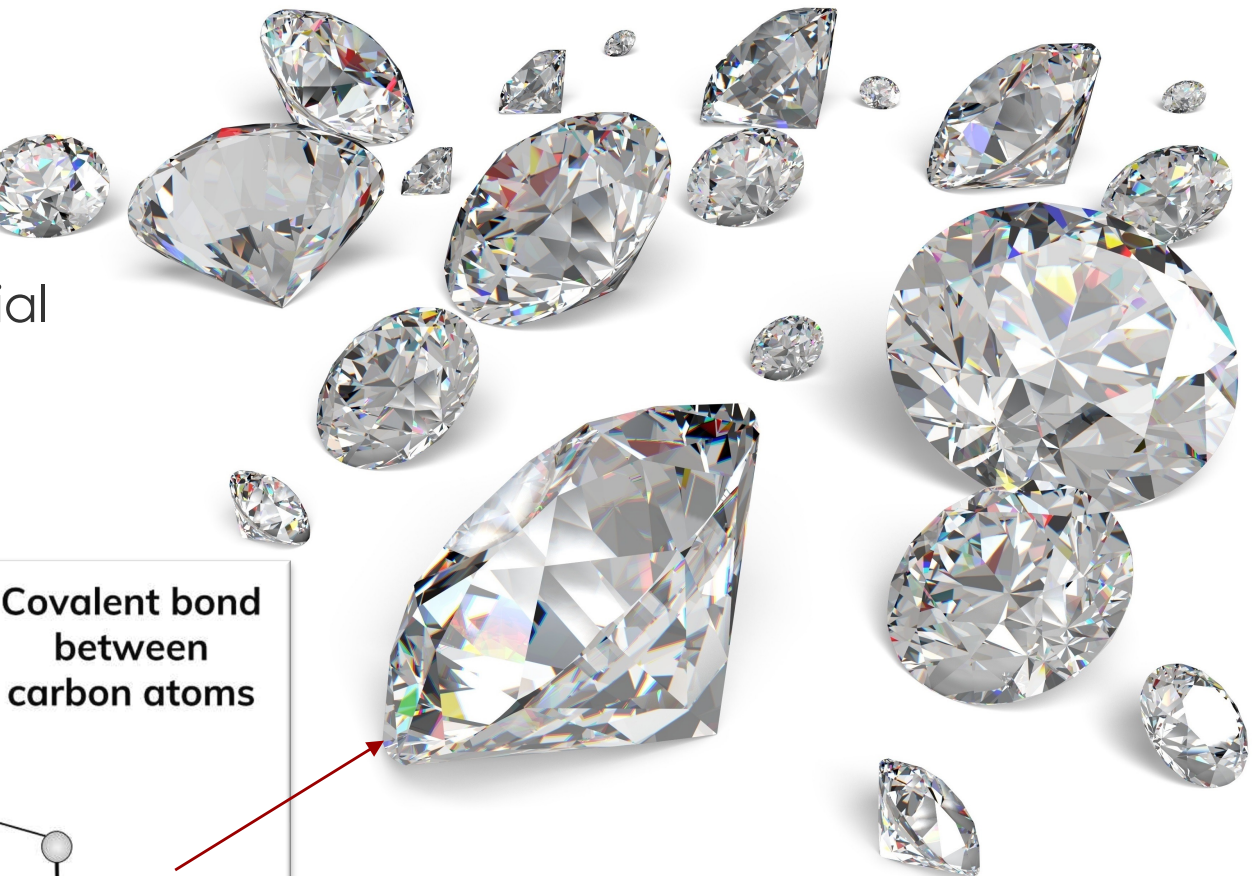


- Luminosity upgrades of the LHC will increase the luminosity by factor ~ 3 .
- Luminosity \sim Radiation damage.
- Need new technologies in the innermost layers to survive the radiation levels.

May 2022

diamond

- Allotrope of Carbon
- Hardest natural material
- Tetrahedral structure
 - Sp₃ bonds





	Diamond	Silicon	
Band Gap [eV]	5.5	1.1	→ Lower leakage current
Average Ionisation Density for MIP [eh/ μ m]	36	81	→ Lower signal

	Diamond	Silicon	
Band Gap [eV]	5.5	1.1	→ Lower leakage current
Average Ionisation Density for MIP [eh/ μ m]	36	81	→ Lower signal
Displacement Energy [eV]	43	25	→ Radiation Hardness

	Diamond	Silicon	
Band Gap [eV]	5.5	1.1	→ Lower leakage current
Average Ionisation Density for MIP [eh/ μ m]	36	81	→ Lower signal
Displacement Energy [eV]	43	25	→ Radiation Hardness
Thermal Conductivity [W/cm.K]	10-20	1.5	→ Room temperature operation

	Diamond	Silicon	
Band Gap [eV]	5.5	1.1	→ Lower leakage current
Average Ionisation Density for MIP [eh/ μ m]	36	81	→ Lower signal
Displacement Energy [eV]	43	25	→ Radiation Hardness
Thermal Conductivity [W/cm.K]	10-20	1.5	→ Room temperature operation
Atomic Number	6	14	→ Tissue equivalence

	Diamond	Silicon	
Band Gap [eV]	5.5	1.1	→ Lower leakage current
Average Ionisation Density for MIP [eh/ μ m]	36	81	→ Lower signal
Displacement Energy [eV]	43	25	→ Radiation Hardness
Thermal Conductivity [W/cm.K]	10-20	1.5	→ Room temperature operation
Atomic Number	6	14	→ Tissue equivalence
Electron Mobility [cm ² /V.s]	1900-3800	1350	→ Fast signal
Hole Mobility [cm ² /V.s]	2300-4500	480	

Natural and synthetic diamond

- Natural diamonds have a **high defect concentration**
 - Grow in different structure to synthetic diamonds
 - Compete with jewellery market
 - There are radiation sensors using natural diamond

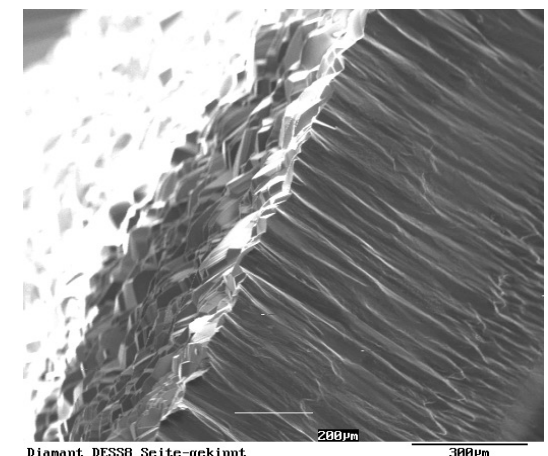
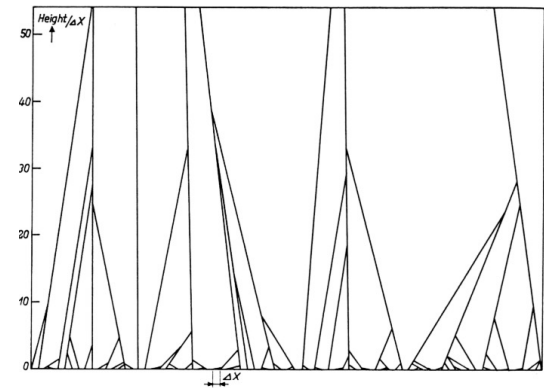


GIA.edu



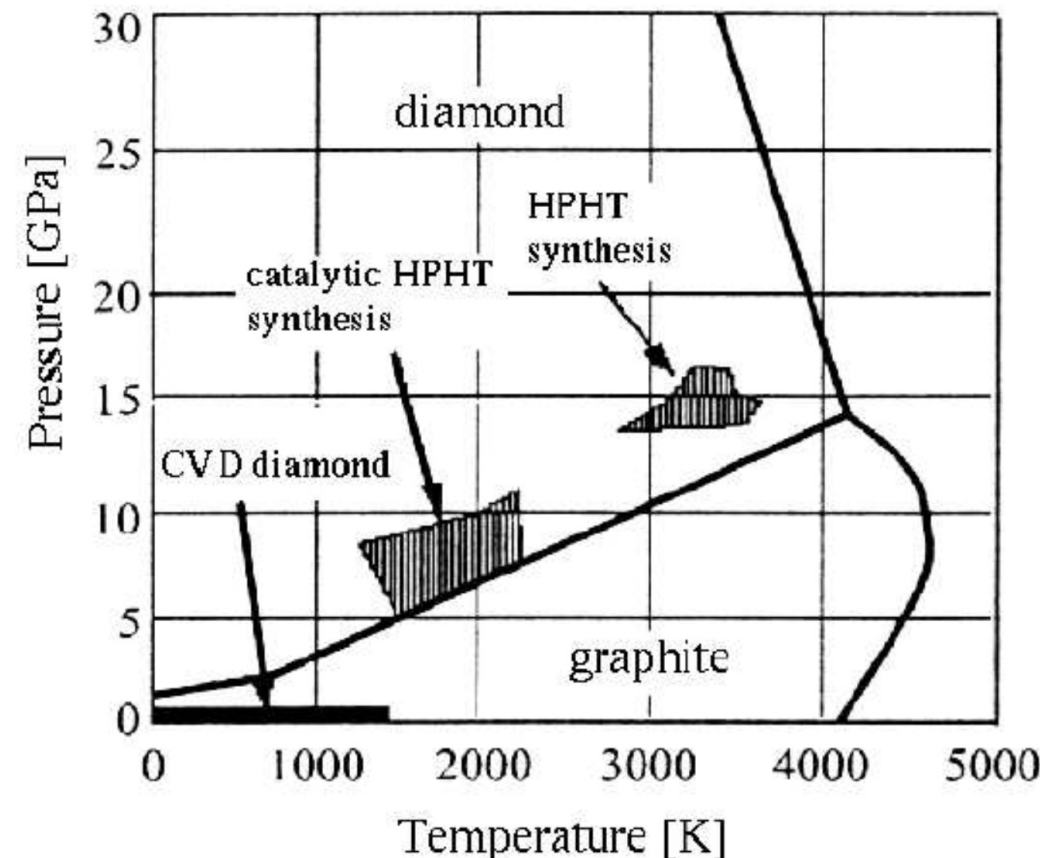
Diamond

- 1941 – Diamond as particle detector (Stetter)
- 1953- CVD process, synthesis of diamond (Eversole)
- ~1980 – polycrystalline CVD diamond.
- 1994 – first diamond strip detector
- 1996 – first diamond pixel detector
- 2011 – first 3D diamond detector



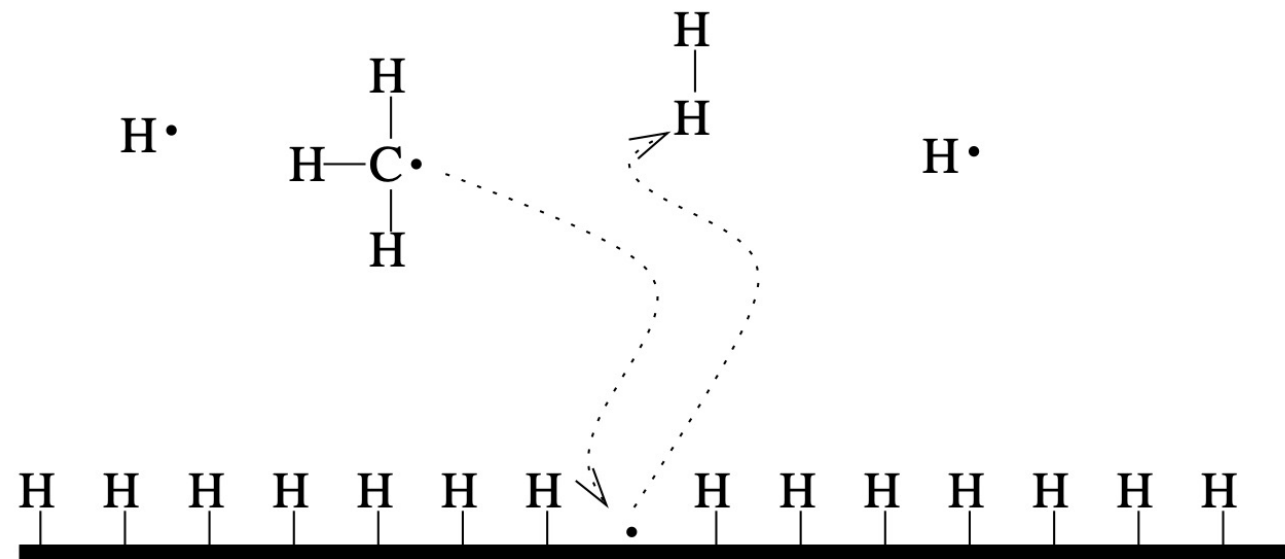
Synthesis of Diamond

- Chemical Vapour Deposition (CVD) of diamond in the graphit phase space.



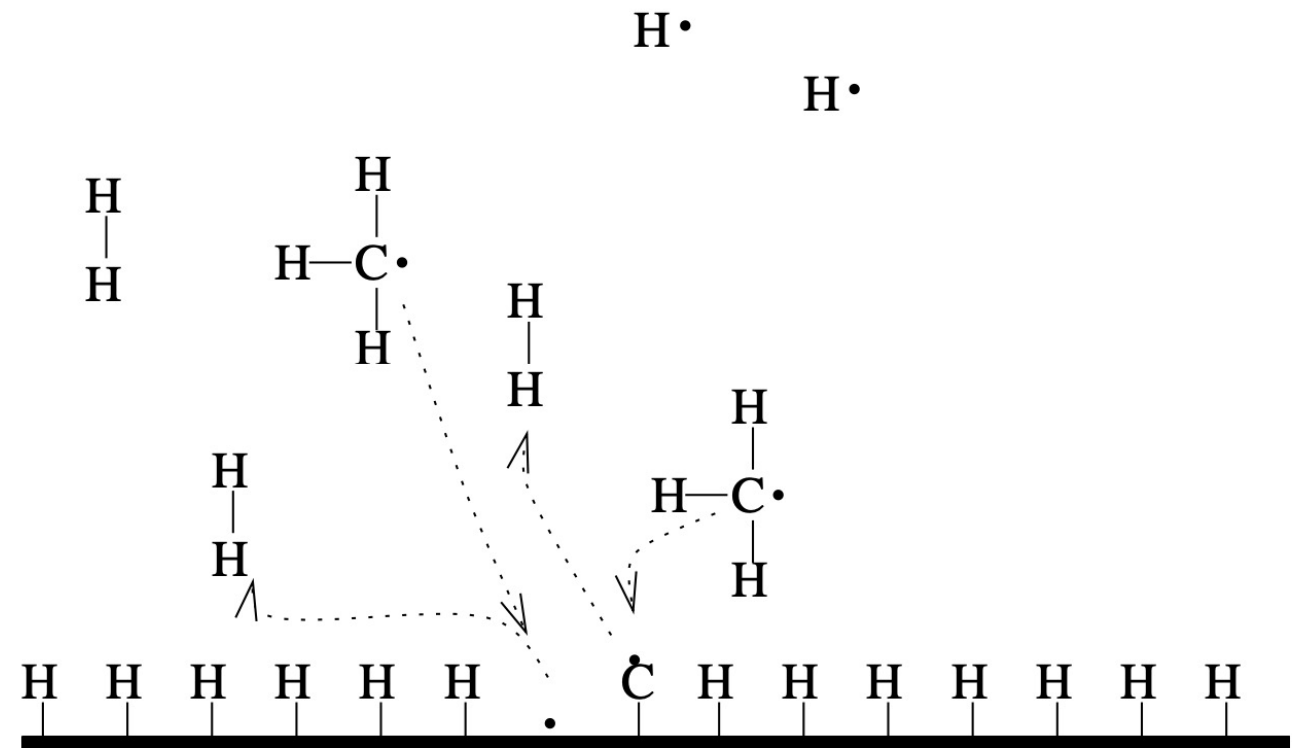
Synthesis of Diamond

- Hydrogen terminated substrate surface
- Methan and Hydrogen gas are heated with microwaves to form a plasma
- Radicals form



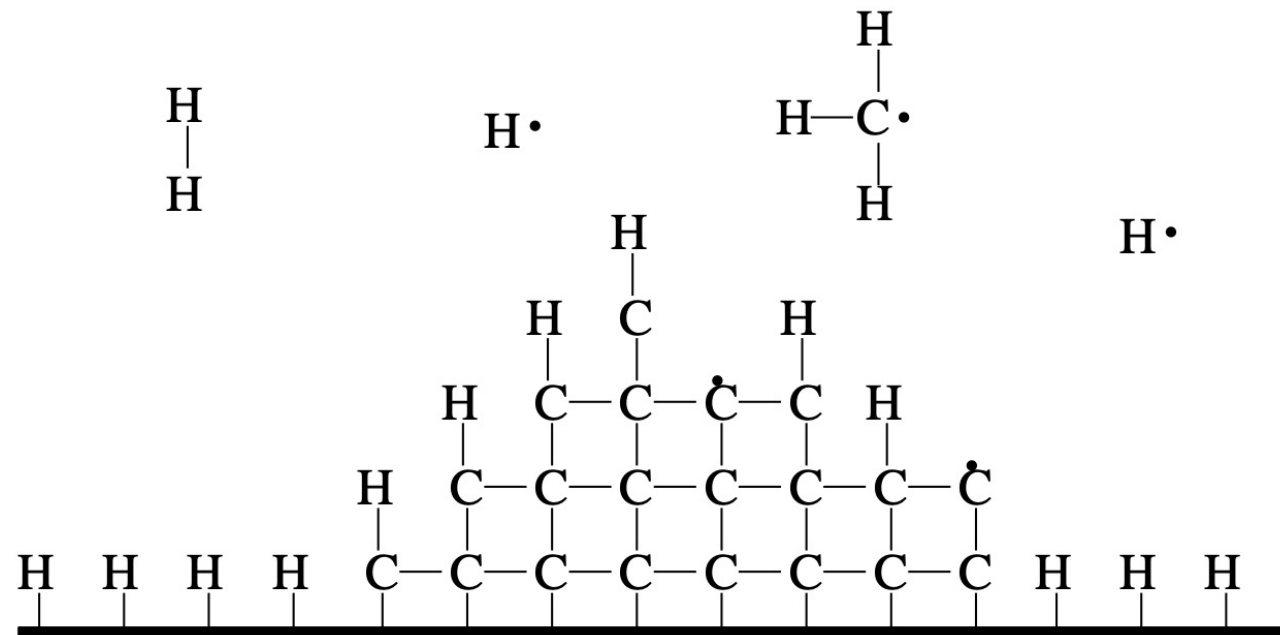
Synthesis of Diamond

- Hydrogen atoms are replaced with Carbon



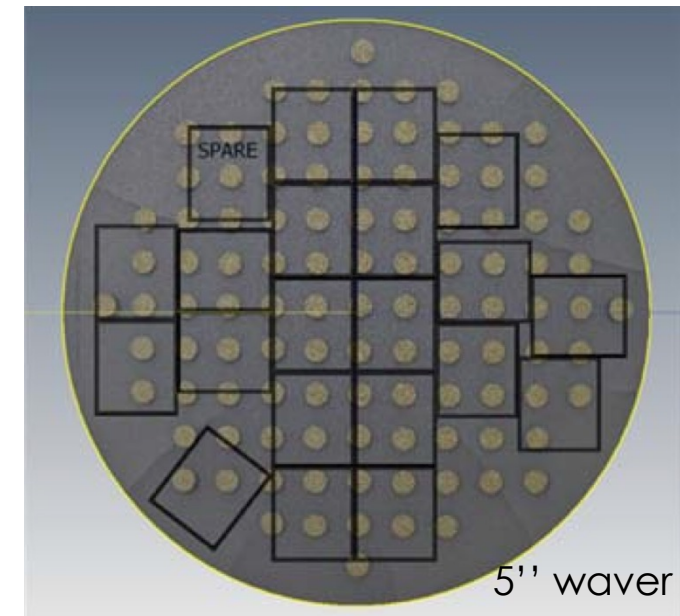
Synthesis of Diamond

- SP₂ bonds (graphite) are weaker than SP₃ bonds (diamond)
- Hydrogen radicals will etch away graphite, but leave diamond
- A diamond film is grown



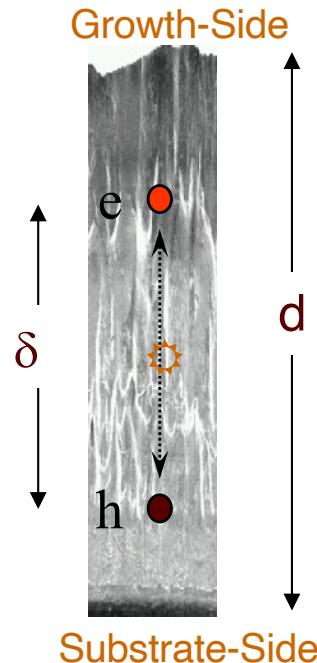
Development of CVD Diamond for detector applications

- Today two main manufacturers of detector grade diamond
 - **ElementSix Ltd**
 - large **polycrystalline** wafers
 - **single crystal** diamonds
 - **II-VI Semiconductors**
 - large **polycrystalline** wafers
 - relatively recent entry
- Alternative sources
 - Diamond on Iridium (Dol) (Audiatec, Germany)
 - Hetero-epitaxially grown -> **large area**
 - **Highly oriented crystallites.**



May 2022

■ Principle of detector operation



$$Q = \frac{d}{t} Q_0$$

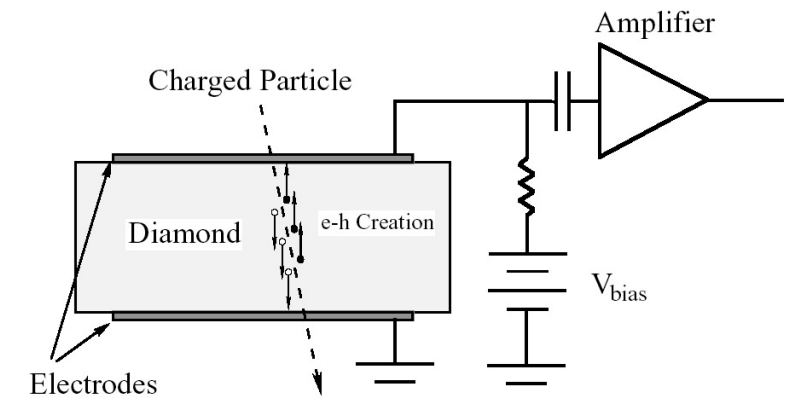
$$\delta = \mu E \tau$$

$$\varepsilon = Q / Q_0$$

collected charge

"collection distance"

collection efficiency



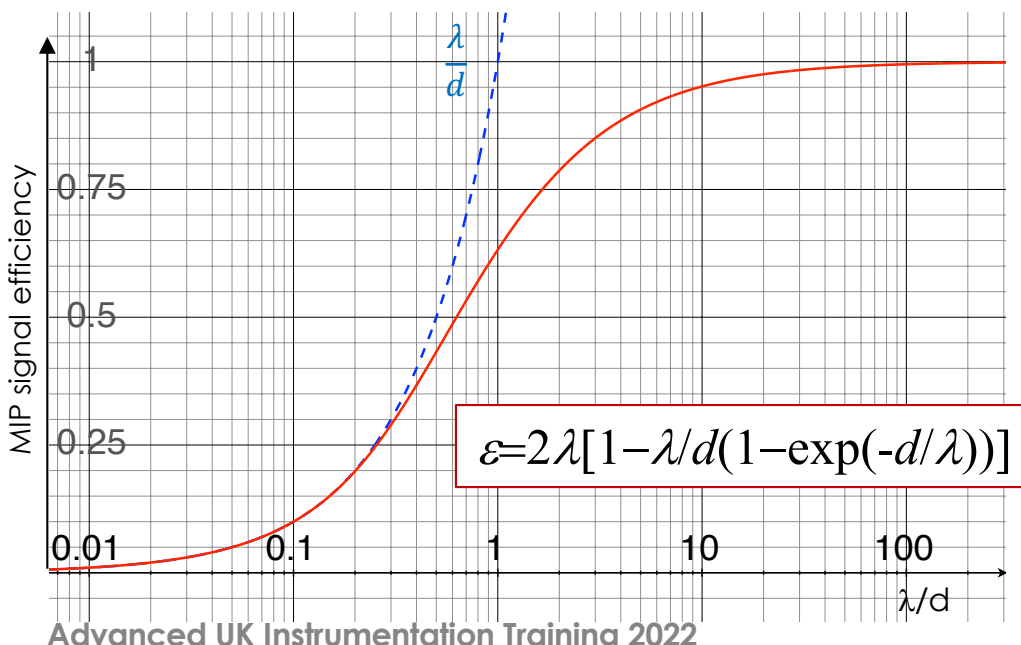
$$\mu = \mu_e + \mu_h$$
$$\tau = \frac{\mu_e \tau_e + \mu_h \tau_h}{\mu_e + \mu_h}$$

- MIP signal is measured, expressed in charge collection distance defined as $\delta [\mu\text{m}] = Q_m [\text{e}] / 36 [\text{e}/\mu\text{m}]$
- More accurately the “Schubweg” (λ).
 - Relation between MIP signal efficiency ϵ , “collection distance” δ , and “Schubweg” λ :

$$\epsilon = \frac{Q_m}{Q_0}$$

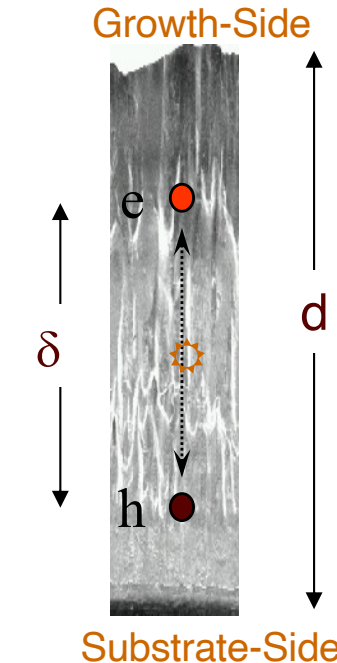
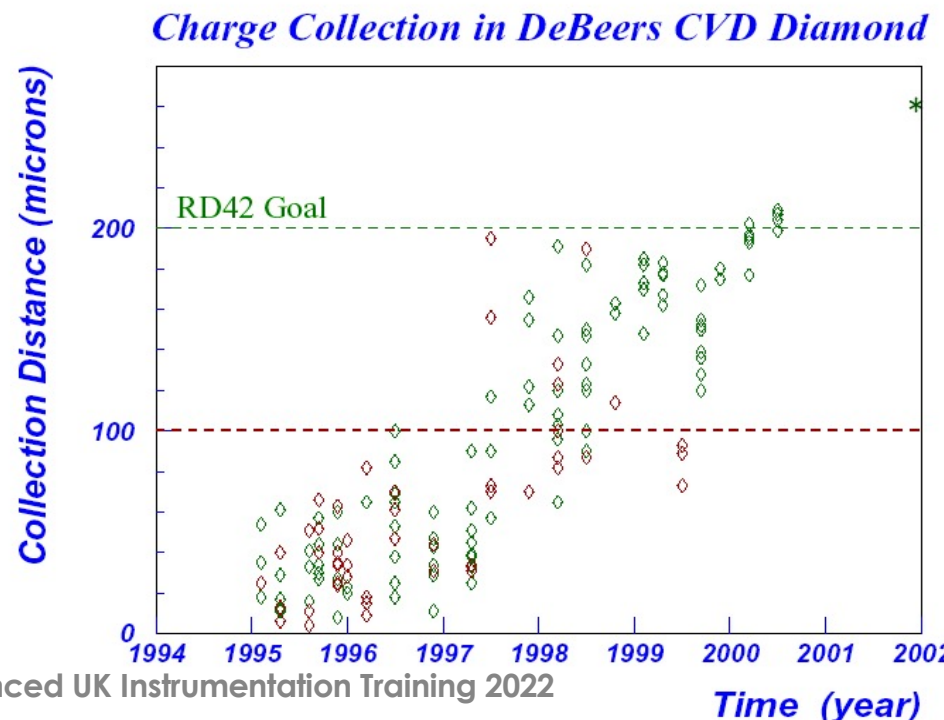
$$\delta = Q_m / 36 [\text{e}\mu\text{m}^{-1}]$$

$$\epsilon = 2\lambda[1 - \lambda/d \cdot (1 - \exp(-d/\lambda))]$$



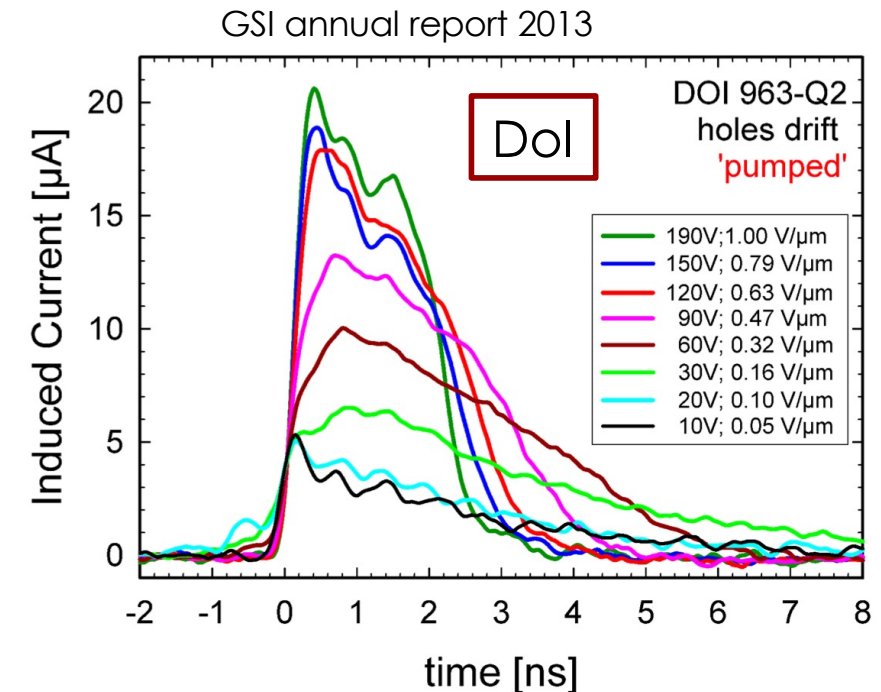
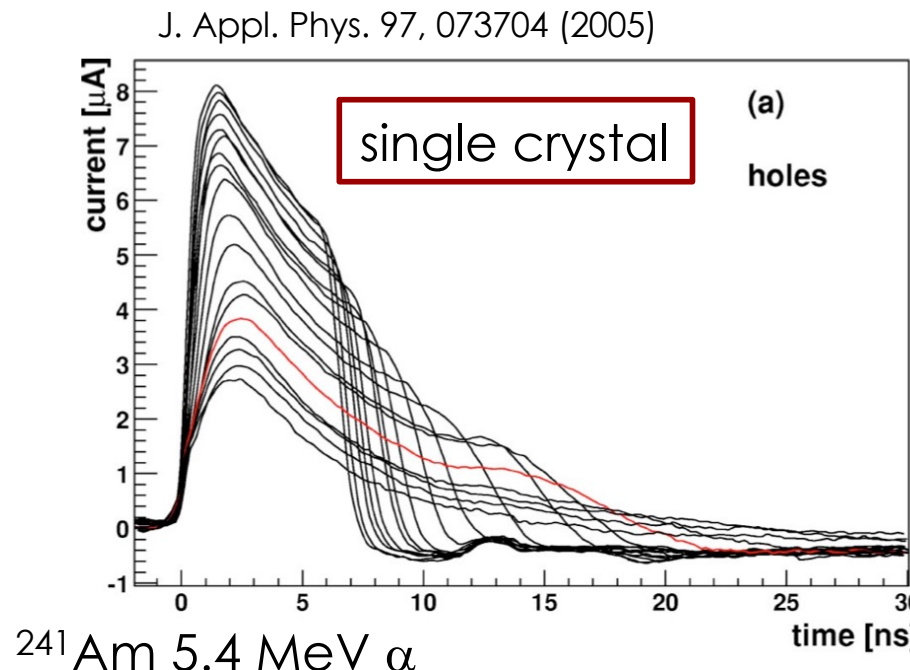
Development of CVD Diamond for detector applications

- Impressive progress over the last 20 years.
- Current state of the art for **polycrystalline** CVD diamond
 $\delta \sim 250 \mu\text{m}$ ($\sim 9000 \text{ e/MIP}$) **commercially available**.



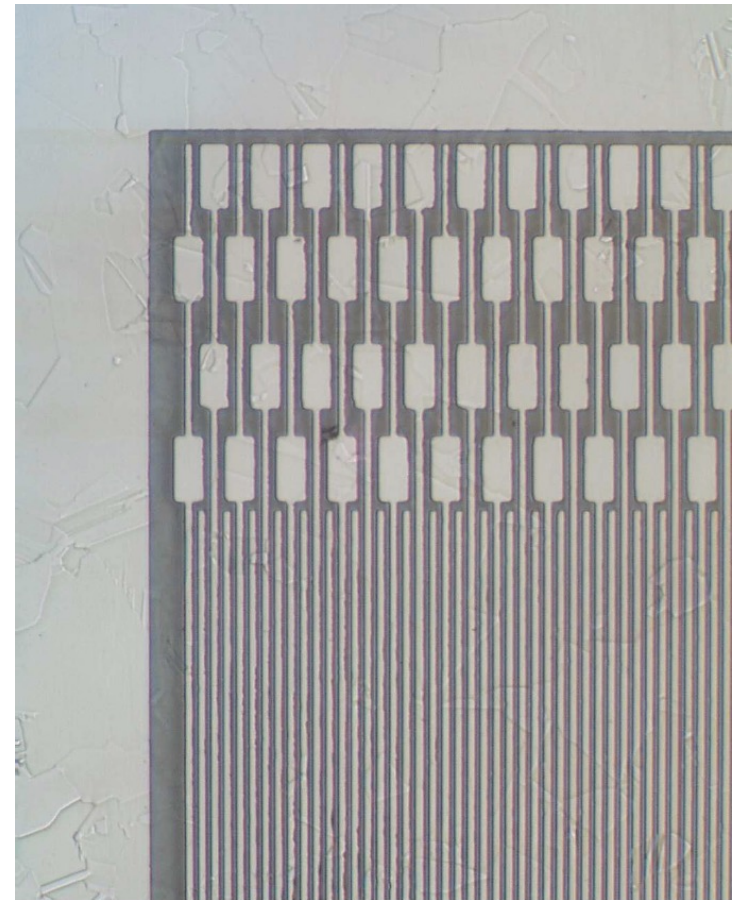
Development of CVD Diamond for detector applications

- Impressive progress over the last 20 years.
- **Single crystal diamond ~ 100% efficient**
- **Diamond on iridium ~ 97% efficient**

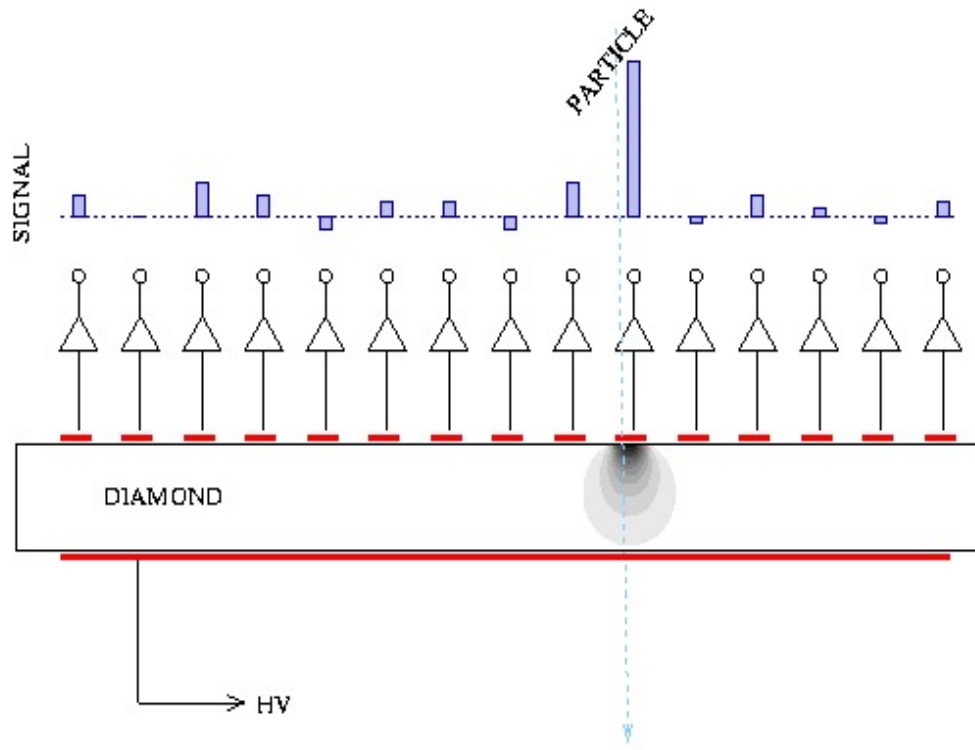


Strip Detectors

- First position sensitive diamond detectors where strip detectors.
- Many prototypes tested starting around 1994

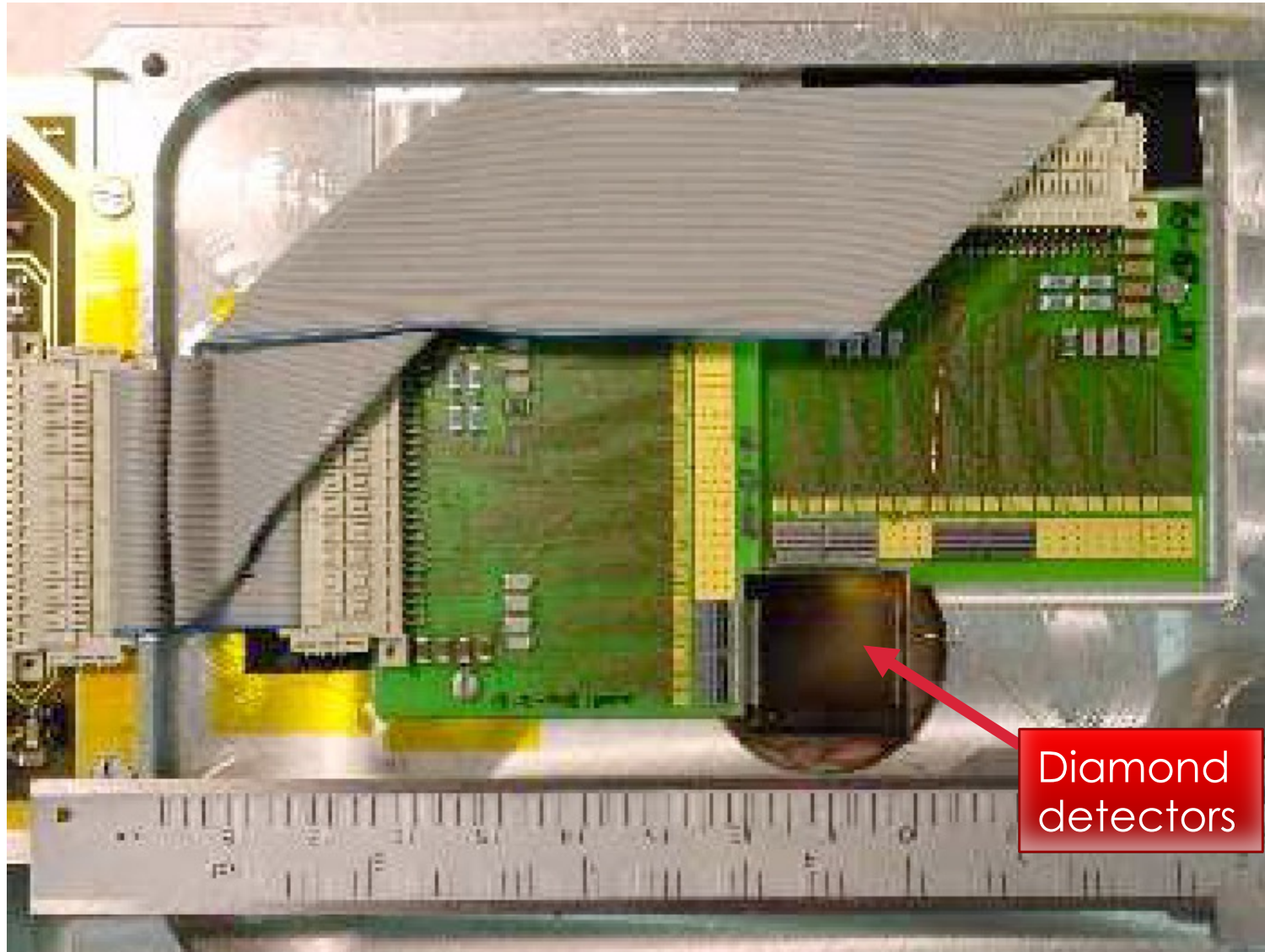


Principle

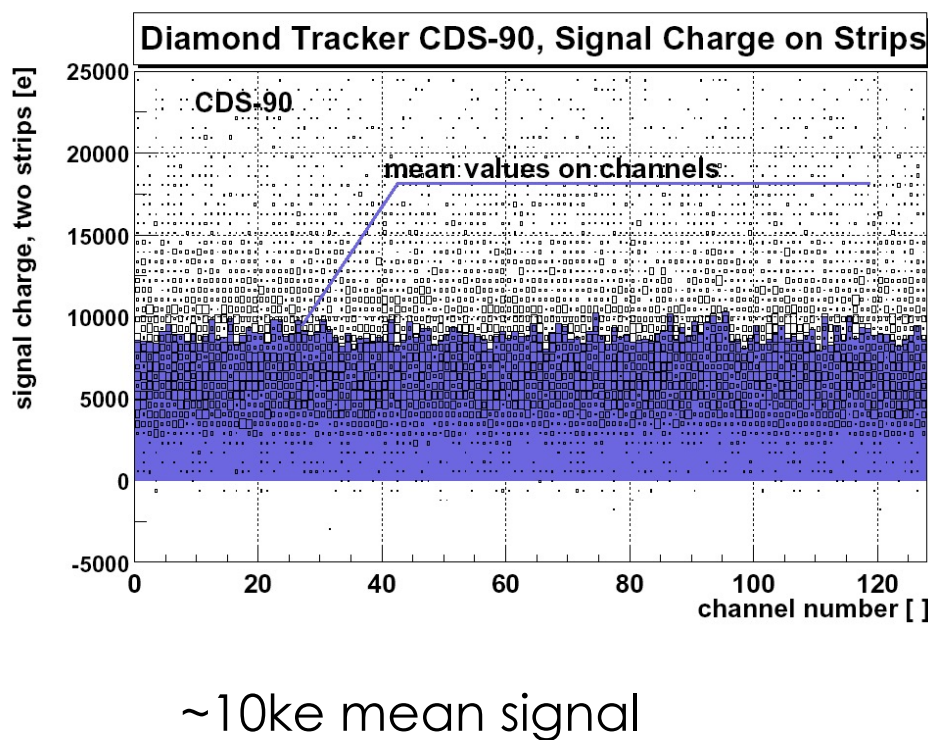


- The charge signal is picked up by the strip(s) next to the particle track.
- The charge is shared by multiple strips if the charge collection is incomplete.
- The position of the particle track can be reconstructed by calculating the charge weighted impact point
(Center of Gravity)

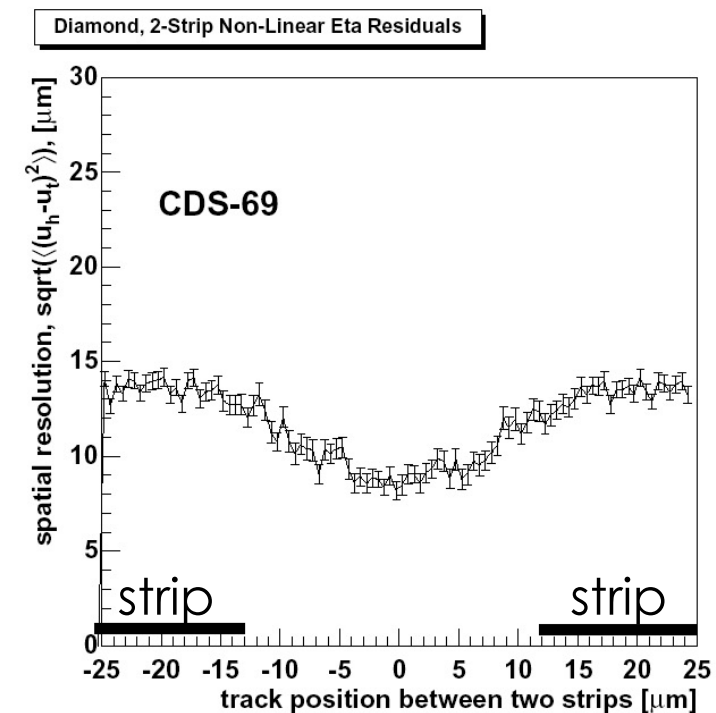
- A Diamond Testbeam Telescope



PH Distribution on each Strip

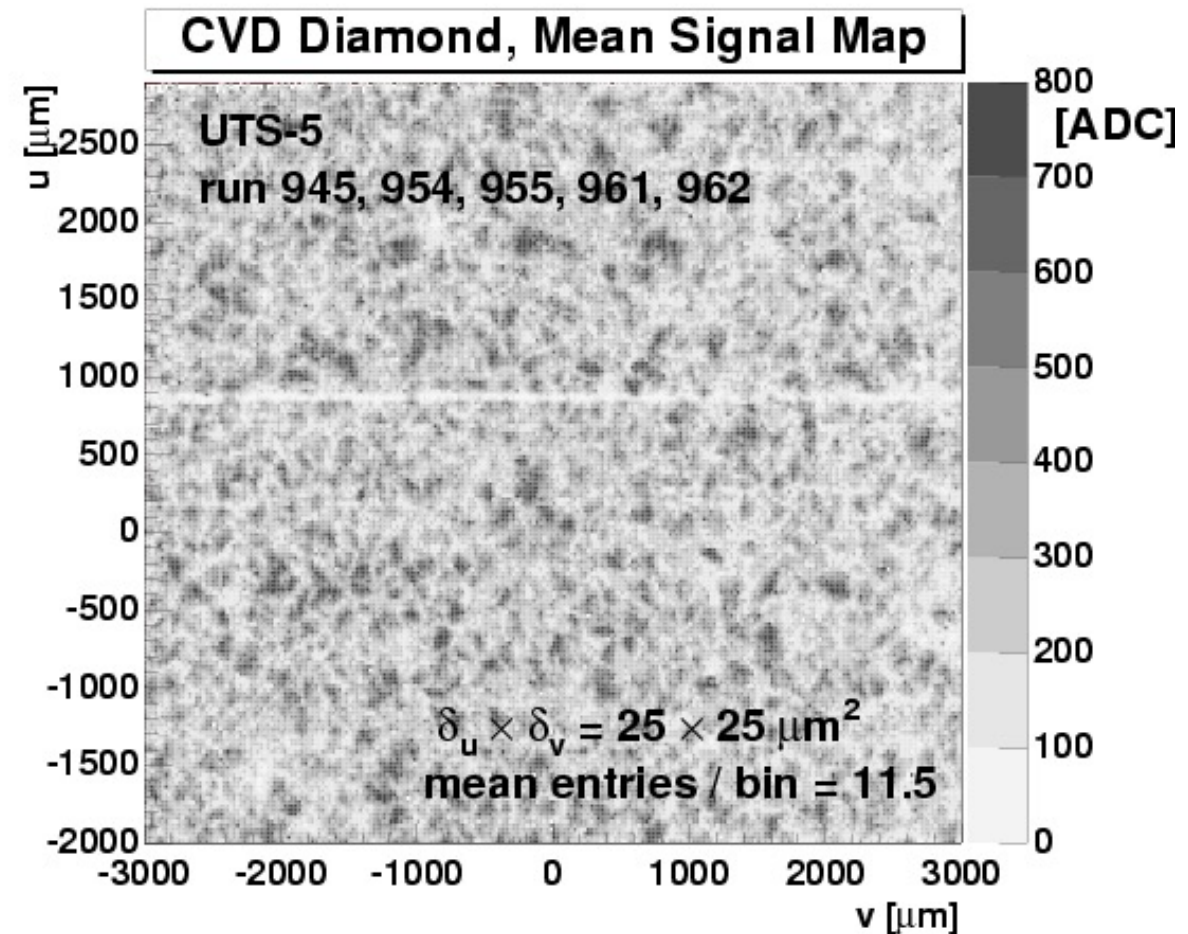


Residual versus Track Position



Uniformity in Charge Collection of CVD Diamonds

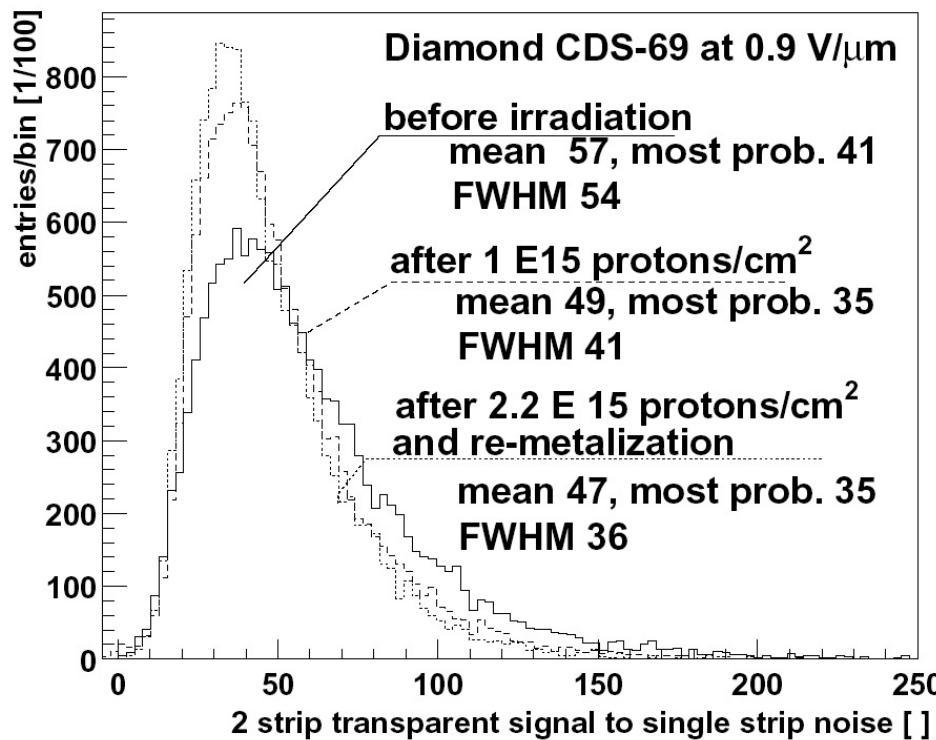
- Measured with MIPS
- Polycrystalline CVD diamond exhibits non-uniform signal response due to crystallite structure.
- Similar patterns observed as with photon beam measurement



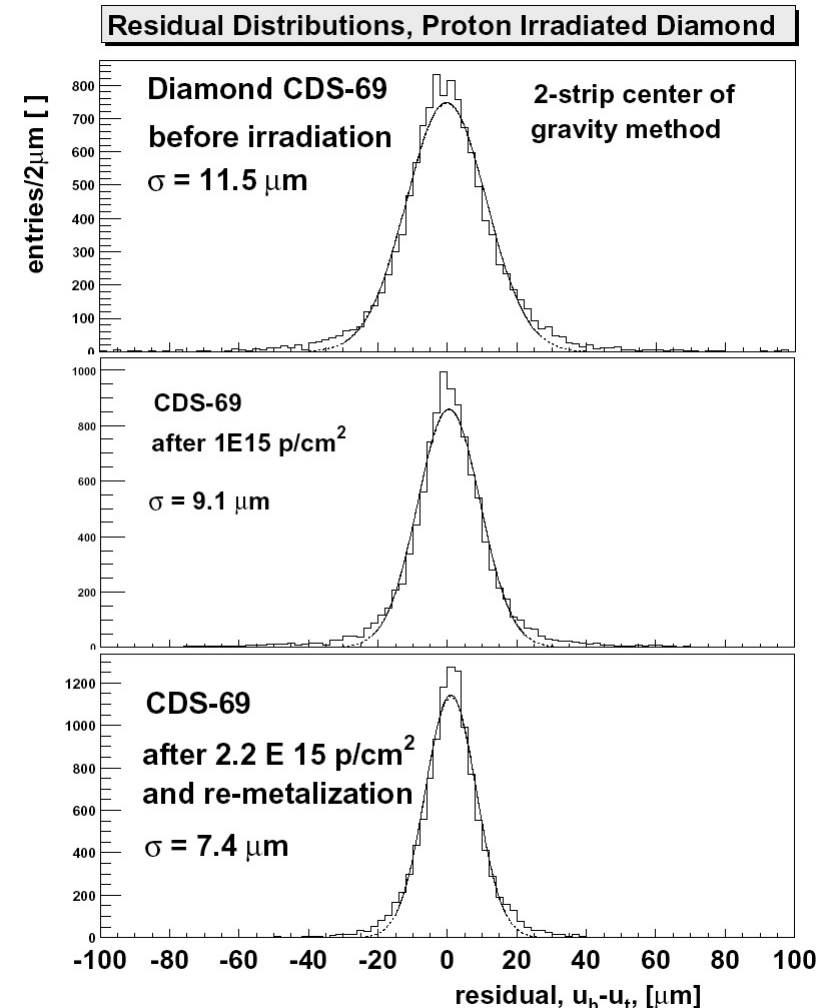
Irradiated Strip Detectors

■ Proton Irradiation

Signal from Irradiated Diamond Tracker



15% loss of S/N after 2e15 p cm⁻²



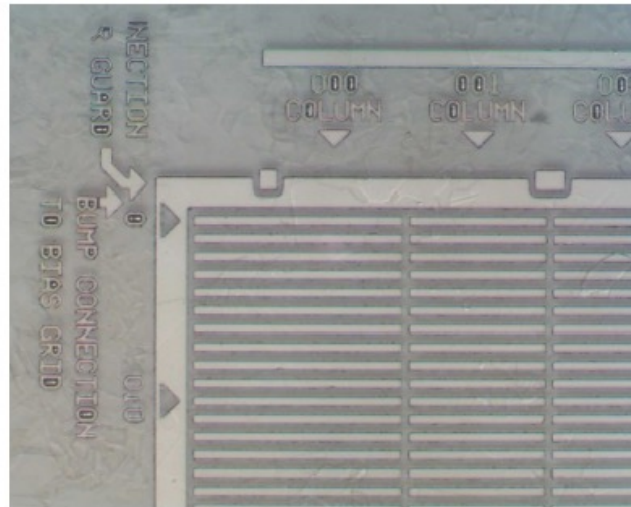
35% improvement in resolution

Pixel Detectors

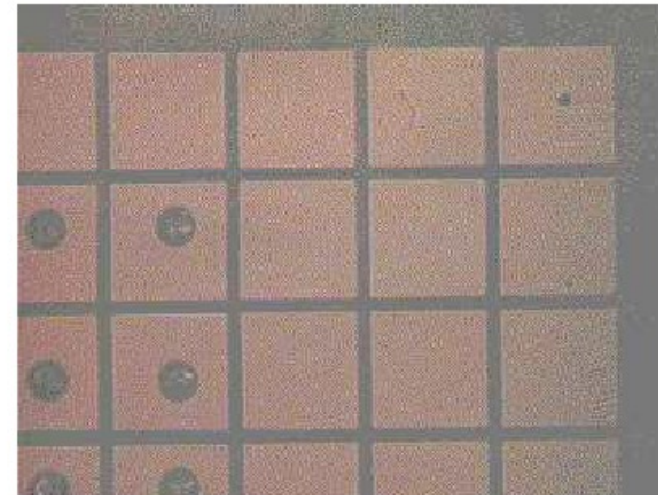
- Several prototypes of Diamond pixel detectors have been developed and tested since around 1996.
- Read-out chips use ROC (CMS), FE-I4 (ATLAS)
- More recently tested 3D pixel detectors (see later).
- Some historic examples in the following.

- Diamond Pixel Detectors

ATLAS FE/I Pixels (Al)



CMS Pixels (Ti-W)



- ◆ Atlas pixel pitch $50\mu\text{m} \times 400\mu\text{m}$
- ◆ Over Metalisation: Al
- ◆ Lead-tin solder bumping at IZM in Berlin
- ◆ CMS pixel pitch $125\mu\text{m} \times 125\mu\text{m}$
- ◆ Metalization: Ti/W
- ◆ Indium bumping at UC Davis

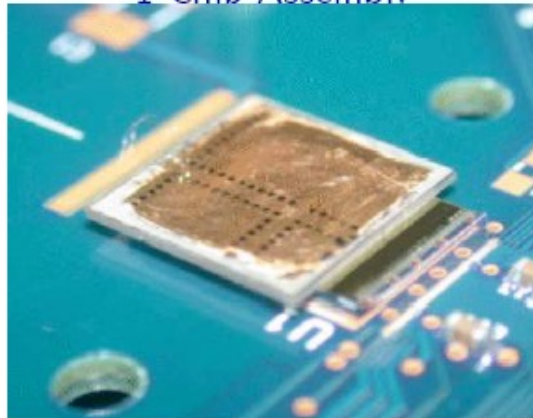
→ Bump bonding yield $\approx 100\%$ for both ATLAS and CMS devices



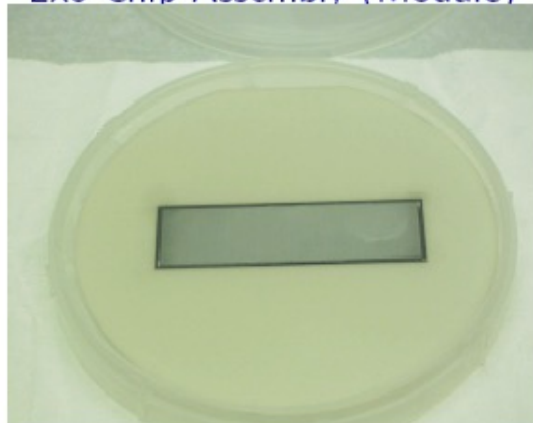
Diamond Pixel Detectors

Results from an ATLAS pixel detector

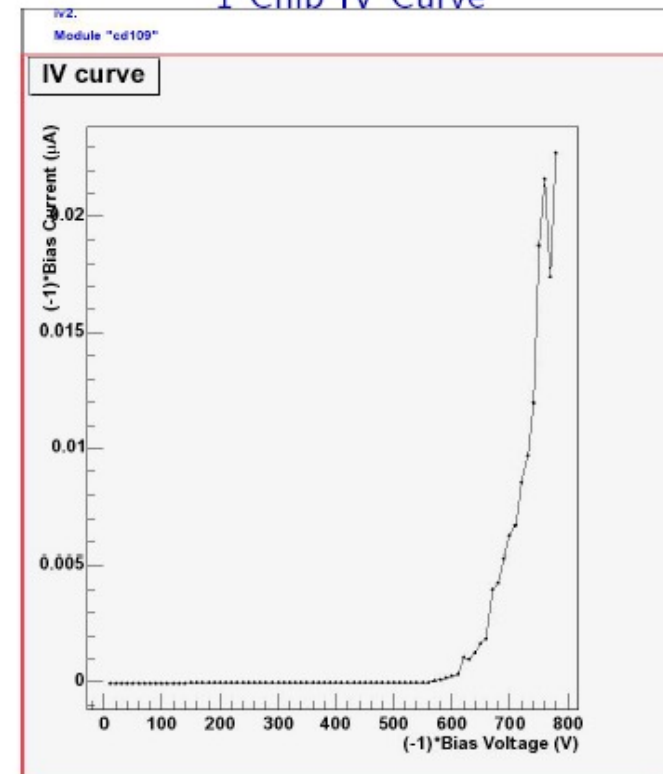
1 Chip Assembly



2x8 Chip Assembly (Module)



1 Chip IV Curve



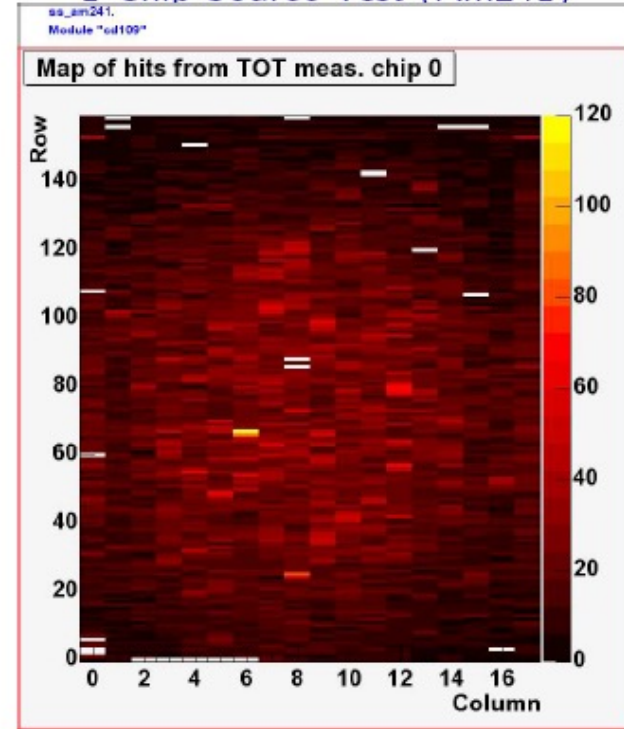


Diamond Pixel Detectors

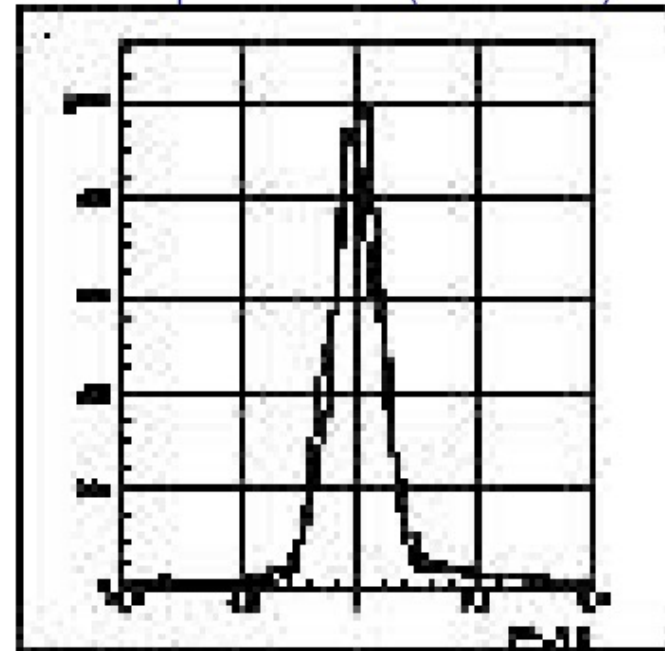
32

Results from an ATLAS pixel detector

1 Chip Source Test (Am241)



1 Chip Beam Test (Resolution)



Americium 241 deposits $\approx 4600e^-$

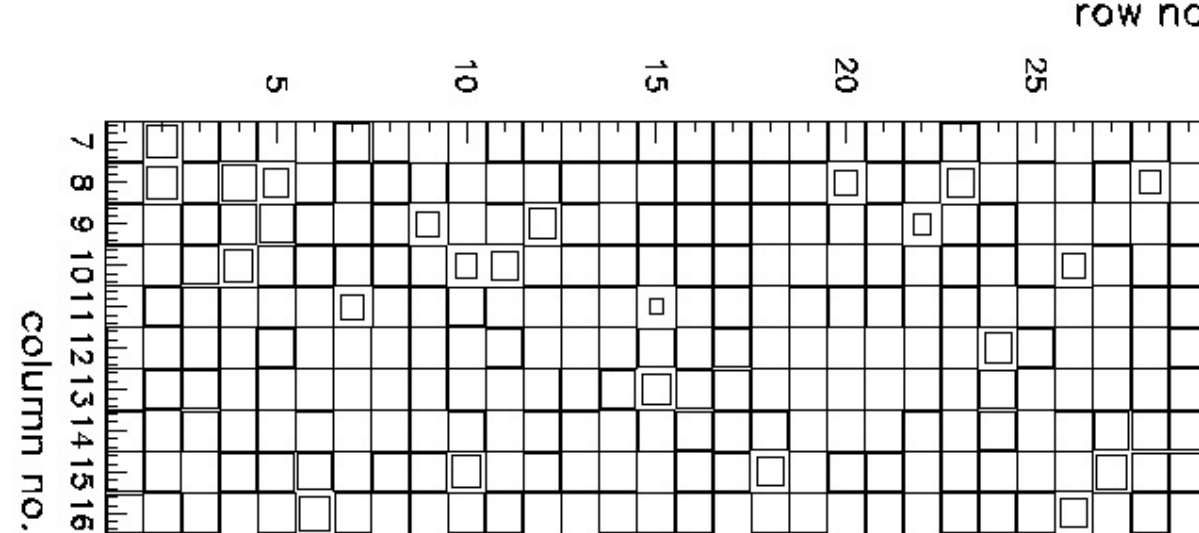
Spatial Resolution $\approx \text{pitch}/\sqrt{12}$ (pitch $50\mu\text{m} \times 400\mu\text{m}$)



Diamond Pixel Detectors

Results from a CMS pixel detector

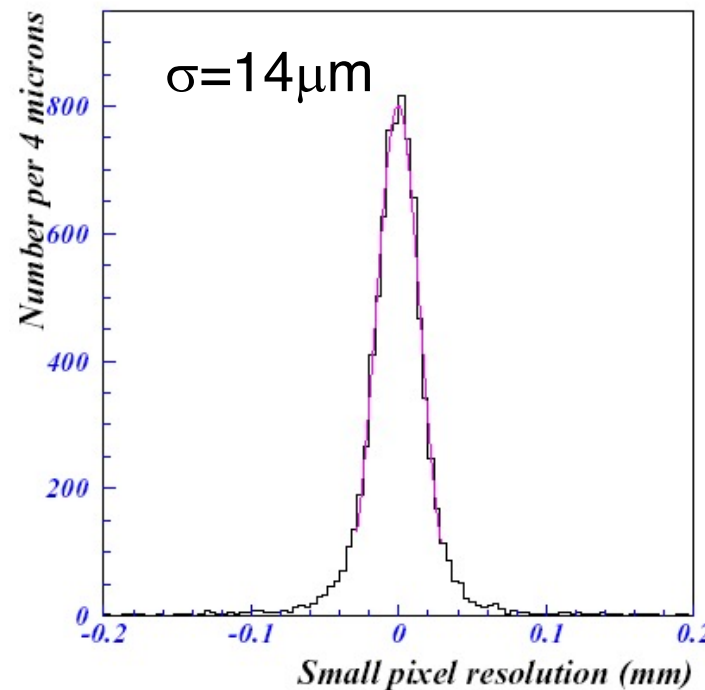
Efficiency vs Pixel



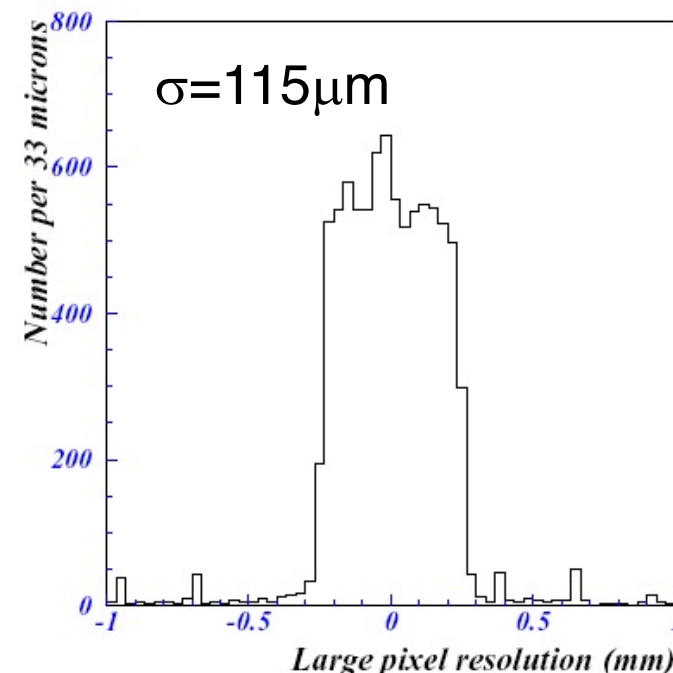
- Inefficient pixels due to bump bonding and/or electronics - shown in pulser tests
- Excellent correlation between beam telescope and pixel tracker data!

- Results from Atlas Diamond Pixel Detectors

Spatial Resolution – Short Direction

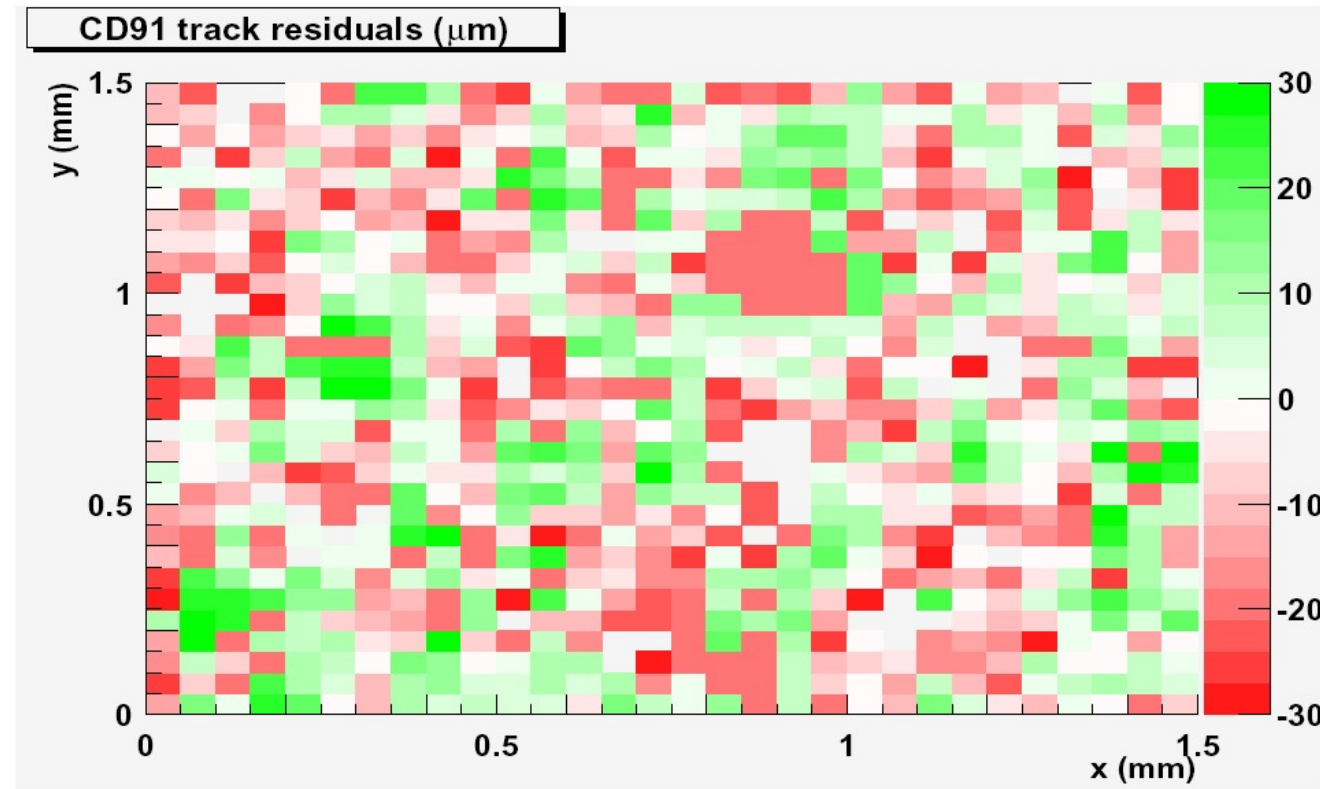


Spatial Resolution – Long Direction



- Efficiency = 80%
- Resolution = digital

- Results from Atlas Diamond Pixel Detectors



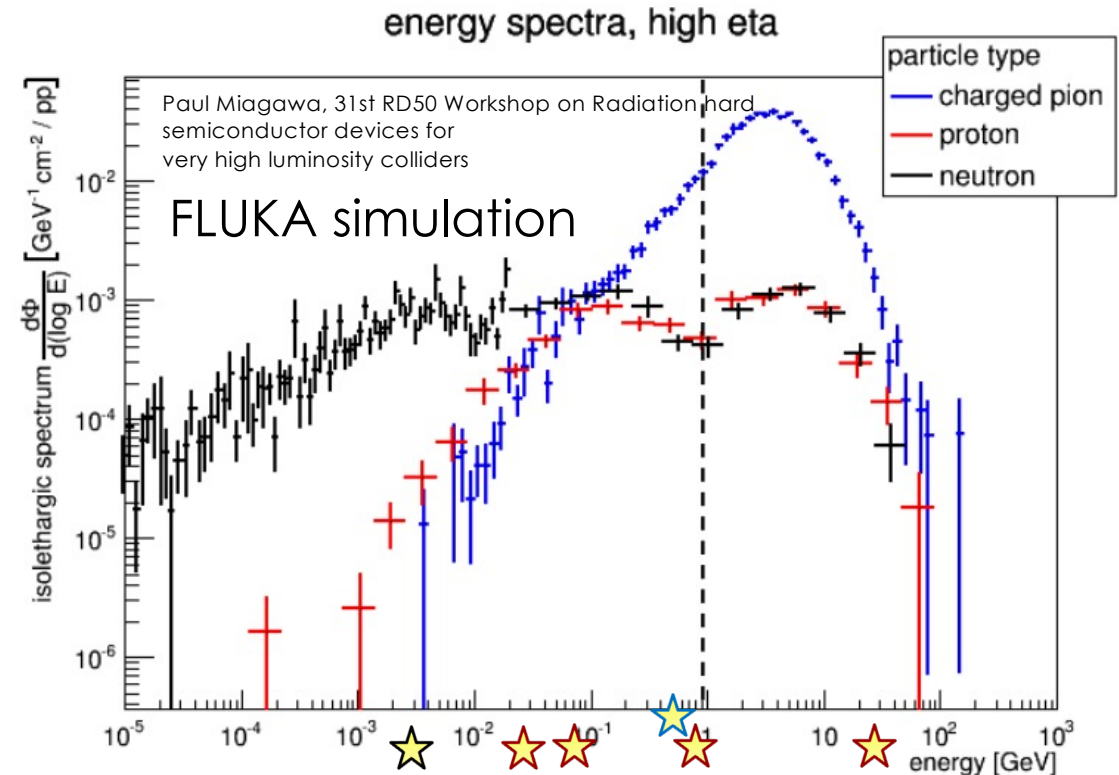
- Large track residuals
- Non-uniformity of response qualitatively reproduces by modeling

Tommaso Lari (INFN)
Alexander Oh (CERN)
Norbert Wermes (University Bonn)

Radiation Tolerance

Tests of Radiation Tolerance

- Irradiate with **proton, pions** and **neutrons**.
 - Energies within the expected radiation profile at HL-LHC.
 - HL-LHC fluence requirement about $2e10^{16}$ neq.



	Proton ★	Pion ★	Neutron ★
Energy	25MeV – 24GeV	300 MeV	1-10 MeV
Fluence	$1.27e16 \text{ p cm}^{-2}$	$6e14 \pi \text{ cm}^{-2}$	$1.3e16 \text{ n cm}^{-2}$

- Assume simple effective model for radiation damage:

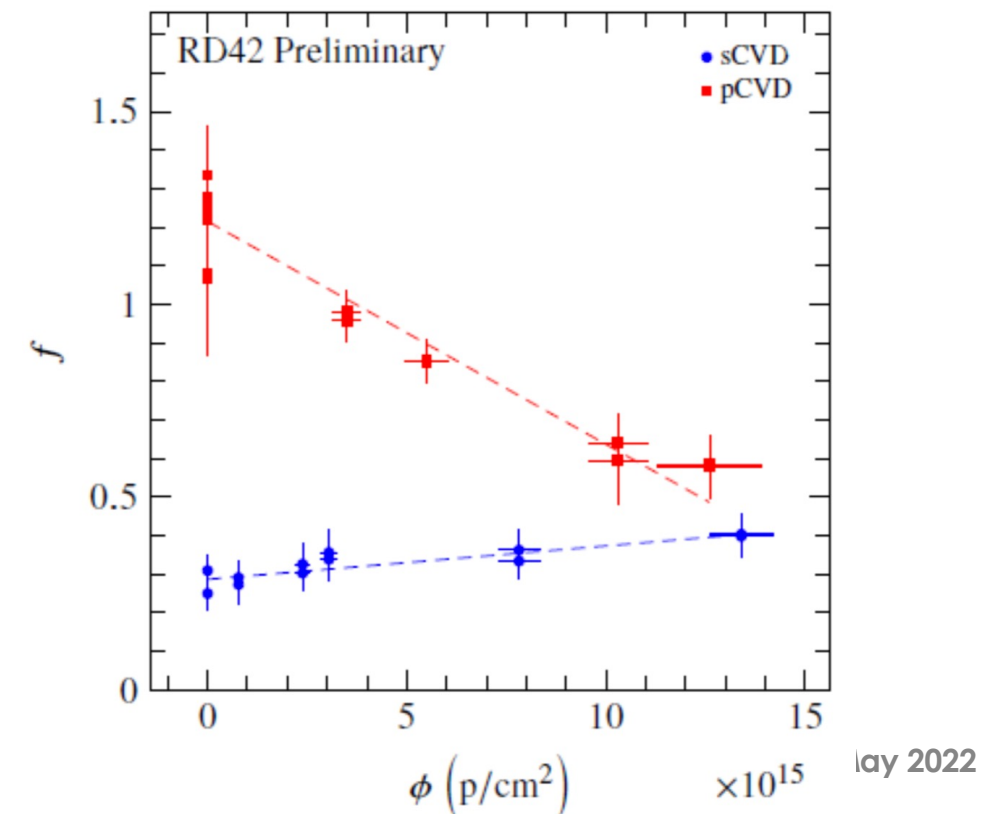
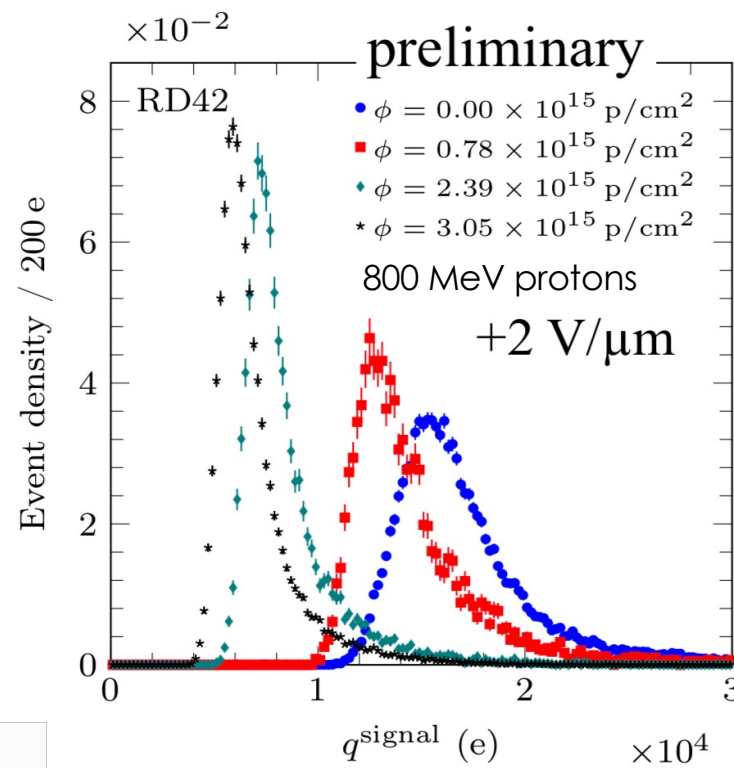
Radiation damage constant
is fitted with simple model:

$$\frac{1}{\lambda} = \frac{1}{\lambda_0} + k_\lambda \Phi$$

damage constant
particle flux

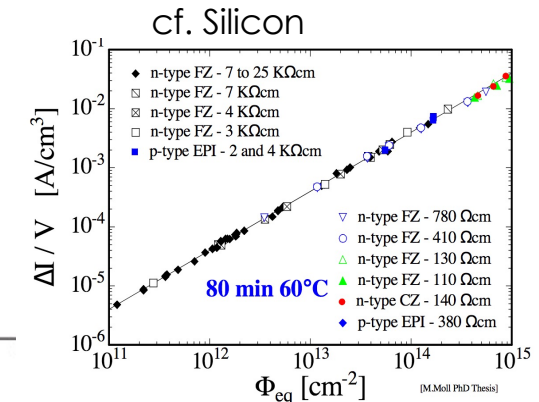
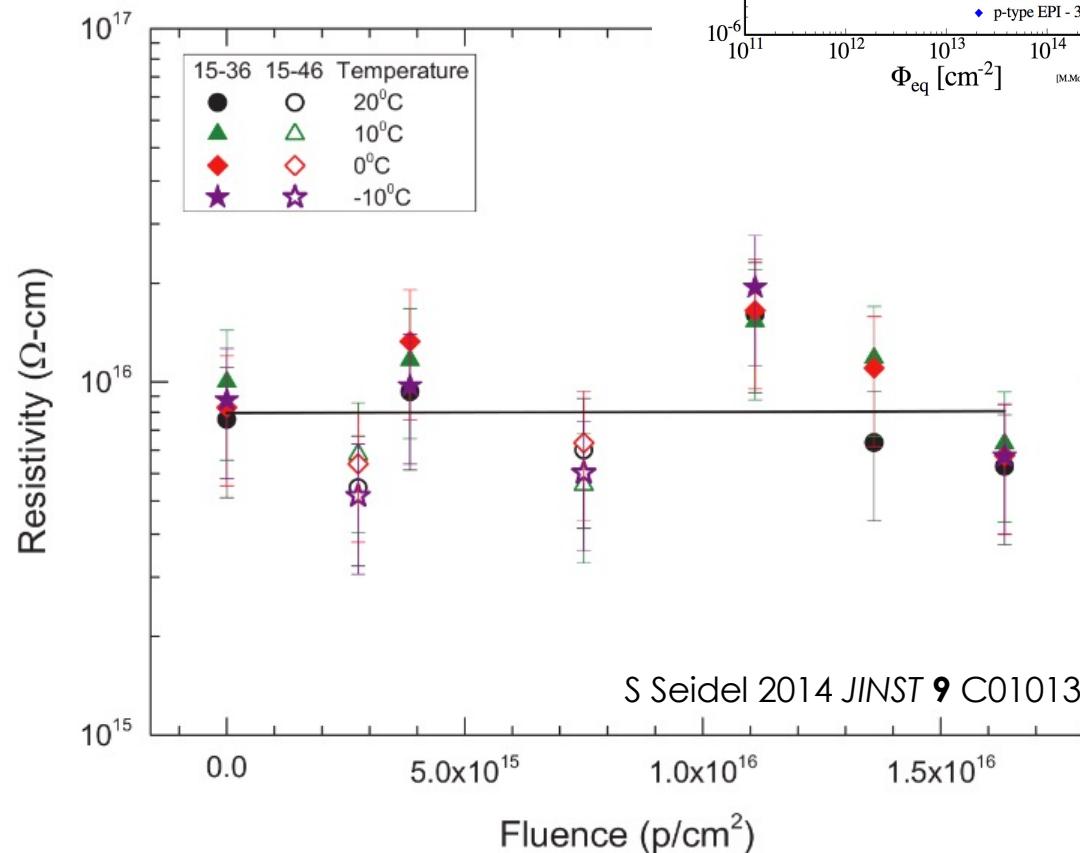
Radiation Tolerance: Characterization

- Typical Landau Spectra after irradiation of pCVD.
- For pCVD see reduction of **FWHM** / **MP** with irradiation.
 - Expected from polycrystalline nature of material!
 - Single crystal material almost flat.



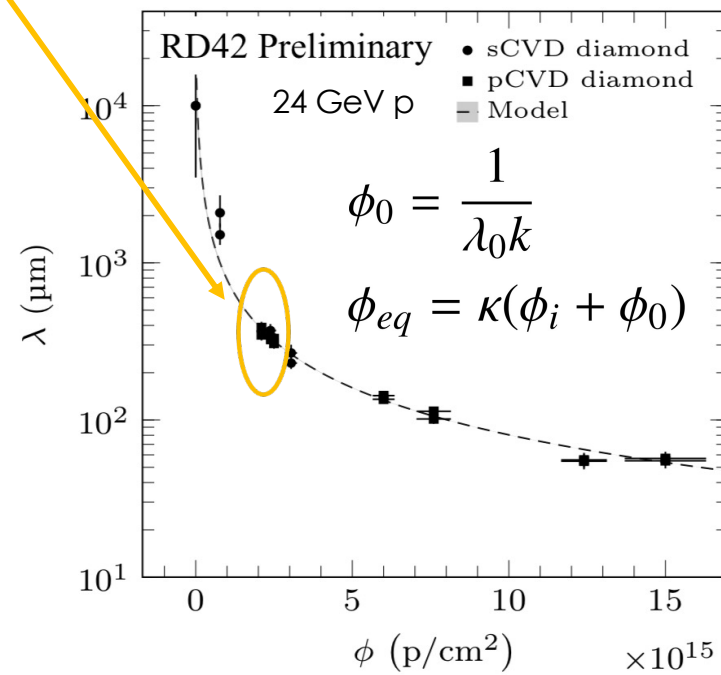
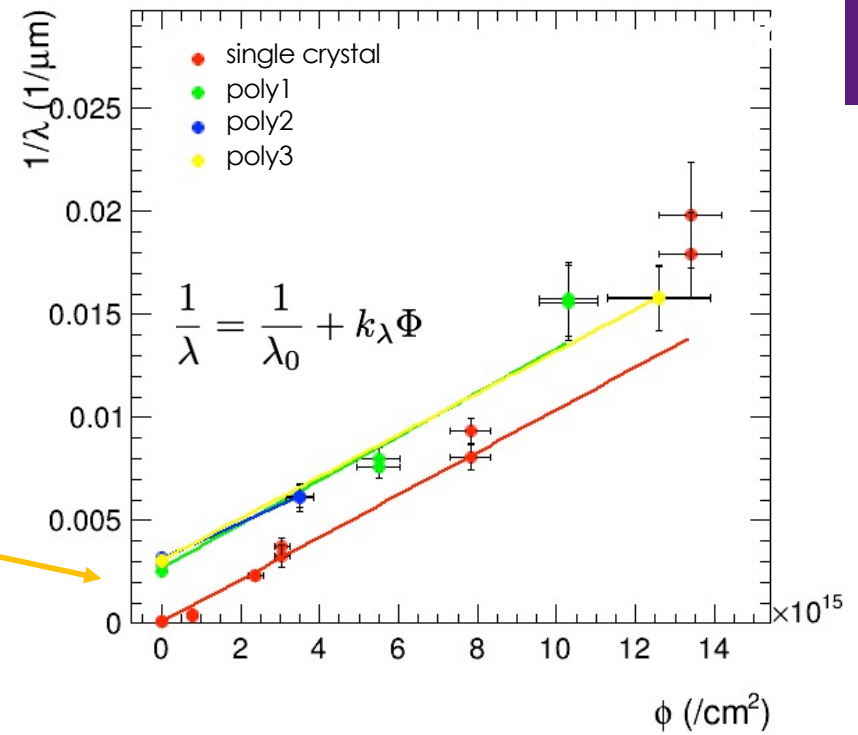
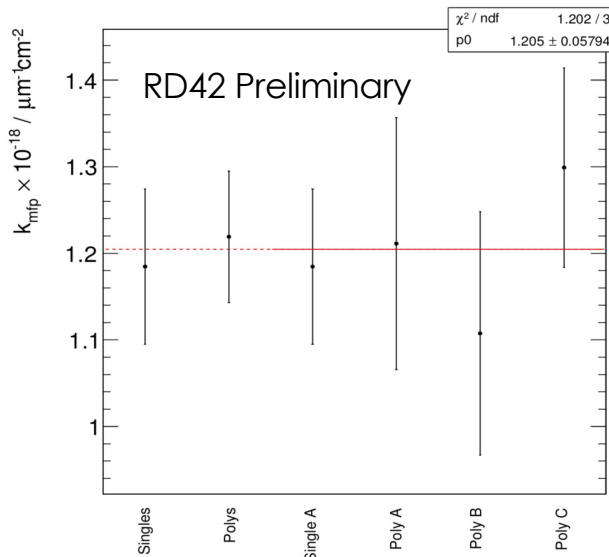
Radiation Tolerance: Characterization

- Resistivity
 - No dose dependence.
 - Due to large bandgap no significant temperature dependence at RT or below.



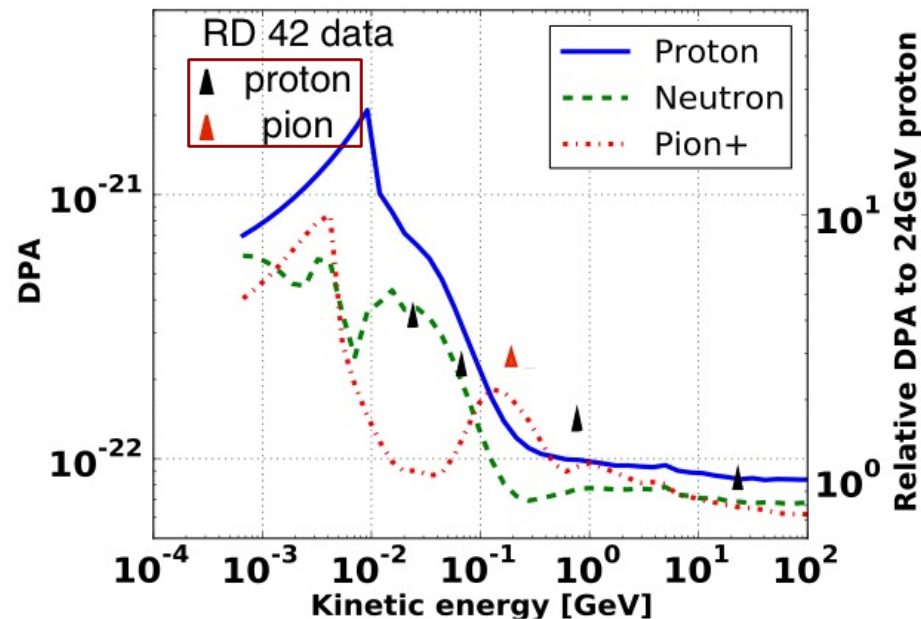
Radiation Tolerance: Characterization

- Damage factor k is determined for each sample.
- **pCVD** diamonds are offset by λ_0 to account for initial finite carrier lifetime.
- Final damage factor averaged over all samples.



Radiation Hardness

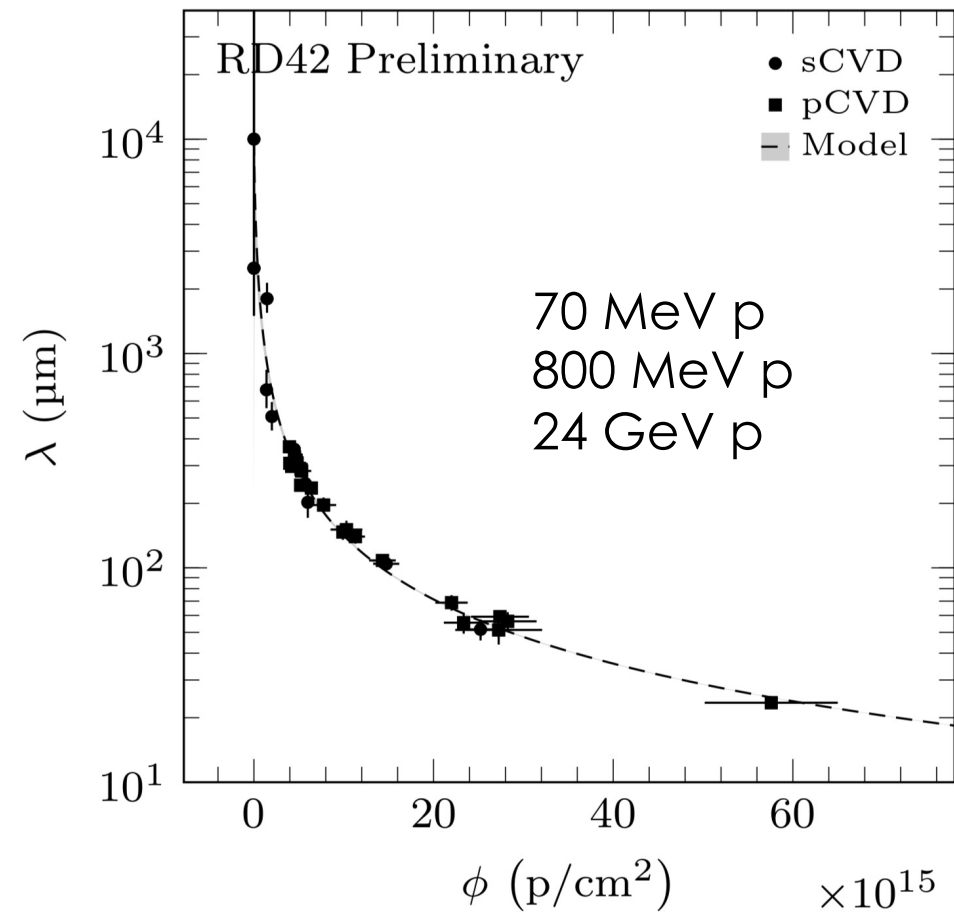
- Describe radiation damage using Norgett-Robinson-Torrens theorem to predict displacements per atom (DPA).
 - (M. Guthoff et al., arXiv:1308.5419)
 - Diamond displacement energy: 43.3 eV
 - Reasonable agreement for $E > 100 \text{ MeV}$.



Radiation Tolerance

■ 24 GeV protons

- $k_\lambda = 0.67 \pm 0.04 \times 10^{-18} \text{ cm}^2 \mu\text{m}^{-1}$
- polycrystalline diamond sample offset by $\Phi \sim 5 \times 10^{15}$ to account for existing traps.
- Poly and single crystal diamond show consistent damage constants.



L. Baeni ETHZ Thesis

<https://www.research-collection.ethz.ch/handle/20.500.11850/222412>

Radiation Tolerance

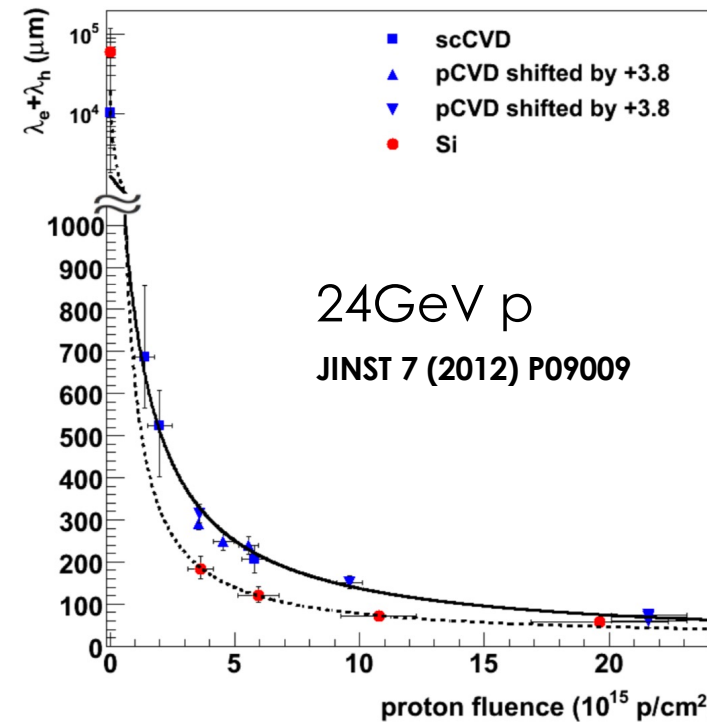
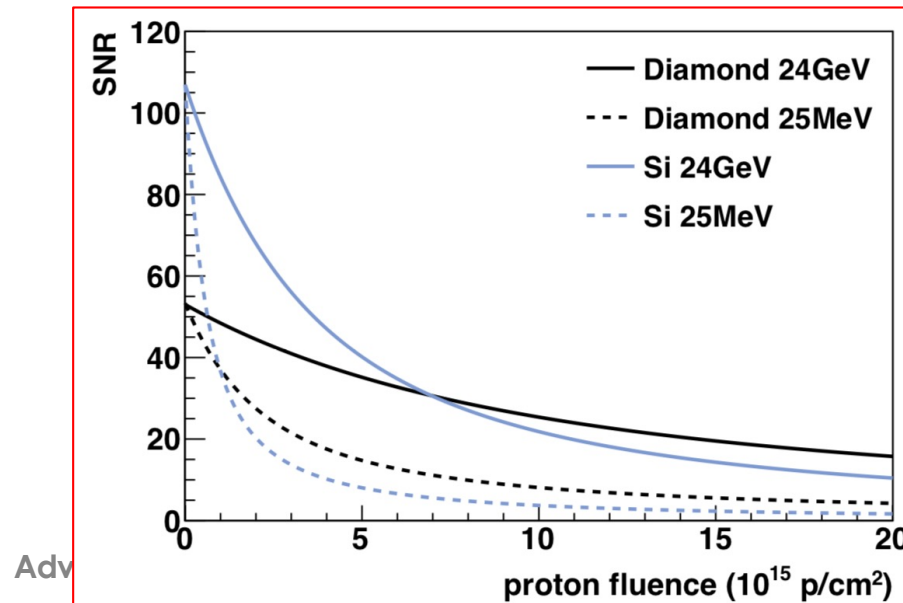
- Summary of RD42 irradiation results:

Particle Species	Relative Damage Constant, κ
24 GeV p	1
800 MeV p	1.54 ± 0.13
70 MeV p	2.5 ± 0.4
25 MeV p	4.5 ± 0.6
fast neutrons	4.5 ± 0.5

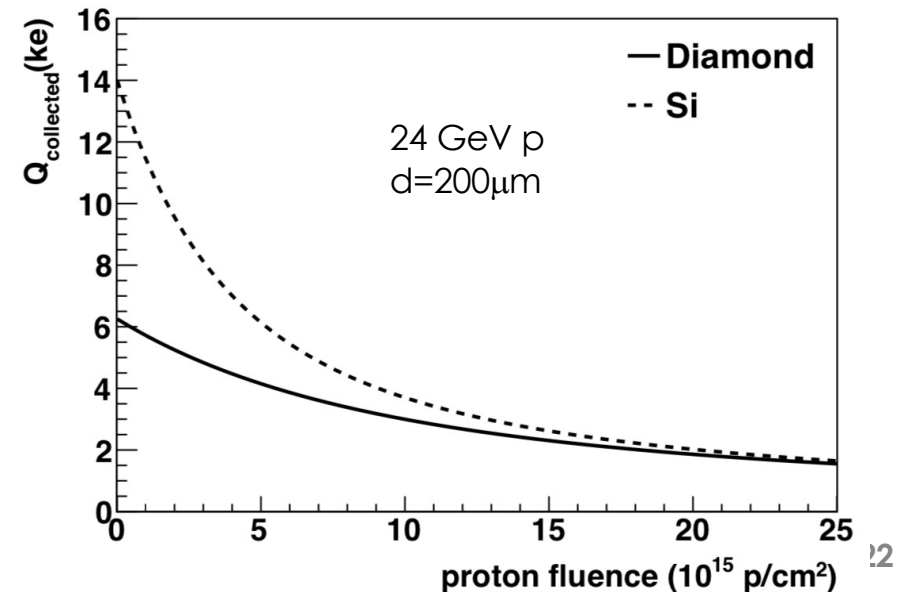
*normalized to 24GeV protons

Radiation Tolerance: Comparison to Si

- k factors typically 2-3 times higher for Silicon.
- A comparison to Si needs to take into account:
 - leakage current
 - capacitance
- Possible figure of merit
Signal to noise ratio:



24GeV p
JINST 7 (2012) P09009

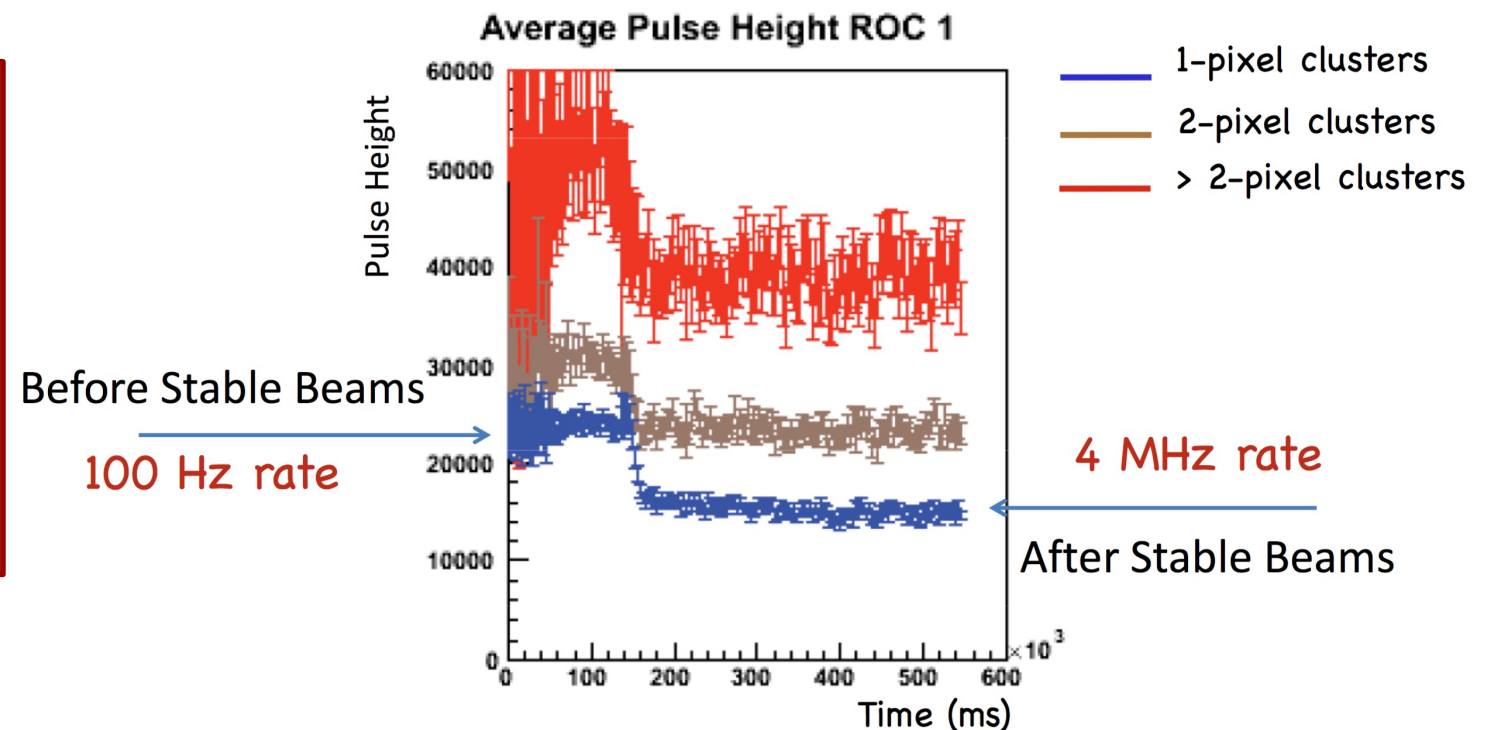


High rate capability

High Rate tests

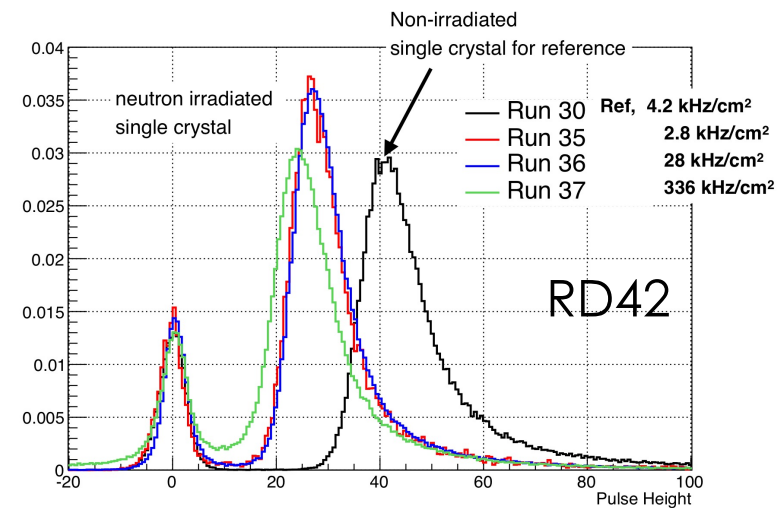
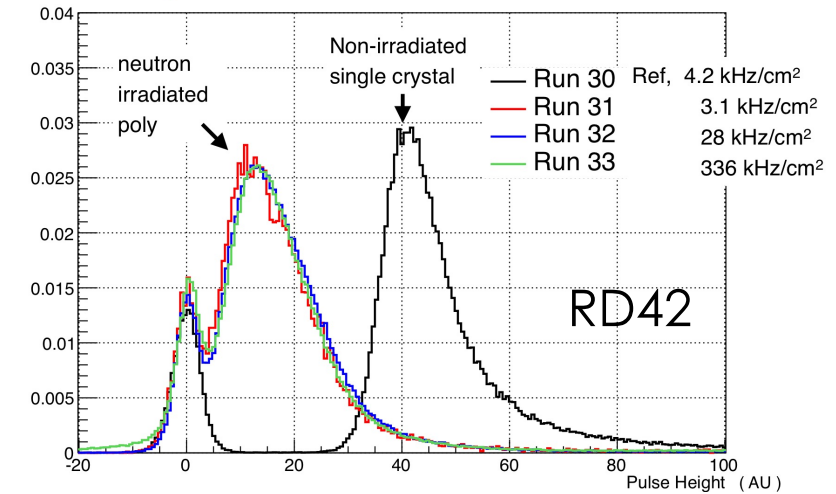
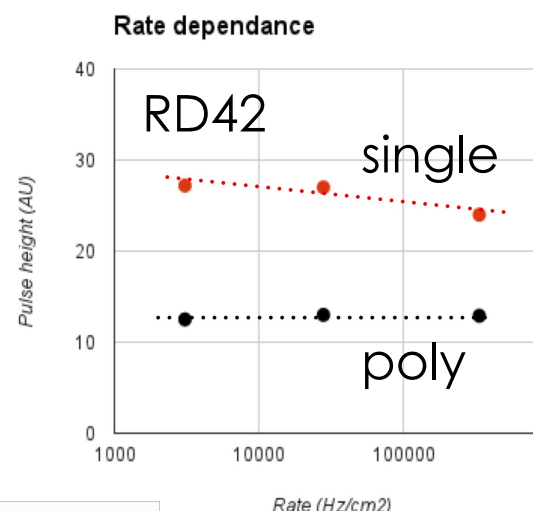
- Tests the pulse height as function of particle rate.
- Test single and poly crystalline diamond.
- Irradiated and un-irradiated.

Investigations triggered by indication of rate dependence of of single crystal diamond pixel detector installed in CMS in 2012.



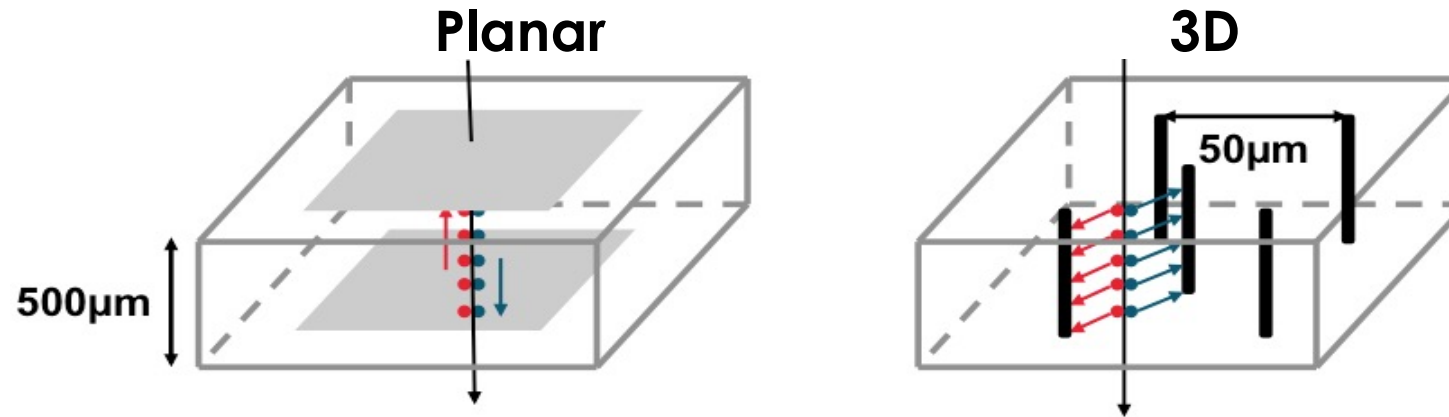
High Rate tests

- single and poly sample irradiated with 5×10^{13} reactor n.
- Tested with 250MeV pions.
- Slight rate dependence observed in irradiated **single crystal** sample.
- No rate dependence observed for irradiated **polycrystalline** sample.



3D diamond detectors

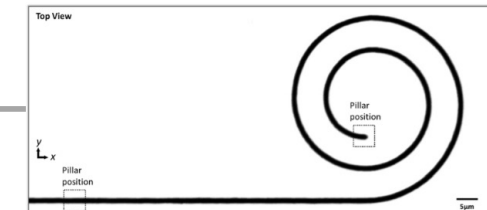
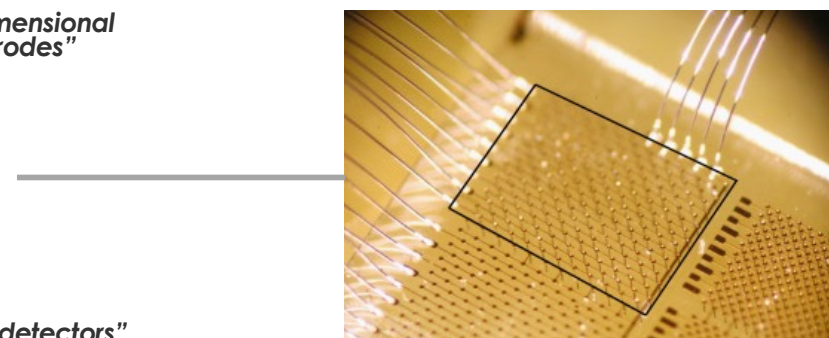
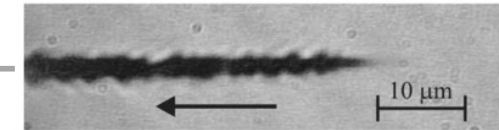
3D Diamond Detectors



- Electrode spacing determines drift distance to induce 1e charge.
- 3D has shorter electrode spacing compared to planar.
- Charge carriers need less drift distance (and time) in 3D than in planar to induce equal signal.
- Influence of traps and resulting limited lifetime suppressed in 3D.

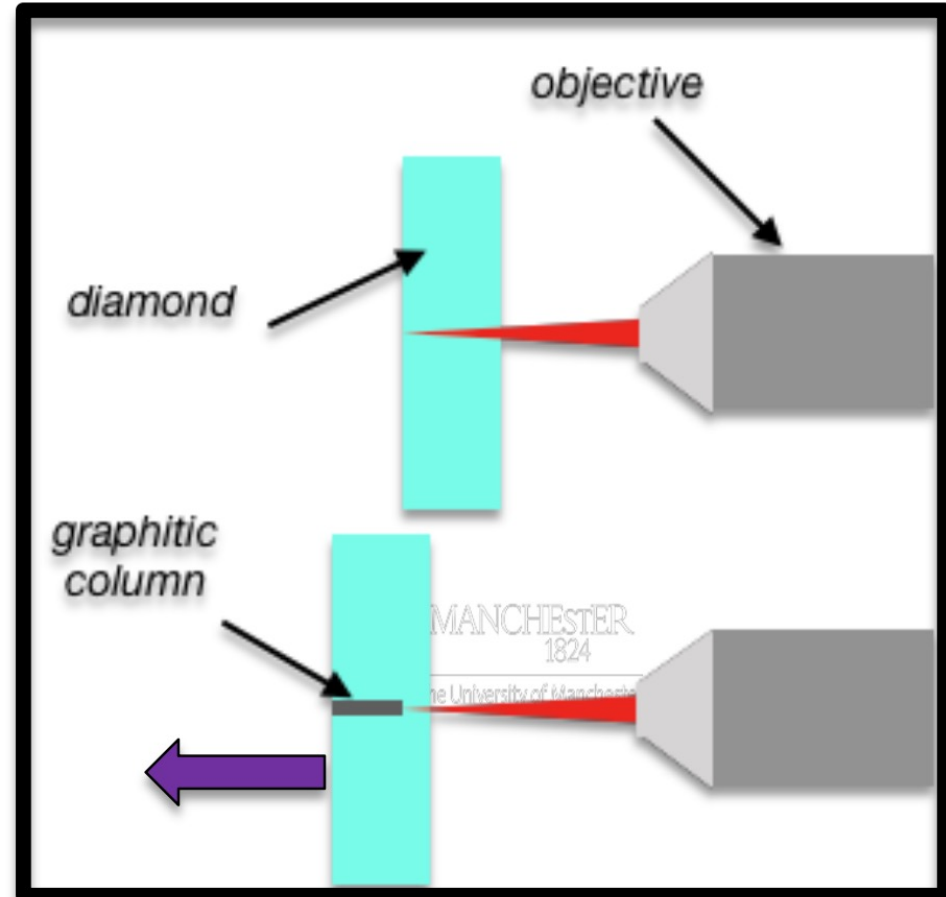
3D Diamond Research - A relatively young field

- Laser induced phase change in diamond.
 - E.g. T.V. Kononenko et al, Diamond & Related Materials 18 (2009) 196–199
"Femtosecond laser microstructuring in the bulk of diamond"
- 3D "Pad" detector
 - A. Oh, B. Caylar, M. Pomorski, T. Wengler, Diamond and Related Materials, 38 , (2013), **"A novel detector with graphitic electrodes in CVD diamond"**
 - S. Lagomarsino et al, Appl. Phys. Lett. 103, 233507 (2013), **"Three-dimensional diamond detectors: Charge collection efficiency of graphitic electrodes"**
- 3D "strip array" detector with position resolution.
 - E.g. F. Bachmaier et al, NIM A, 786, (2015) 97-104,
"A 3D diamond detector for particle tracking"
- Radiation damage studies.
 - Eg. S. Lagomarsino et al, Applied Physics Letters 106, 193509 (2015)
"Radiation hardness of three-dimensional polycrystalline diamond detectors"
- Improvements in graphitization process.
 - Eg. B. Sun et al., Applied Physics Letters 105, 231105 (2014), **"High conductivity micro-wires in diamond following arbitrary paths"**
- 3D pixel detectors
 - RD42, CERN-LHCC-2018-015 ((2018), **Development of Diamond Tracking Detectors for High Luminosity Experiments at the LHC, HL-LHC and Beyond**)
 - L. Anderlini et al, Front. Phys., 04 November 2020, **Fabrication and Characterisation of 3D Diamond Pixel Detectors With Timing Capabilities**



Fabrication

- Conductive columns are created by changing diamond into a graphitic material with a short laser pulse:

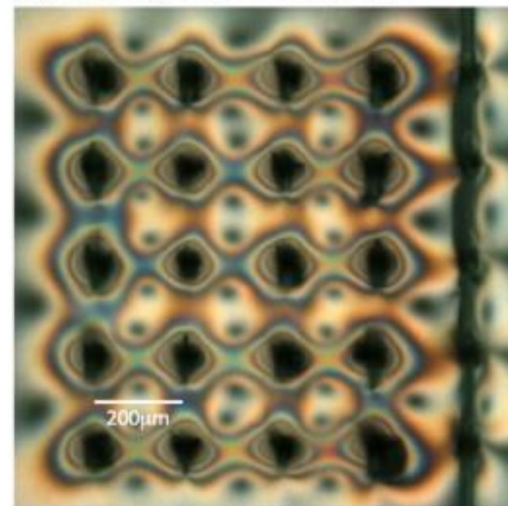


Laser graphitisation of diamond

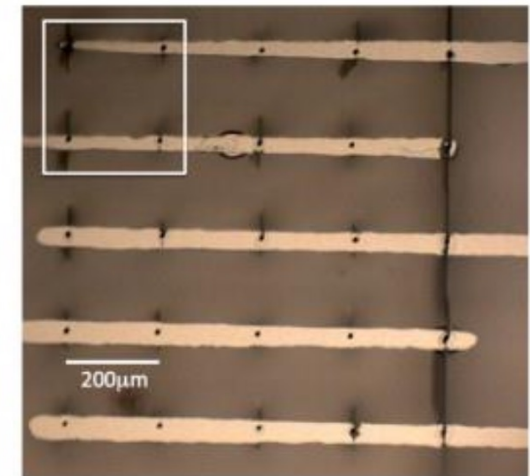
FIRST 3D DIAMOND DEVICE

- Collaboration of **Manchester**, CEA LIST and CERN
- Published **2013**
- Single crystal substrate
- First device made at LIST using **nano-second** pulse nitrogen laser with beam spot diameter of **10µm**

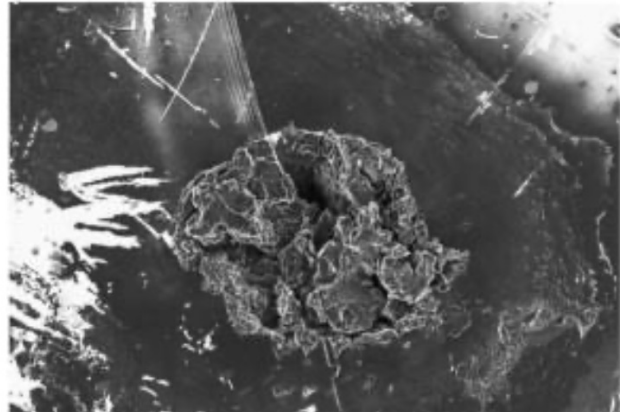
(a) Birefringence microscopy.



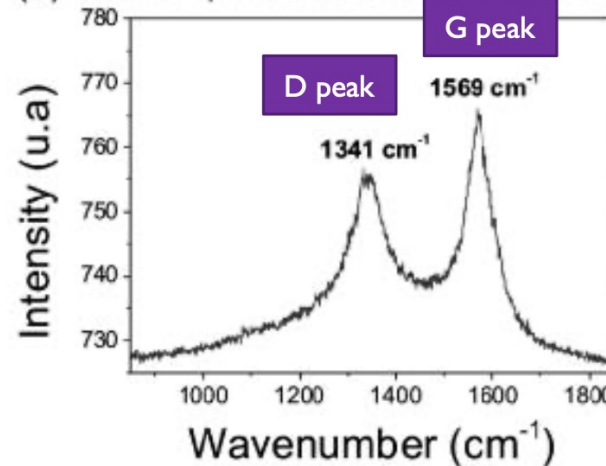
(b) Photograph after metallisation.



(a) SEM picture of a graphitic column.



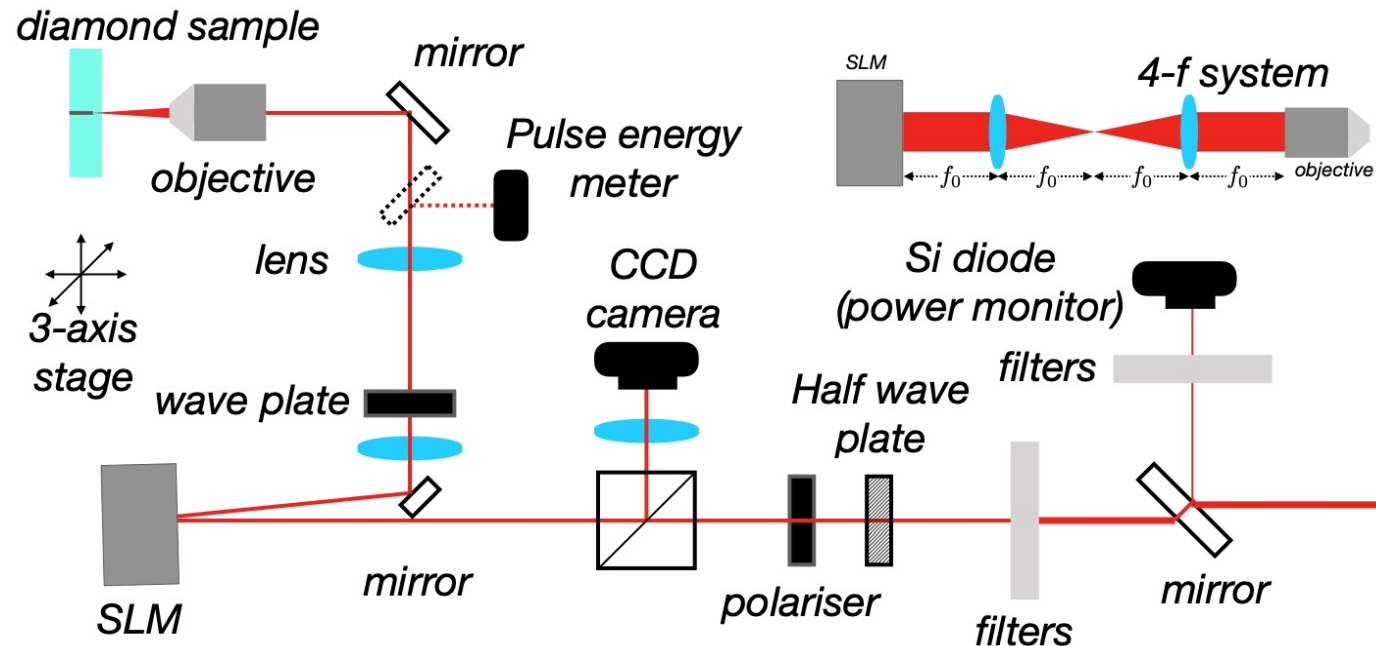
(b) Raman spectrum on the graphitic column.



Oh,A., Caylar, B., Pomorski, M., & Wengler, T. (2013). A novel detector with graphitic electrodes in CVD diamond. *Diamond and Related Materials*, 38, 9–13.

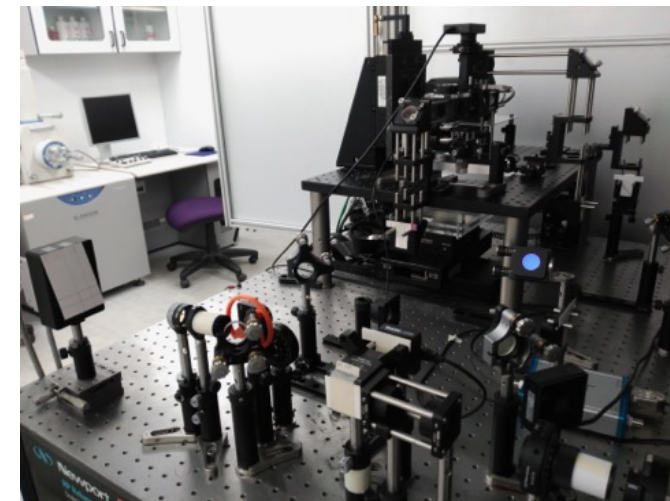
Laser Set-up in Manchester

60



Laser specs:

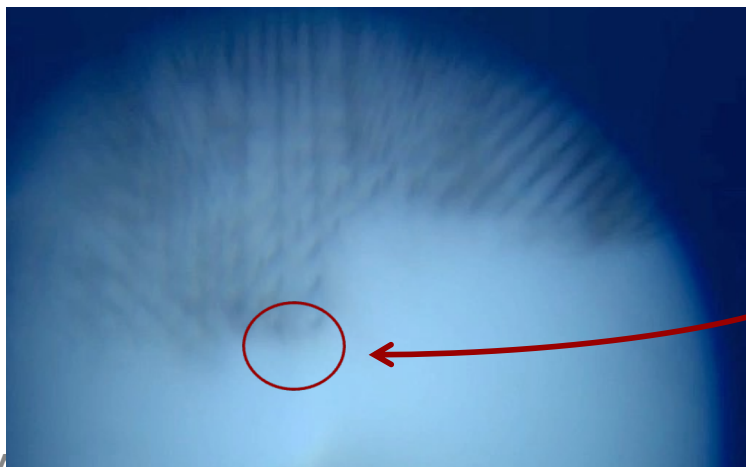
- Wavelength: 800 nm
- Repetition rate: 1 kHz
- Pulse duration: 100 fs
- Max power: 1 W



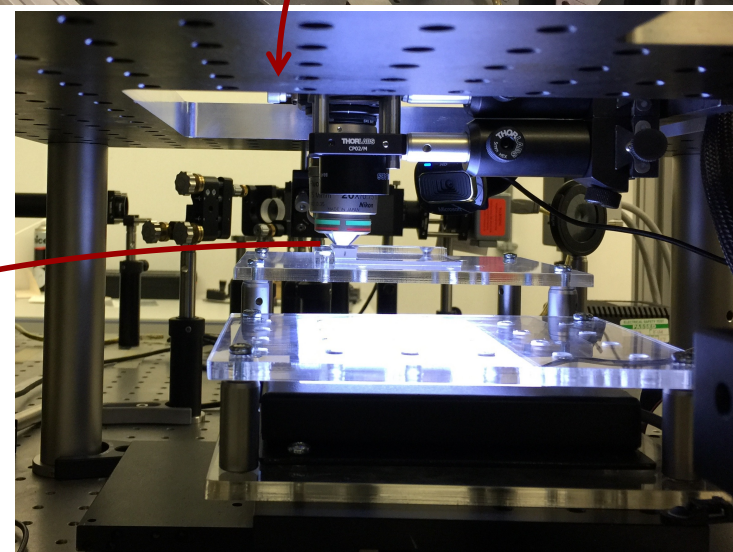
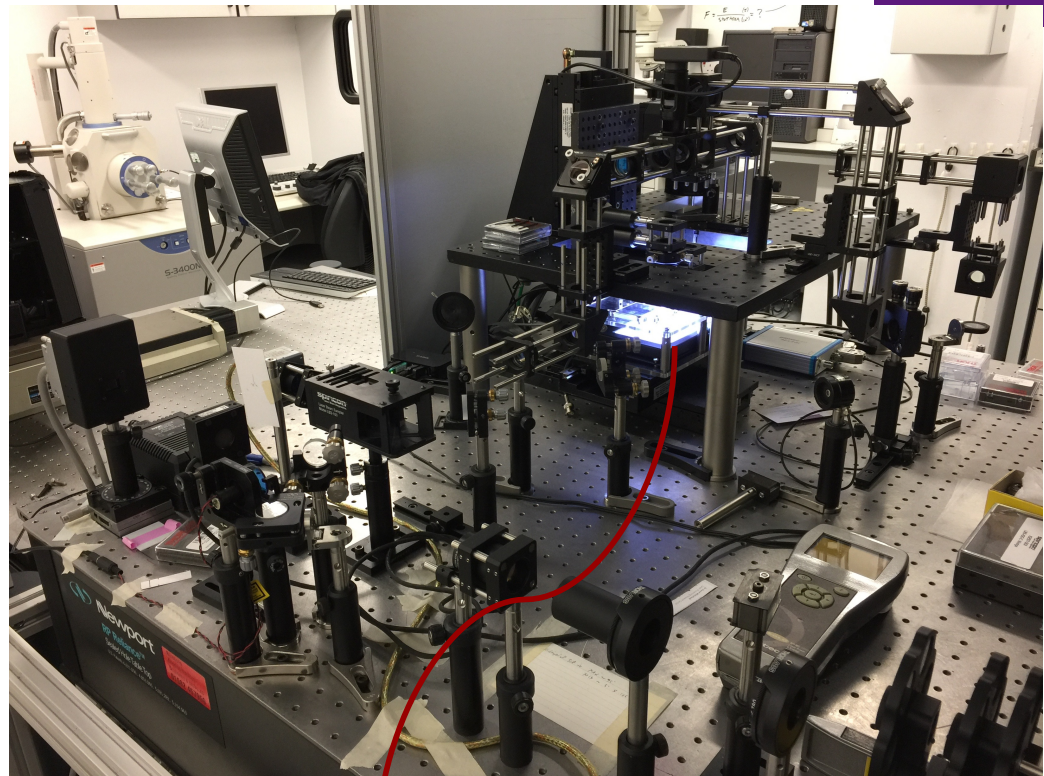
Just moved to MECDI!

University of Manchester, Laser Processing Research Center.

- Wavelength = 800 nm
- Repetition rate = 1 kHz
- Pulse duration = 100 fs
- Spot size = 10 μ m
- Pulse Energy ~ 1 μ J
- Spatial light modulator



Advanced UK Instrumentation Training 2022

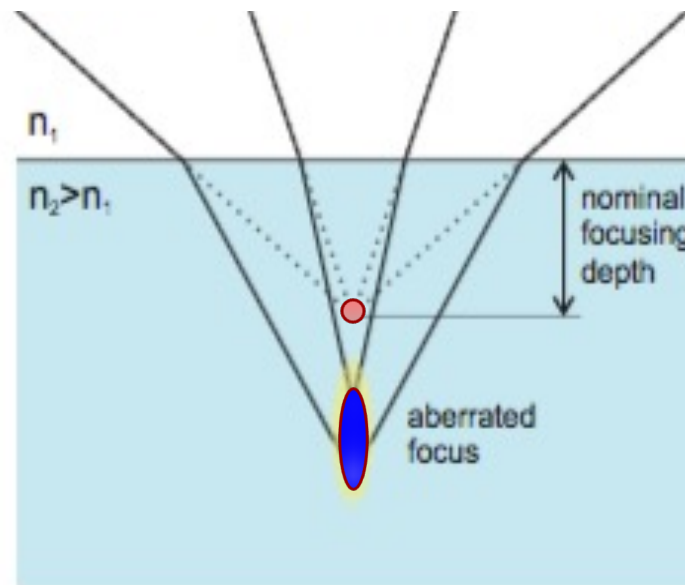


May 2022

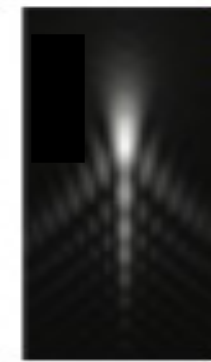
SLM – Phase Spatial Light Modulation

- Comparison SLM vs standard process.

	Std.	SLM
Resistivity	$1 \Omega\text{cm}$	$0.1 \Omega\text{cm}$
Diameter	$\sim 3\mu\text{m}$	$\sim 1\mu\text{m}$
Diamond to graphite ratio	~ 4	~ 0.2



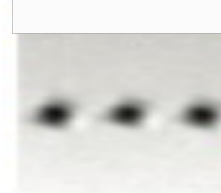
Simulated
depth = $40\mu\text{m}$



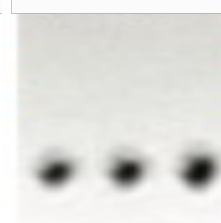
Measured
depth = $40\mu\text{m}$



depth = $80\mu\text{m}$

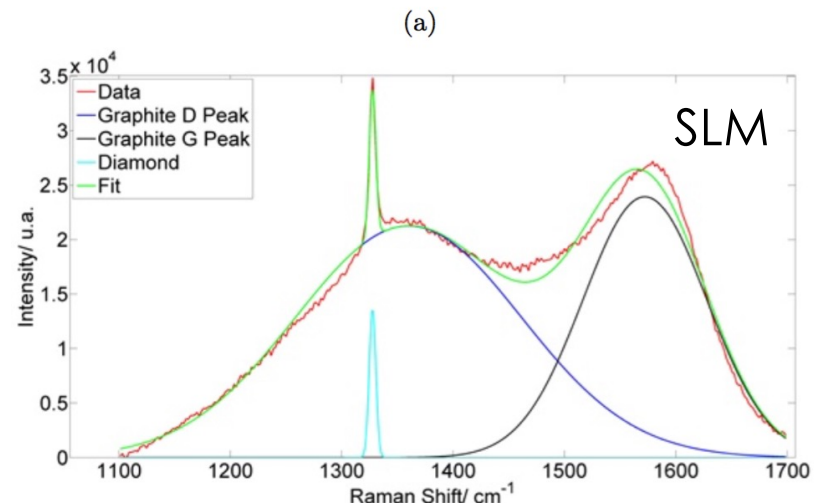
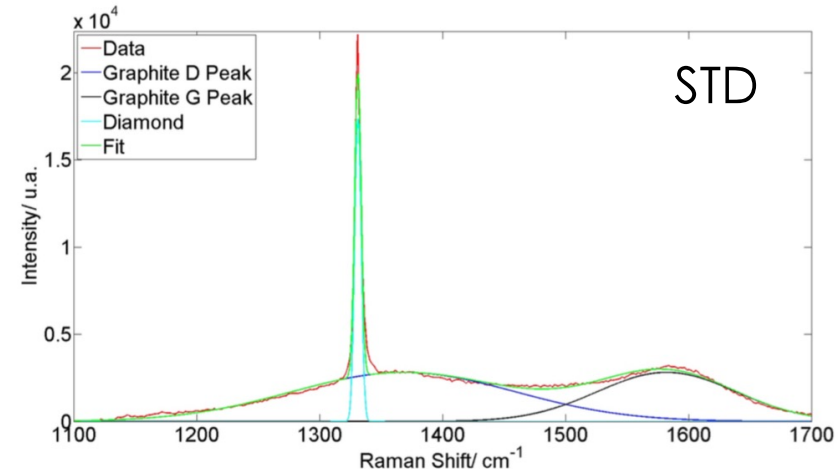
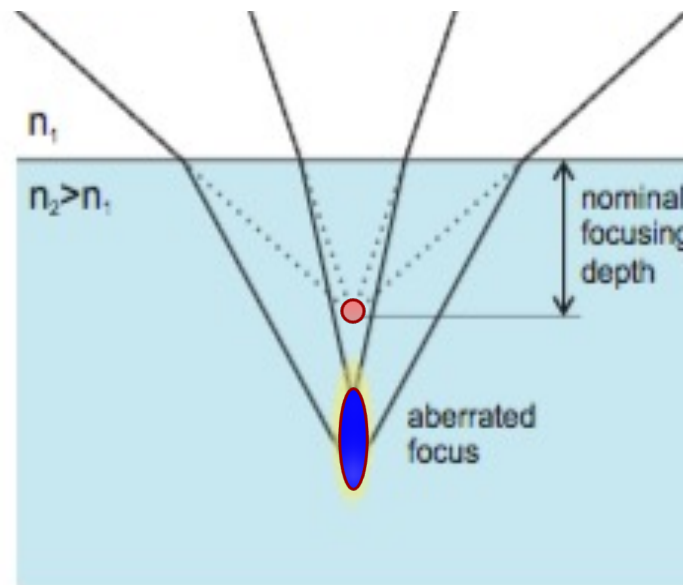


depth = $130\mu\text{m}$



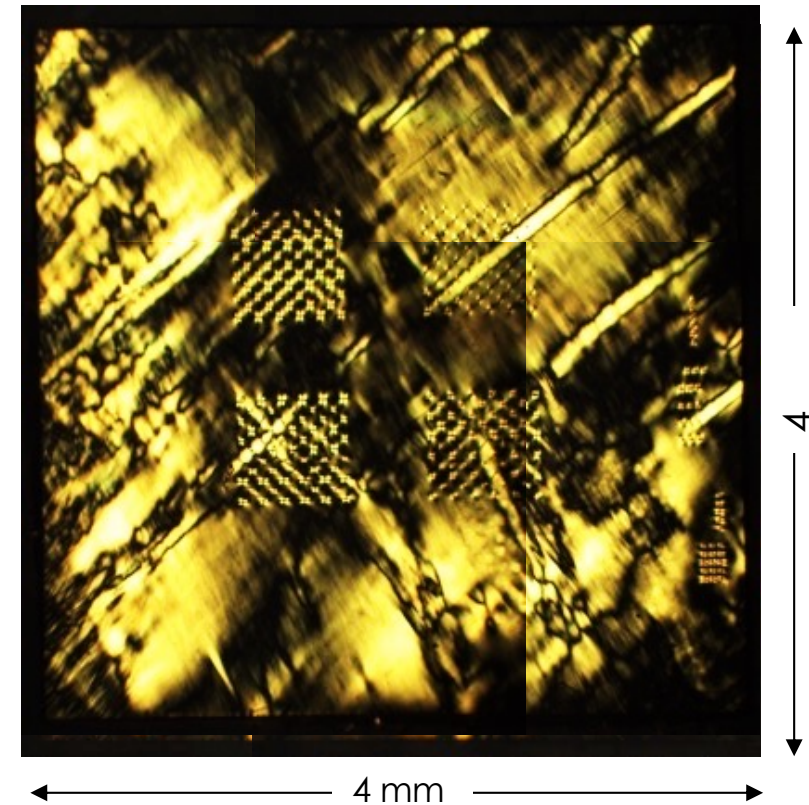
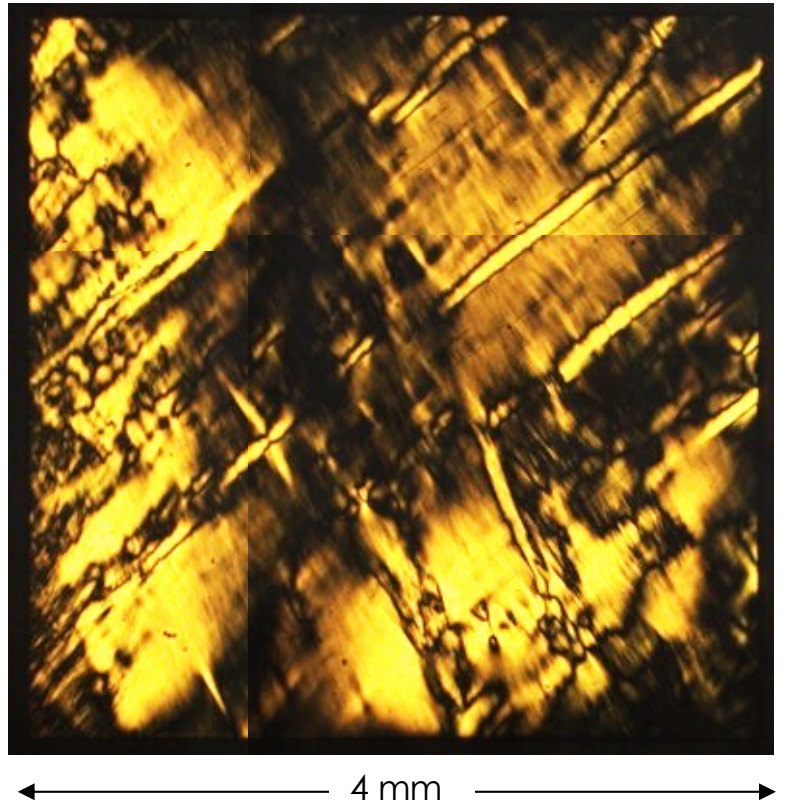
- Comparison SLM vs standard process.

	Std.	SLM
Resistivity	$1 \Omega\text{cm}$	$0.1 \Omega\text{cm}$
Diameter	$\sim 3\mu\text{m}$	$\sim 1\mu\text{m}$
Diamond to graphite ratio	~ 4	~ 0.2



X-polariser image

64

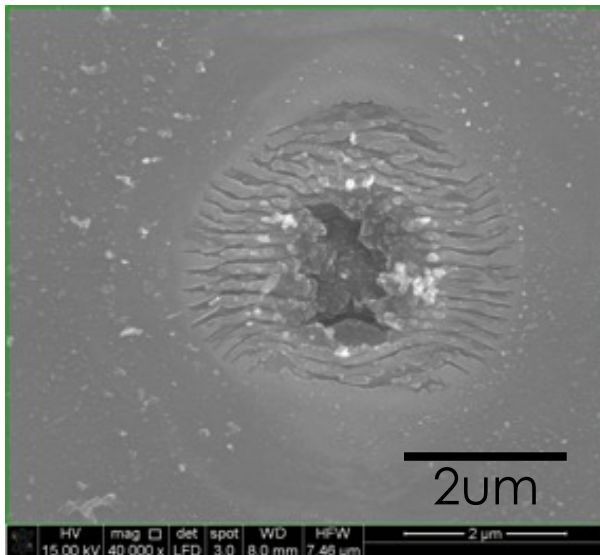


- Optical grade scCVD diamond.
- Post processing.

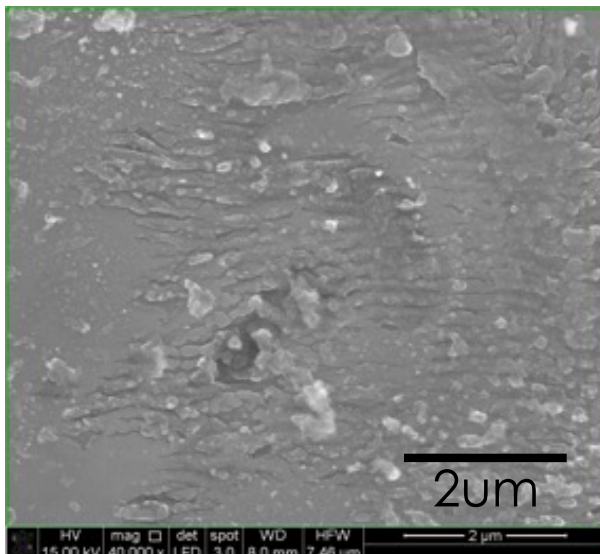
SEM surface image

65

- Seed surface

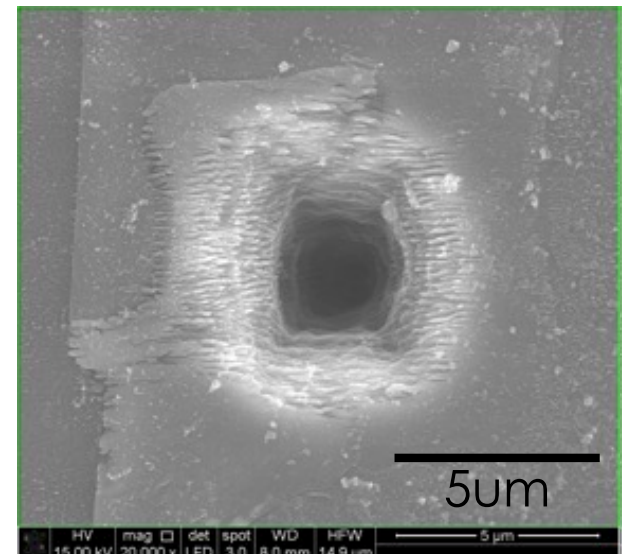
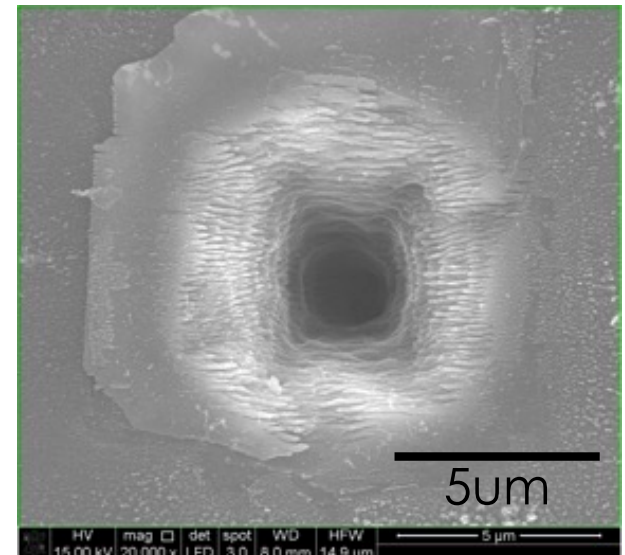


With SLM
10um/s
400nJ



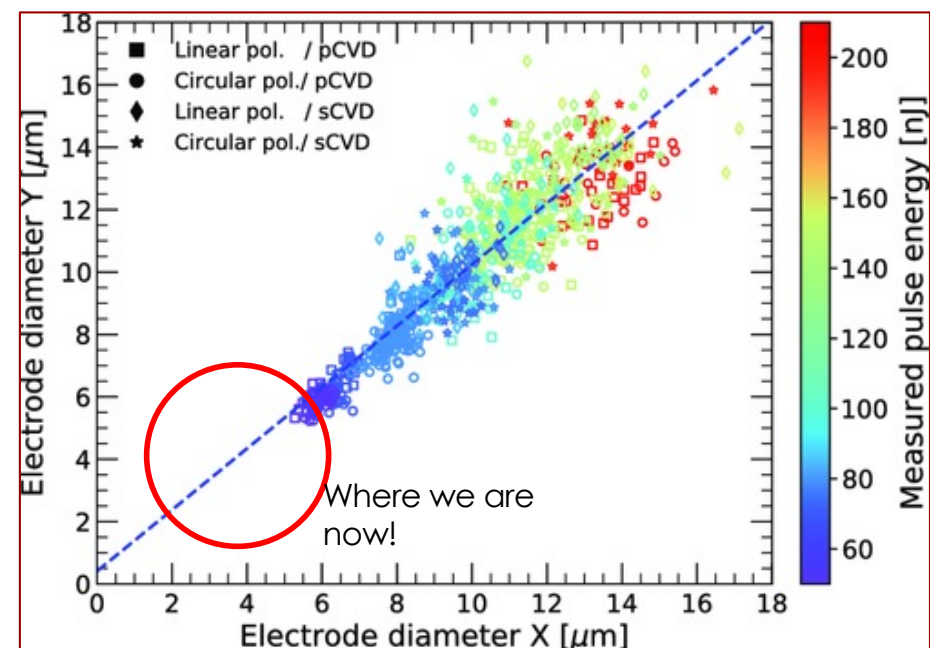
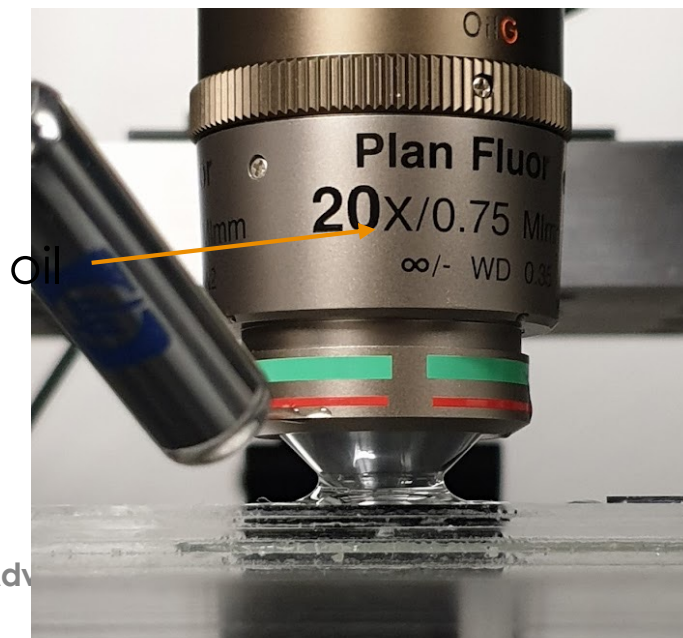
Without SLM
10um/s
400nJ

- Exit surface



Making the thinnest column

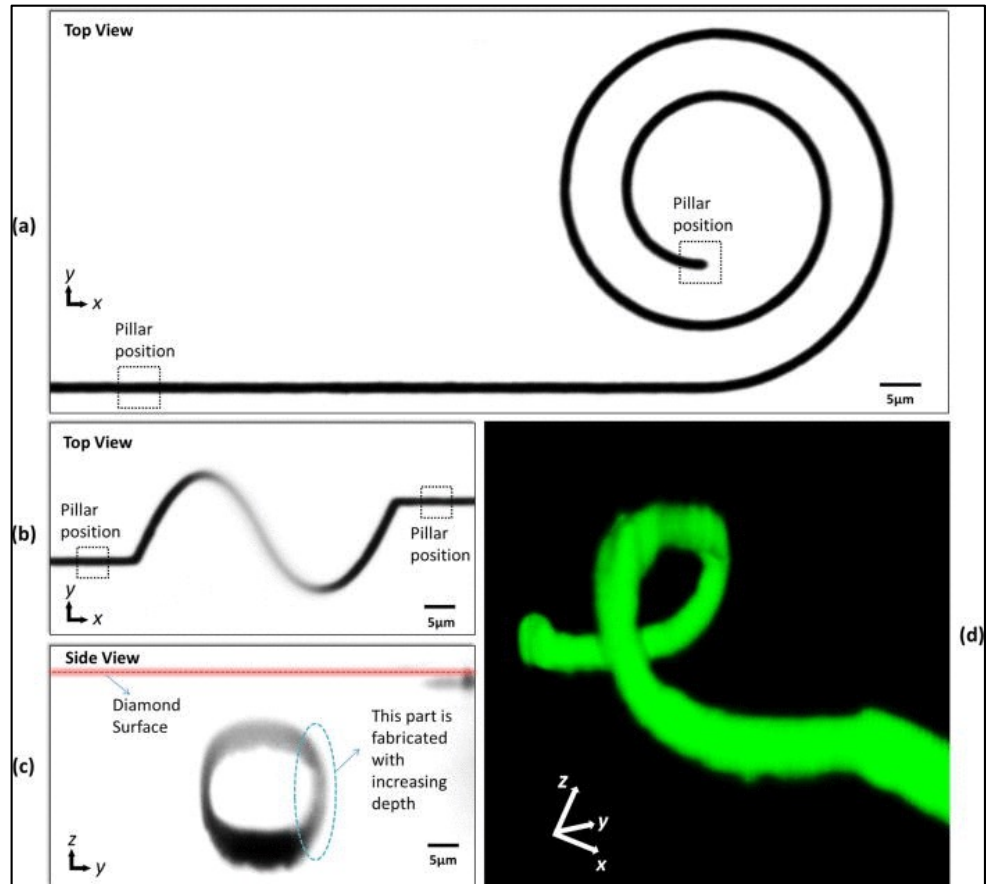
- More energy = thicker column
- Non-linear breakdown of diamond
 - More focused beam spot at depth makes thinner column
 - Immersion Oil helps to reduce refraction loss from air-diamond interface
 - SLM still key!



Lopez Paz, I., Allegre, O., Li, Z., Oh, A., Porter, A. and Whitehead, D. (2019), Study of Electrode Fabrication in Diamond with a Femto-Second Laser. *Phys. Status Solidi A*, 216: 1900236.

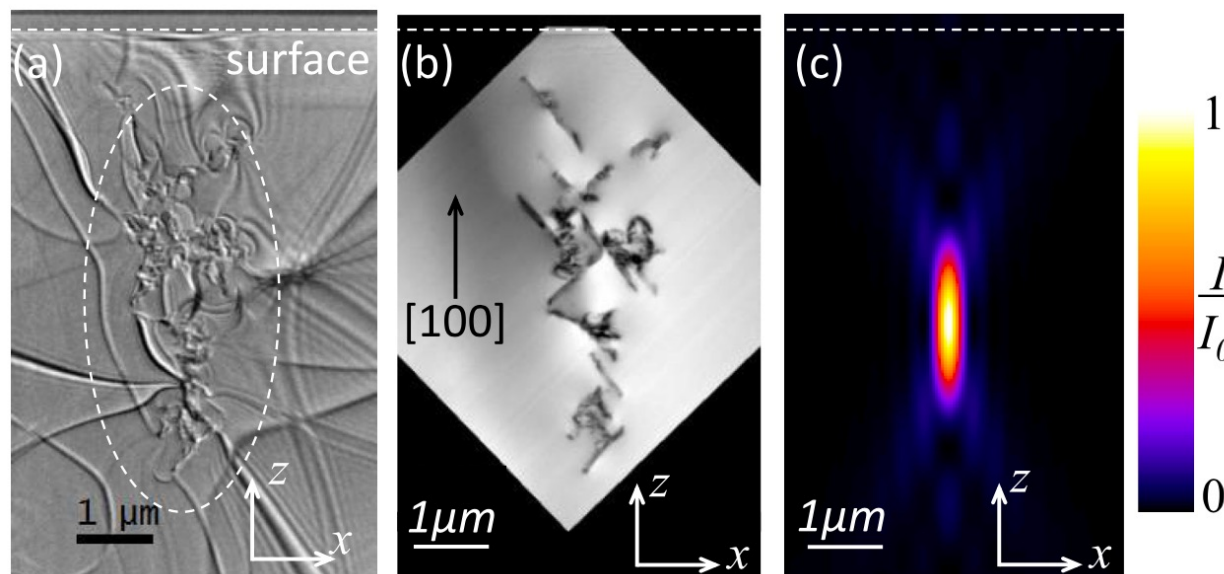
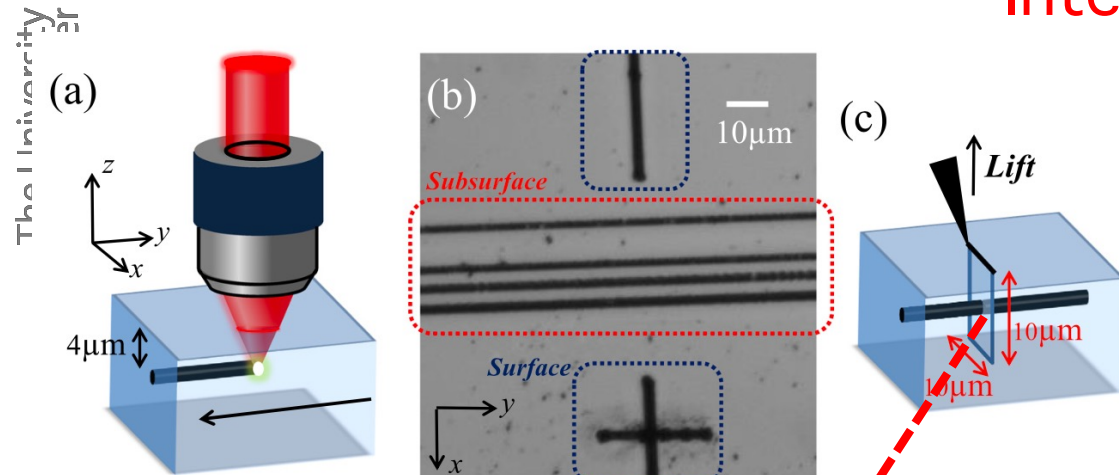
Moving sideways

- Also have the possibility to move in **arbitrary** direction
- Wavefront correction needs to be tailored in real-time
 - For vertical columns have mainly spherical corrections
 - For horizontal processing, the correction is ~elliptical
- Gets even trickier at depth $>200\mu\text{m}$



Sun, B., Salter, P. S., & Booth, M. J. (2014). High conductivity micro-wires in diamond following arbitrary paths. *Applied Physics Letters*, 105(23), 231105.

Internal structure



Patrick S. Salter et al.,
APPLIED PHYSICS LETTERS 111,
081103 (2017)

- Prepare sample with horizontal graphitic wires.
- STEM image of wire cross section.
- Optical and spectral data points to micro-cracks and nano-clusters of sp^2 bonded carbon.
- Micro wires are not macroscopic structures!

Parameter space scan

69

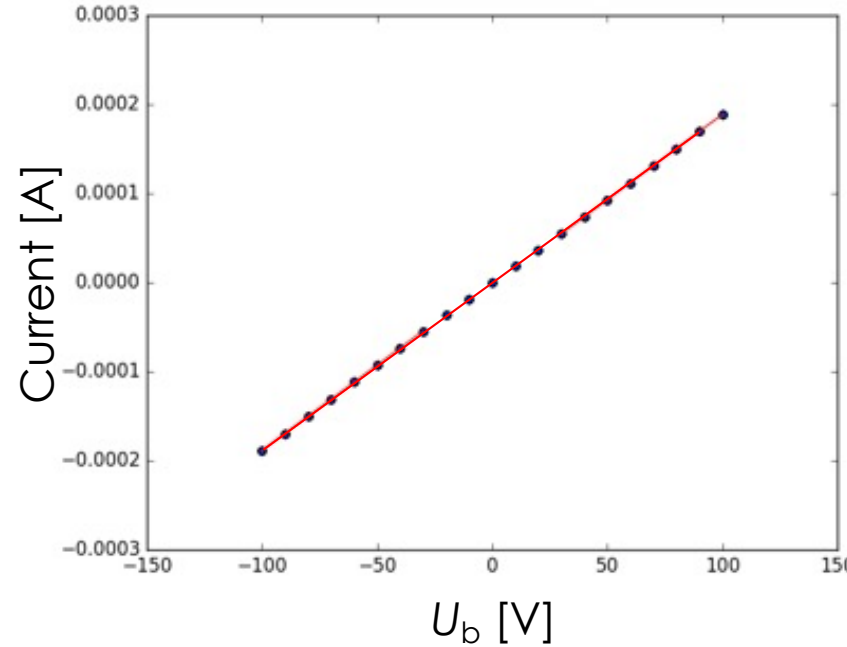
Patrick Salter, Oxford

Iain Haughton, AO, Manchester

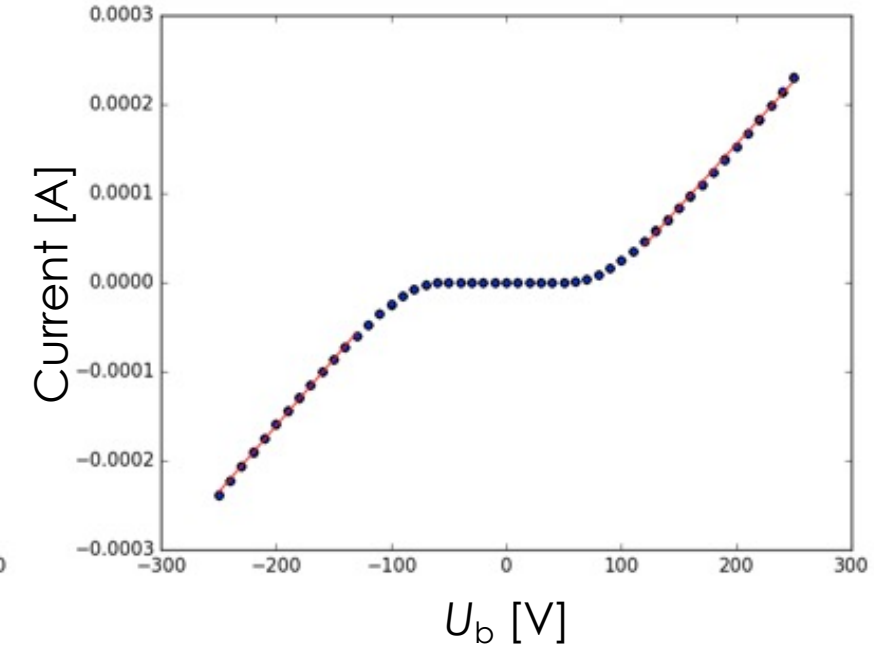
		Laser translation speed			
		5um/s	10um/s	20um/s	30um/s
Laser beam energy	100nJ	x	x		
	200nJ	x	x	x	
	300nJ		x	x	x
	400nJ		x	x	x
	500nJ			x	x
	600nJ				x

- Repeat **with** and **without** SLM correction.

- Ohmic and barrier potential curves observed.



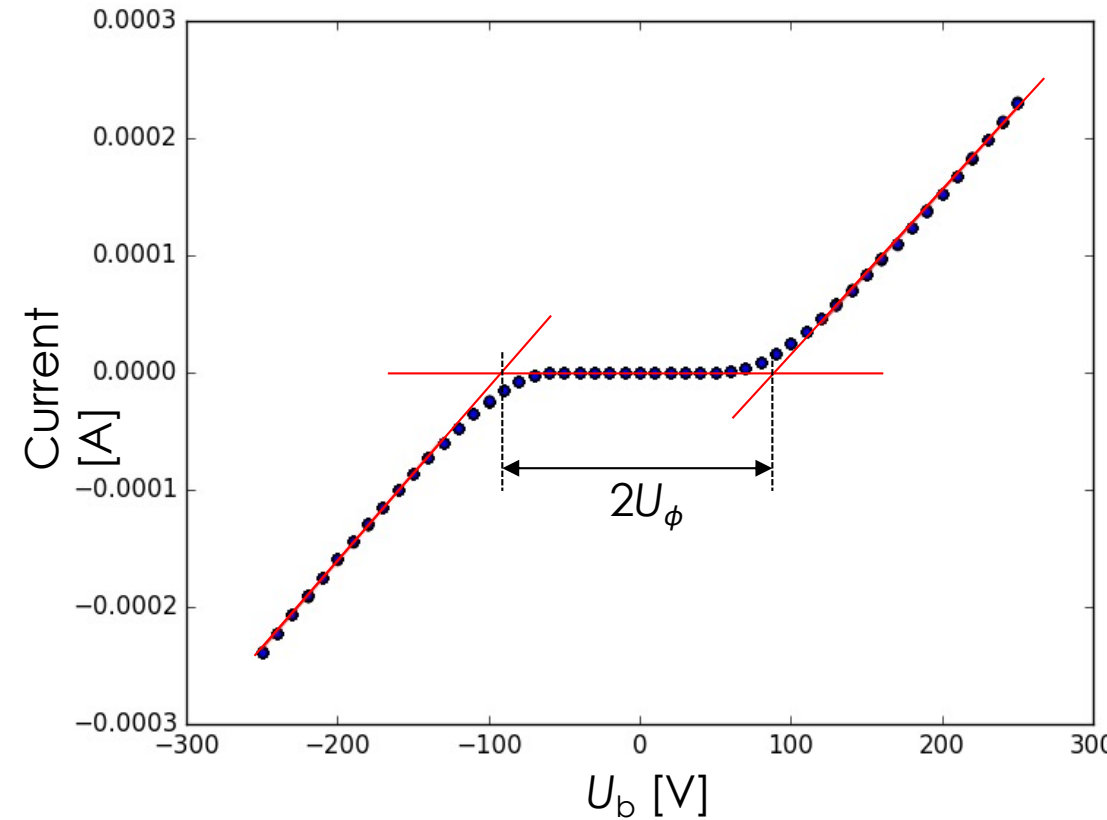
Continuous.



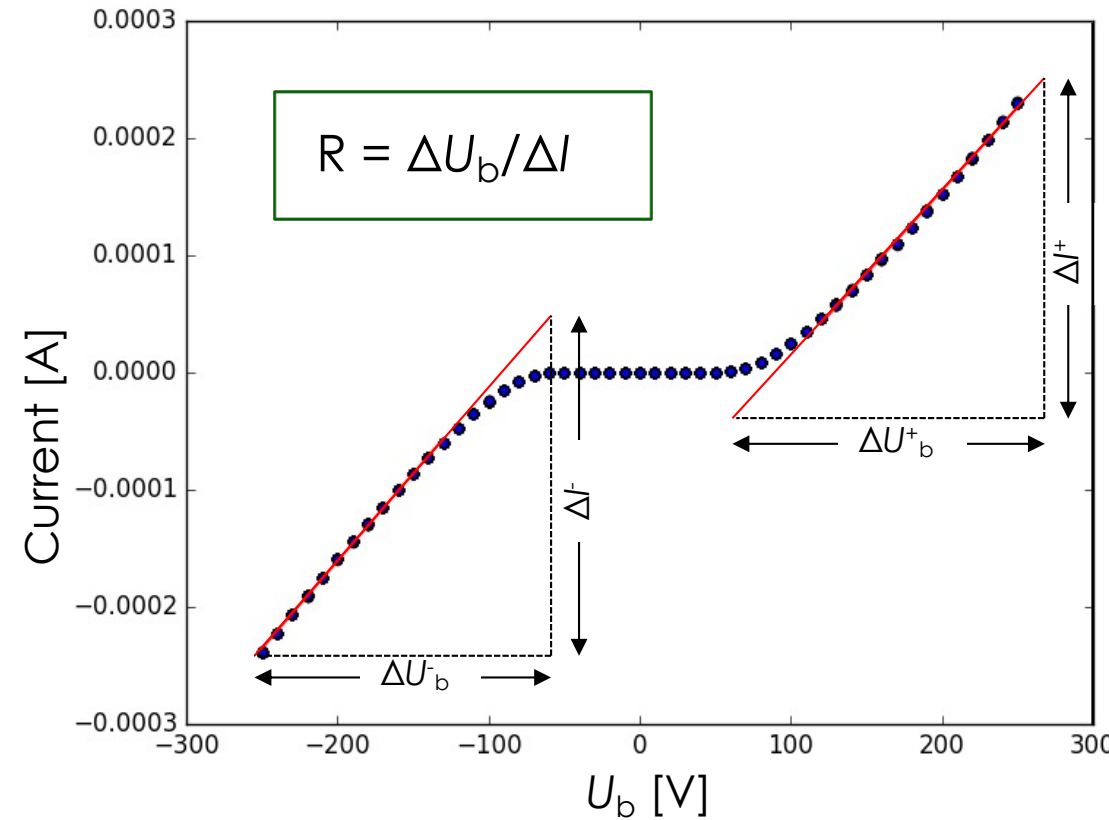
Bulk effect?
Micro gaps?

Barrier potential

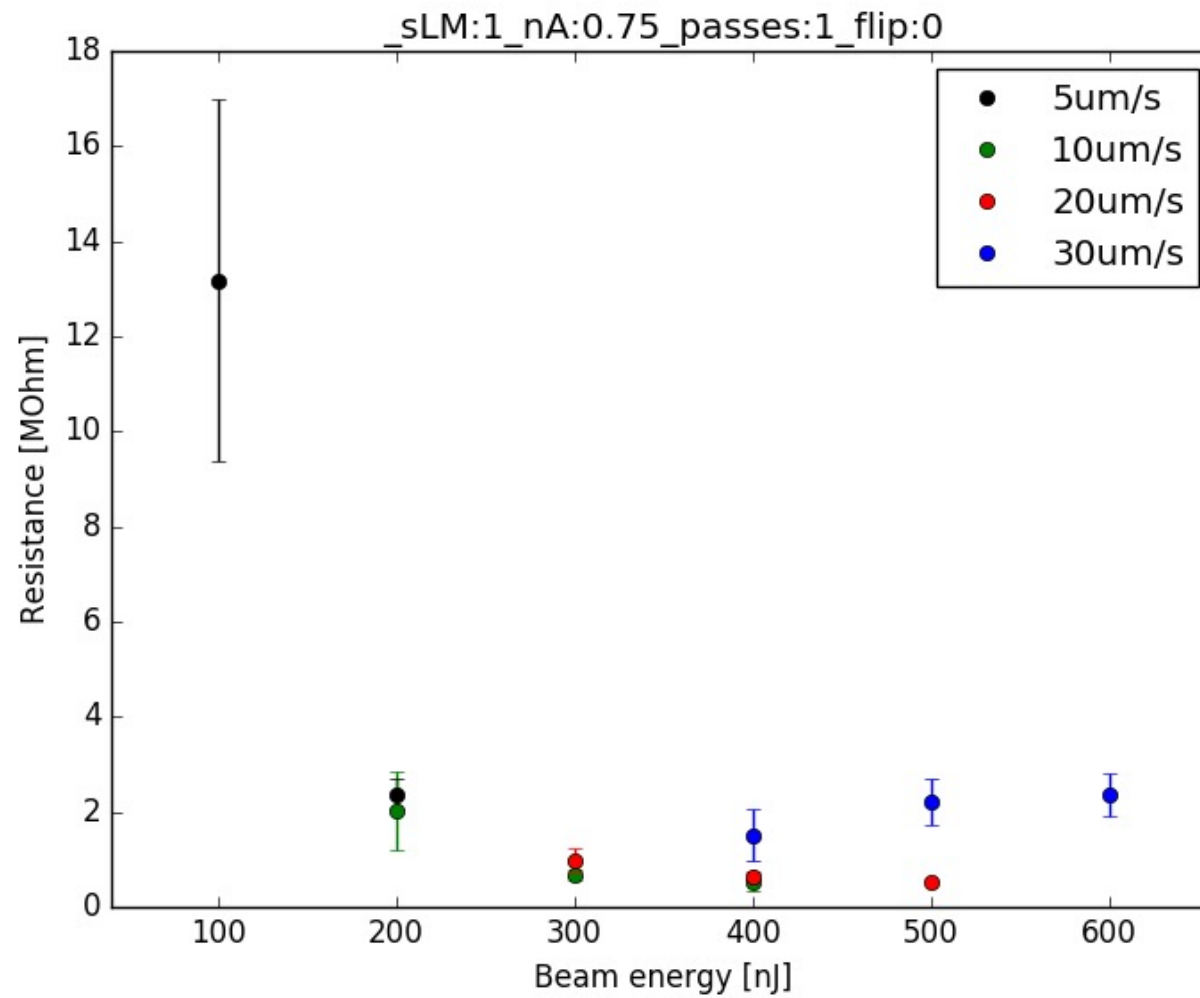
72



Resistance measurement

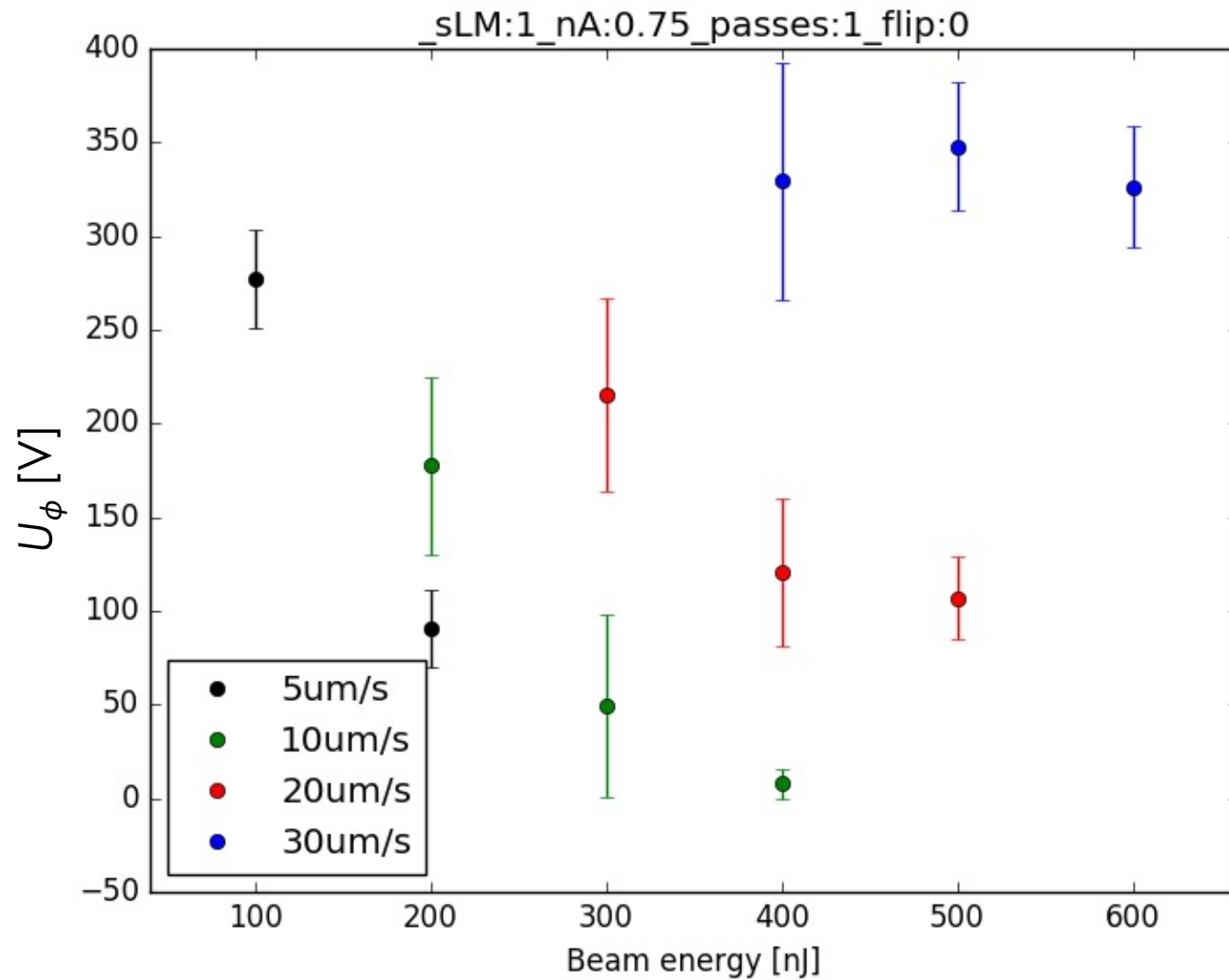


Resistance



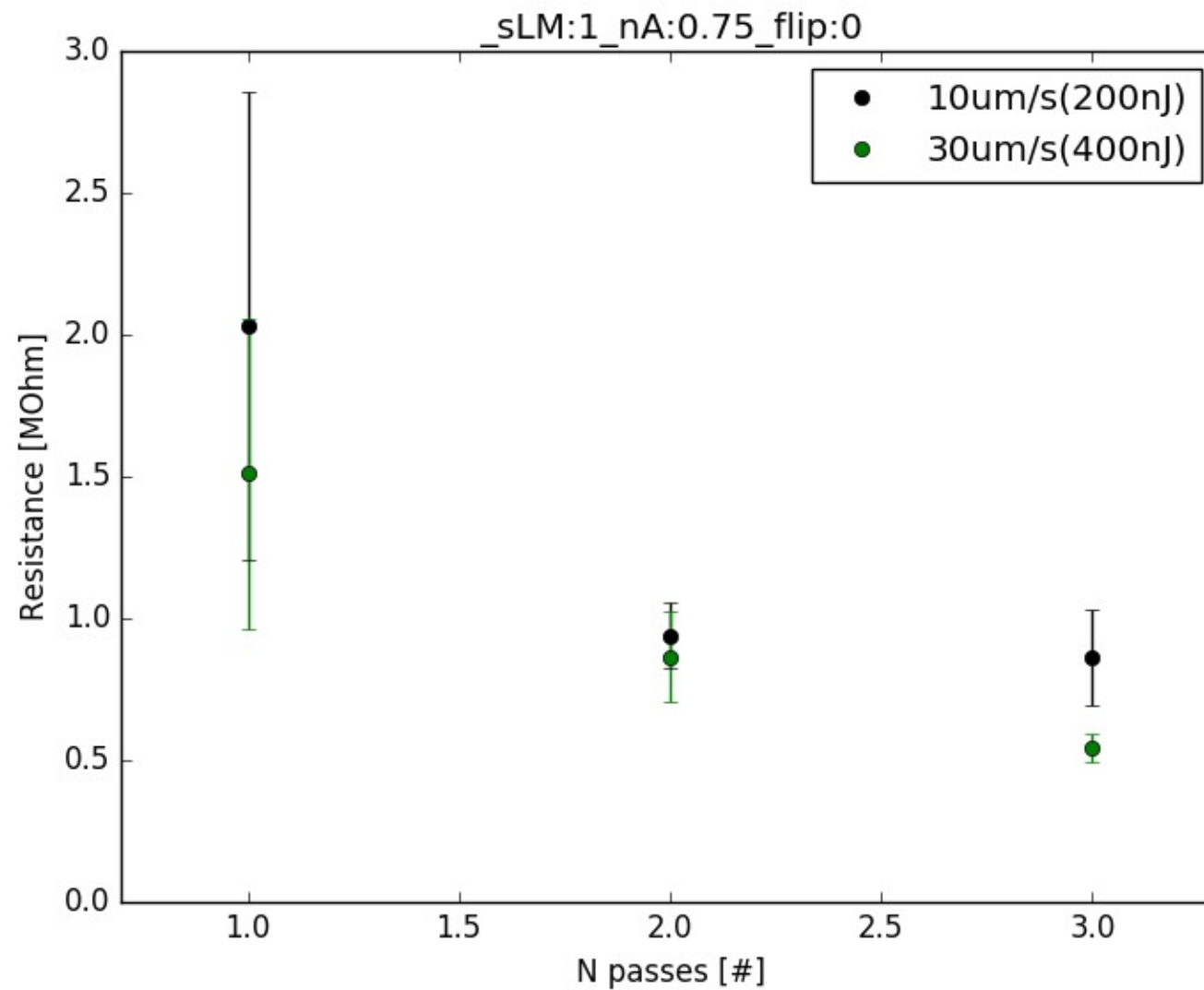
- Resistance increase as power law
→ multi-photon process.

Barrier energy



- Reduction in barrier with increased energy.
- Discrepancy at 30um/s.

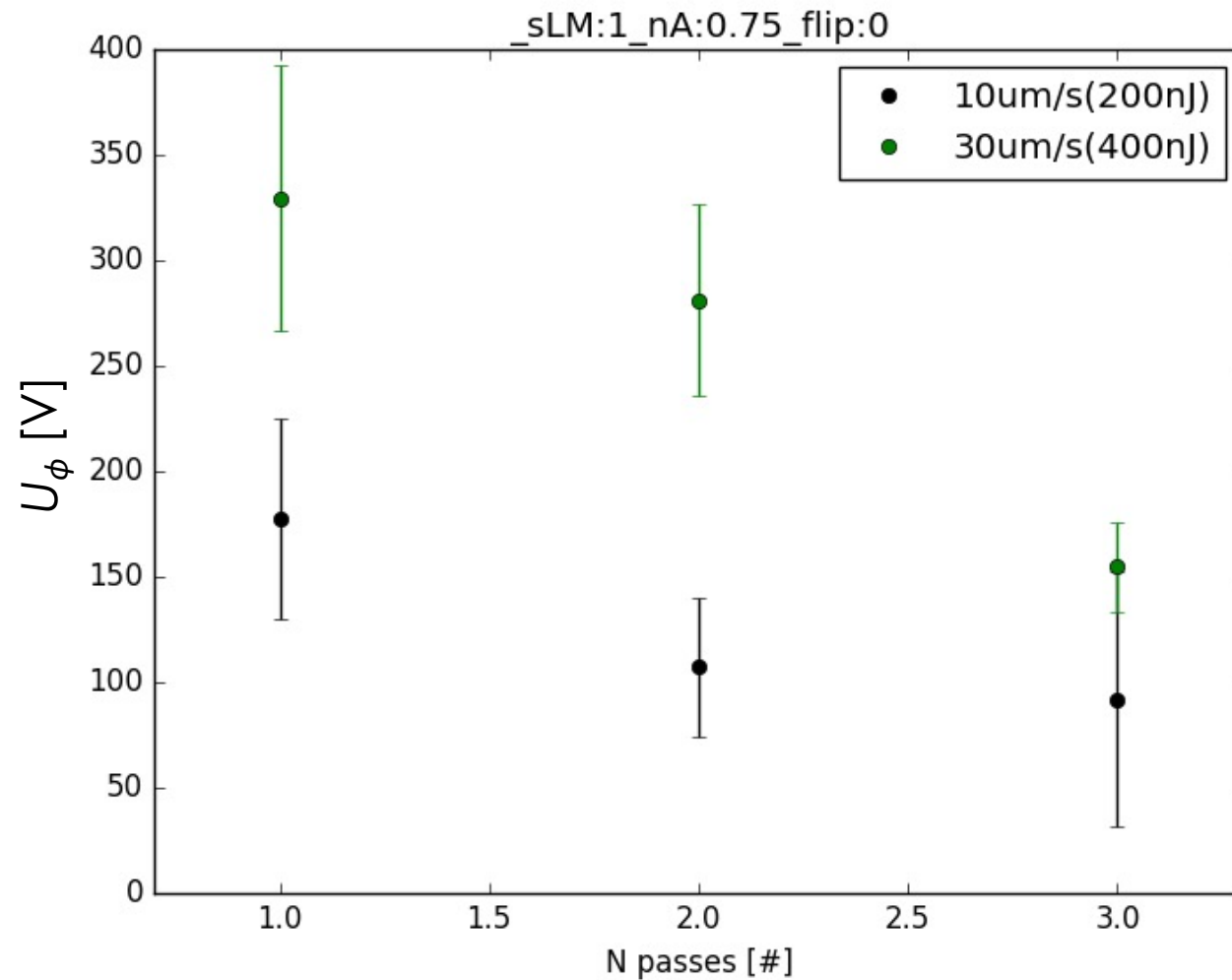
Multiple passes



- Multiple passes reduces resistance and increases uniformity of the columns.

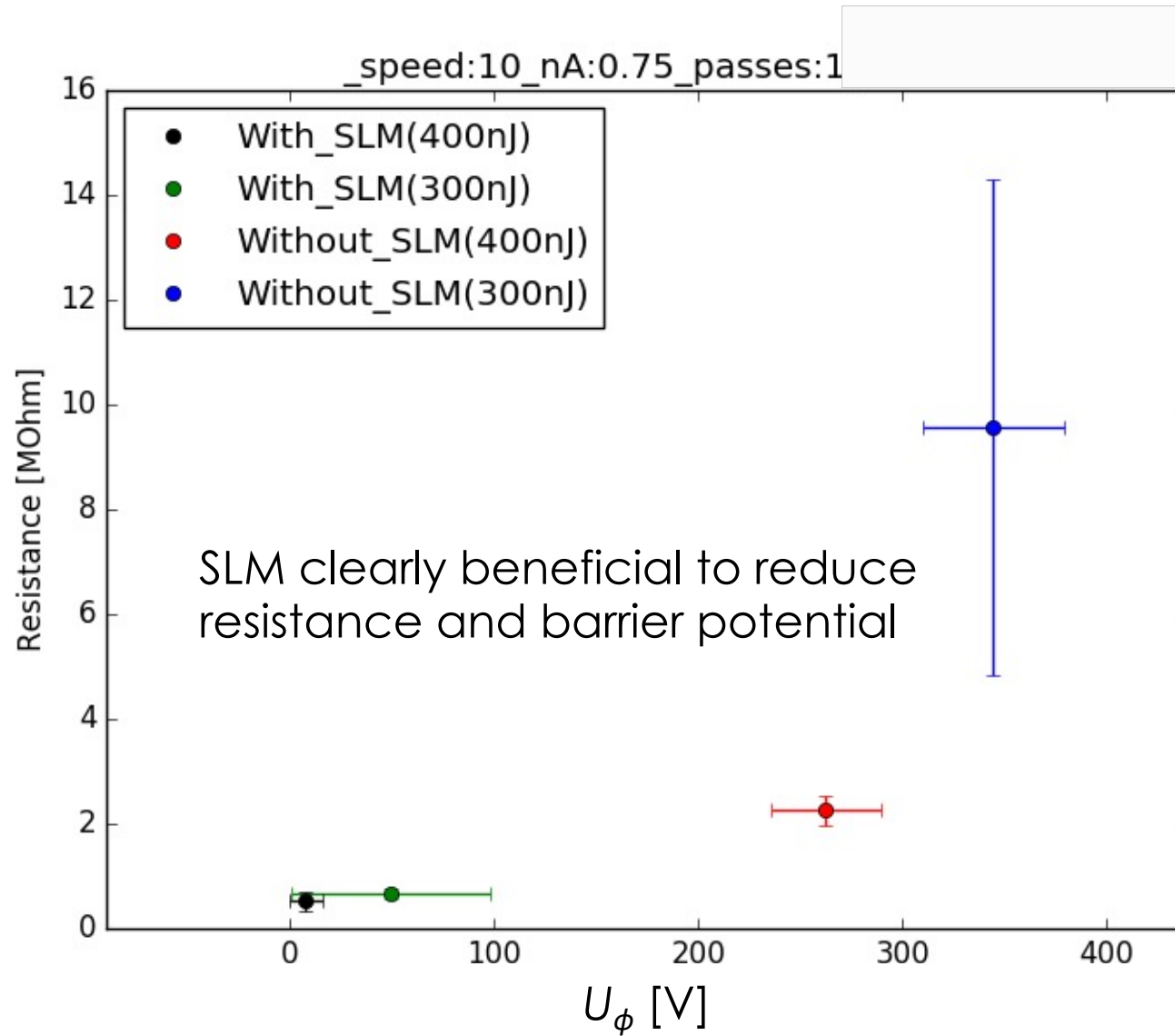
Multiple passes

80



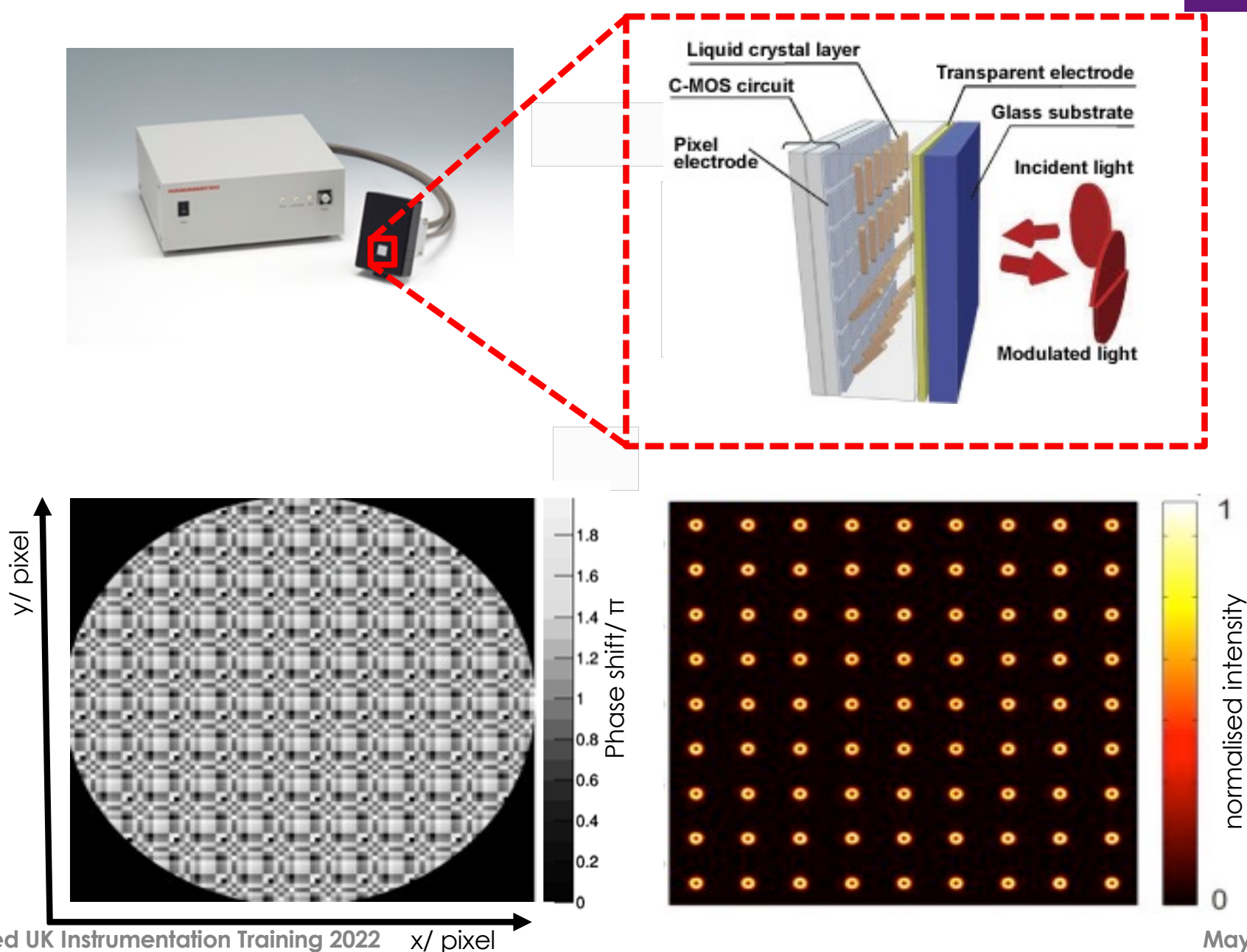
- Multiple passes also reduces U_ϕ .

With and without SLM



SLM parallel processing?

82



3D Diamond detector tests with relativistic charged particles

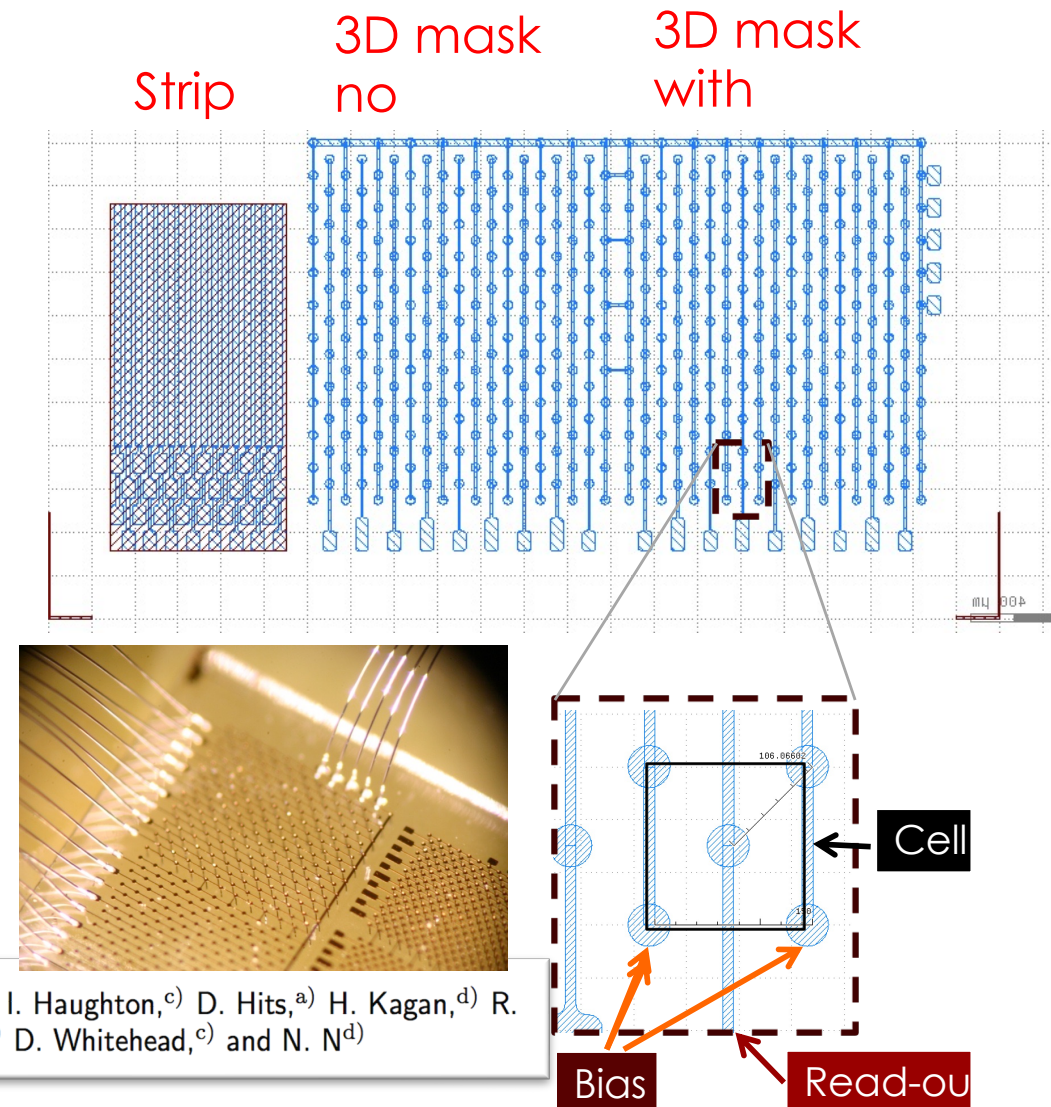
- Types
 - 100x100um cell size ganged to form strips
 - 100x100um cell size, bonded to pixel read-out
 - 50x50um cell size, bonded to pixel read-out
- All detectors made from polycrystalline diamond.
- Beam tests
 - CERN beam line H6 : protons $\sim 120 \text{ GeV}/c$
 - PSI : pions $\sim 250 \text{ MeV}/c$

Thanks for material from the RD42 collaboration!

3D Diamond prototype

■ Proto-type

- Strip detector with back side contact
 - 3D metal only pattern
 - 3D metal + graphitic columns
 - Cubic cell base size $150\mu\text{m}$
 - 99 cells
-
- Measure response with 120 GeV protons.
 - Paper published NIMA "A 3D diamond detector for particle tracking", NIM A, 786 (2015)

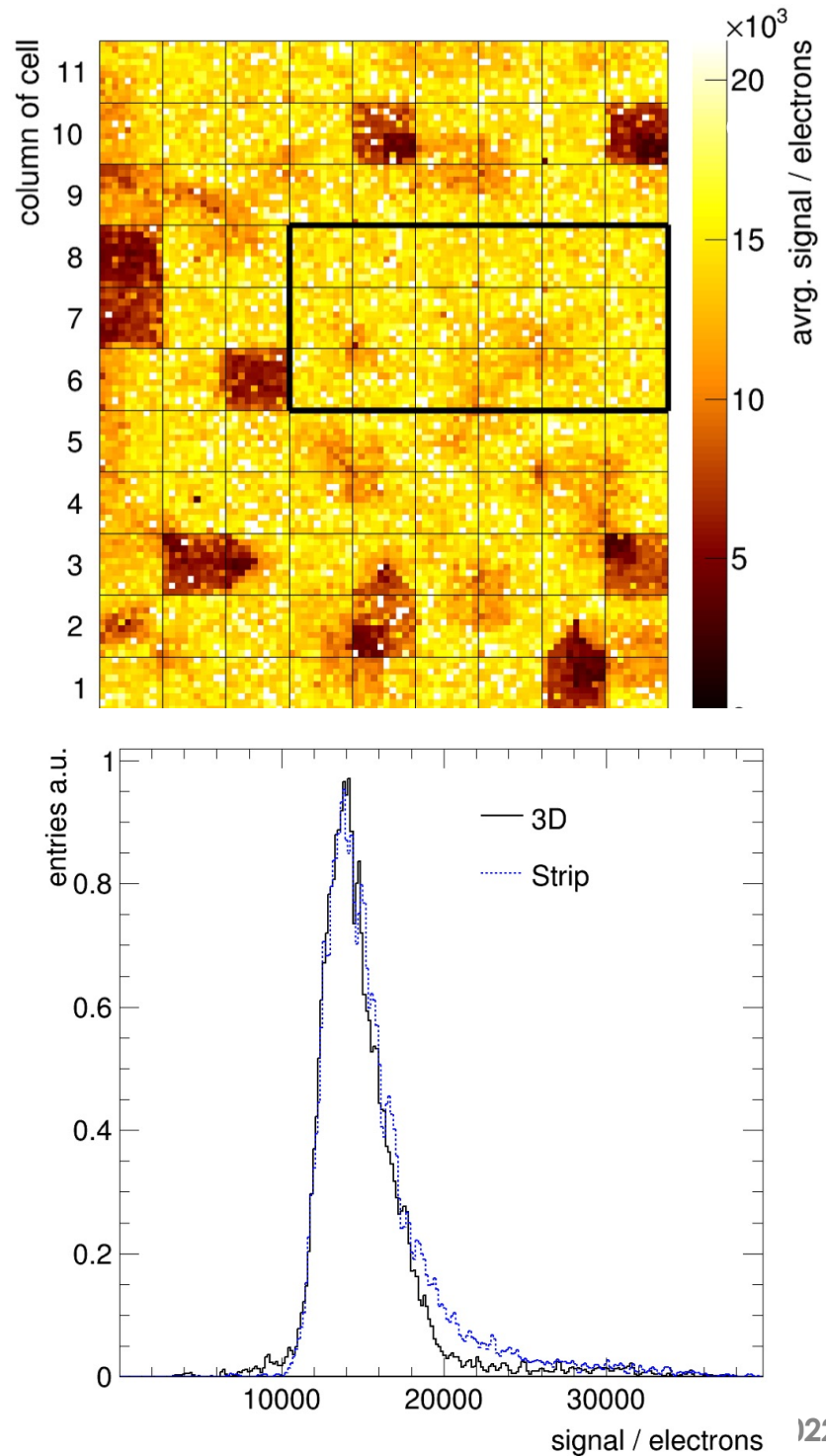


F. Bachmair,^{a)} L. Baeni,^{a)} P. Bergonzo,^{b)} B. Caylar,^{b)} G. Forcolin,^{c)} I. Haughton,^{c)} D. Hits,^{a)} H. Kagan,^{d)} R. Kass,^{d)} L. Li,^{c)} A. Oh,^{c)} M. Pomorski,^{b)} V. Tyzhnevyyi,^{c)} R. Wallny,^{a)} D. Whitehead,^{c)} and N. Nd^{d)}

Analysis steps

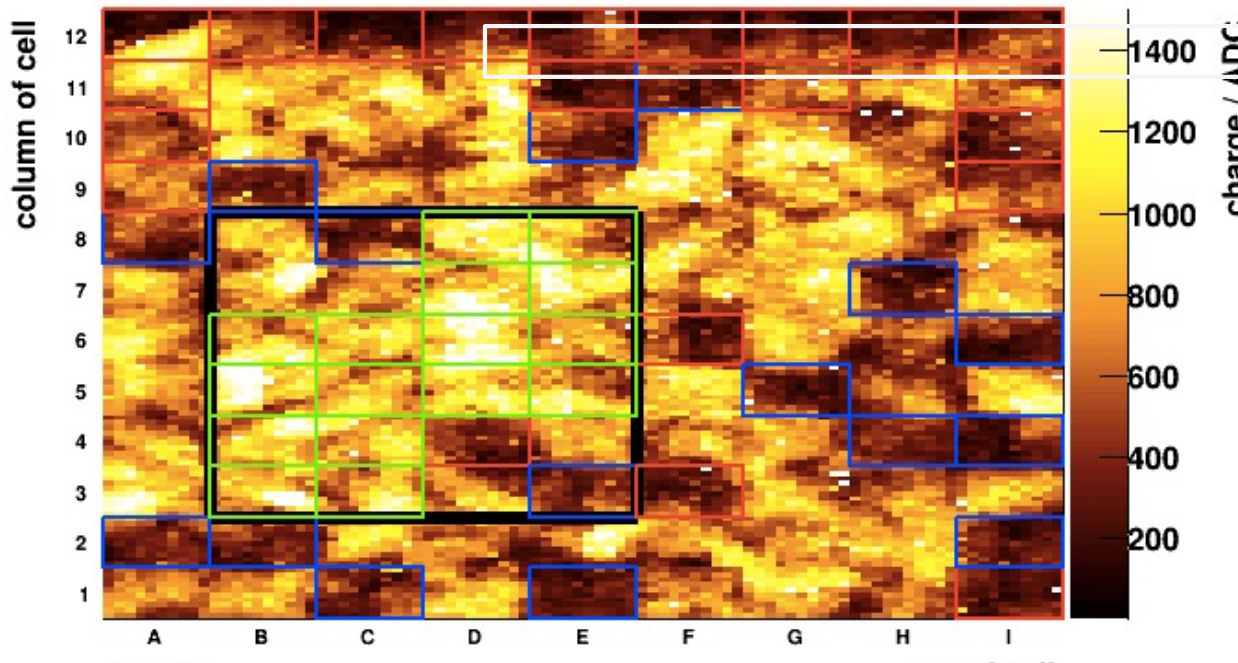
- $U_b(3D)=40V$
- $U_b(\text{strip})=500V$
- Identify **continuous region** of intact cells for analysis.
- Exclude contribution of negative signals.
- **Average charge**
Strip: 16.8ke
3D: 15.9ke
- **MP:**
Strip: 14.7ke
3D: 15ke

3D and Strip show comparable response.
Conclusion -> 3D works!



Test of first 3D pCVD diamond detectors

hPulseHeightVsDetectorHitPostionXY_trans

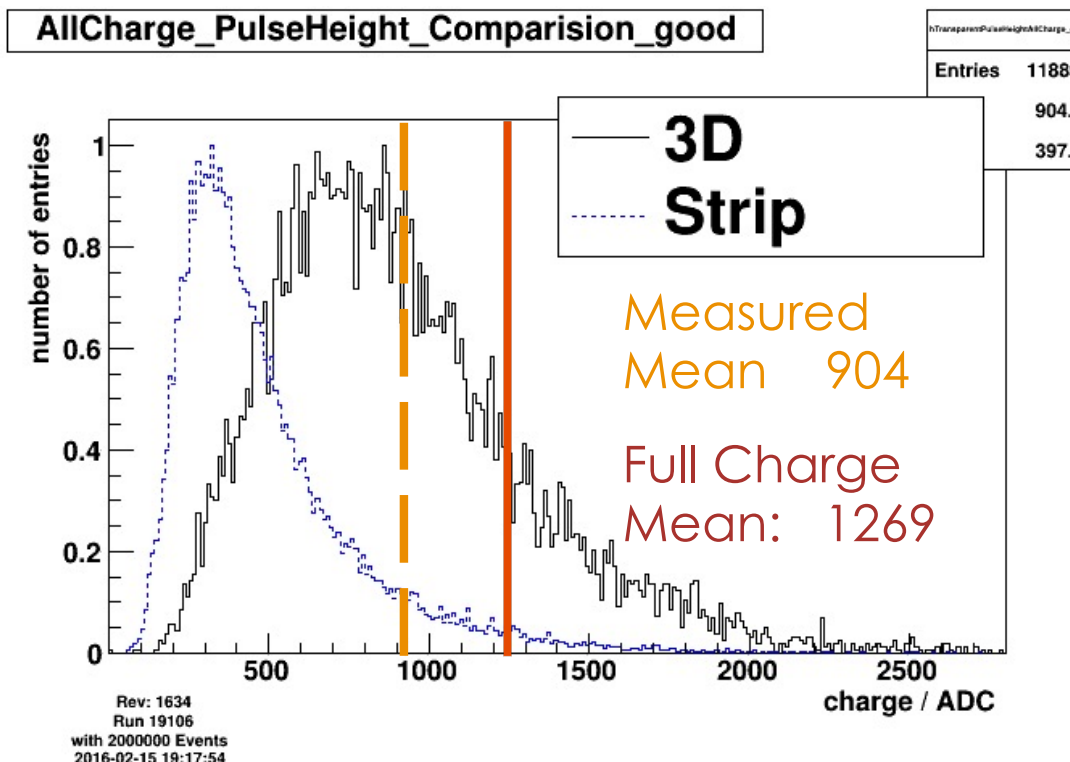


Rev: 1549
Run 19106
with 2000000 Events
2016-02-02 13:34:21

- $U_b(3D)=75V$
- $U_b(\text{strip})=500V$
- Selected 16 adjacent cells

Test of first 3D pCVD diamond detectors

- Red line estimate the Mean for Full Charge Collection (100%)



71% of Full Charge Collection, corresponding to ~13 ke.

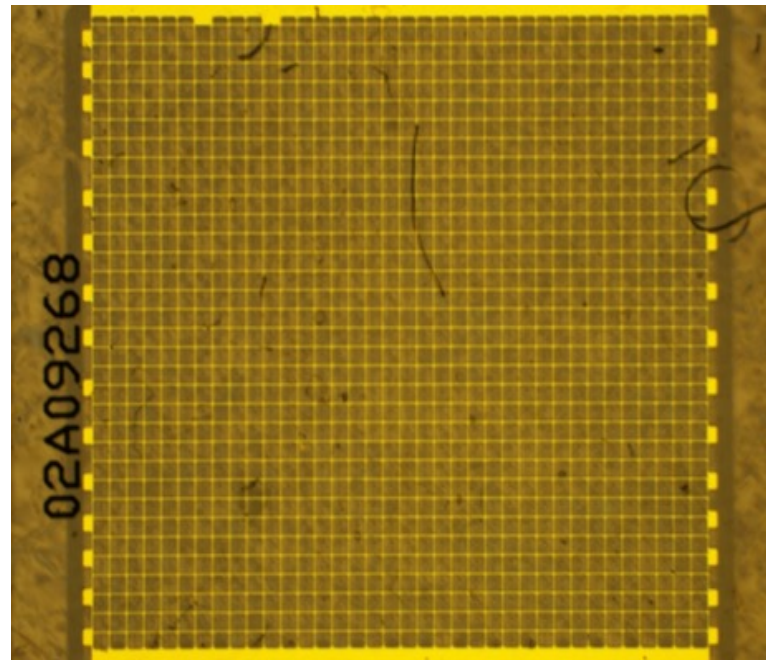
Highest charge collection ever measured for pCVD diamonds

Large area 3D, pCVD, 100x100

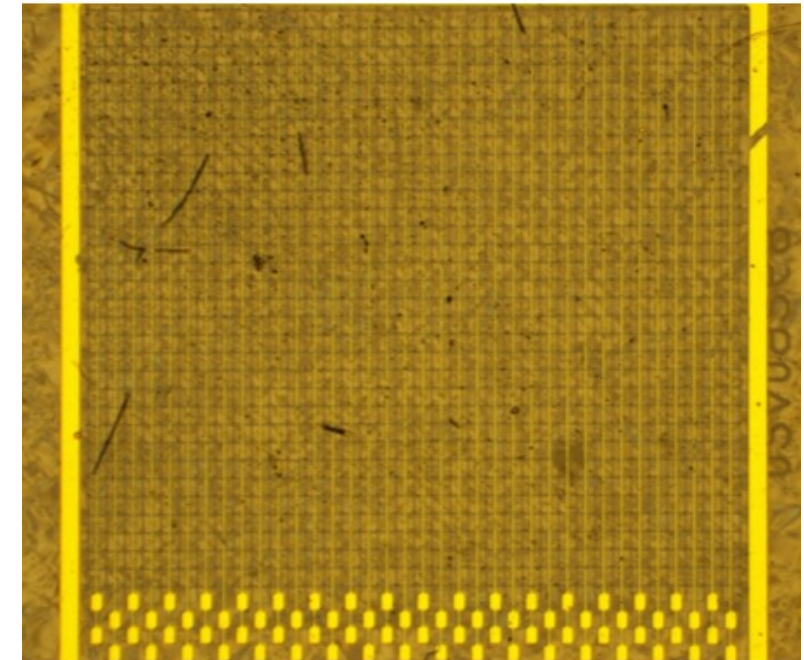
In May/Sept 2016 tested the first full 3D device fabricated in pcCVD with three dramatic improvements:

1. An order of magnitude more cells (1188 vs 99).
2. Smaller cell size (100um vs 150um).
3. Higher column production efficiency (>99% vs ~90%).

HV side

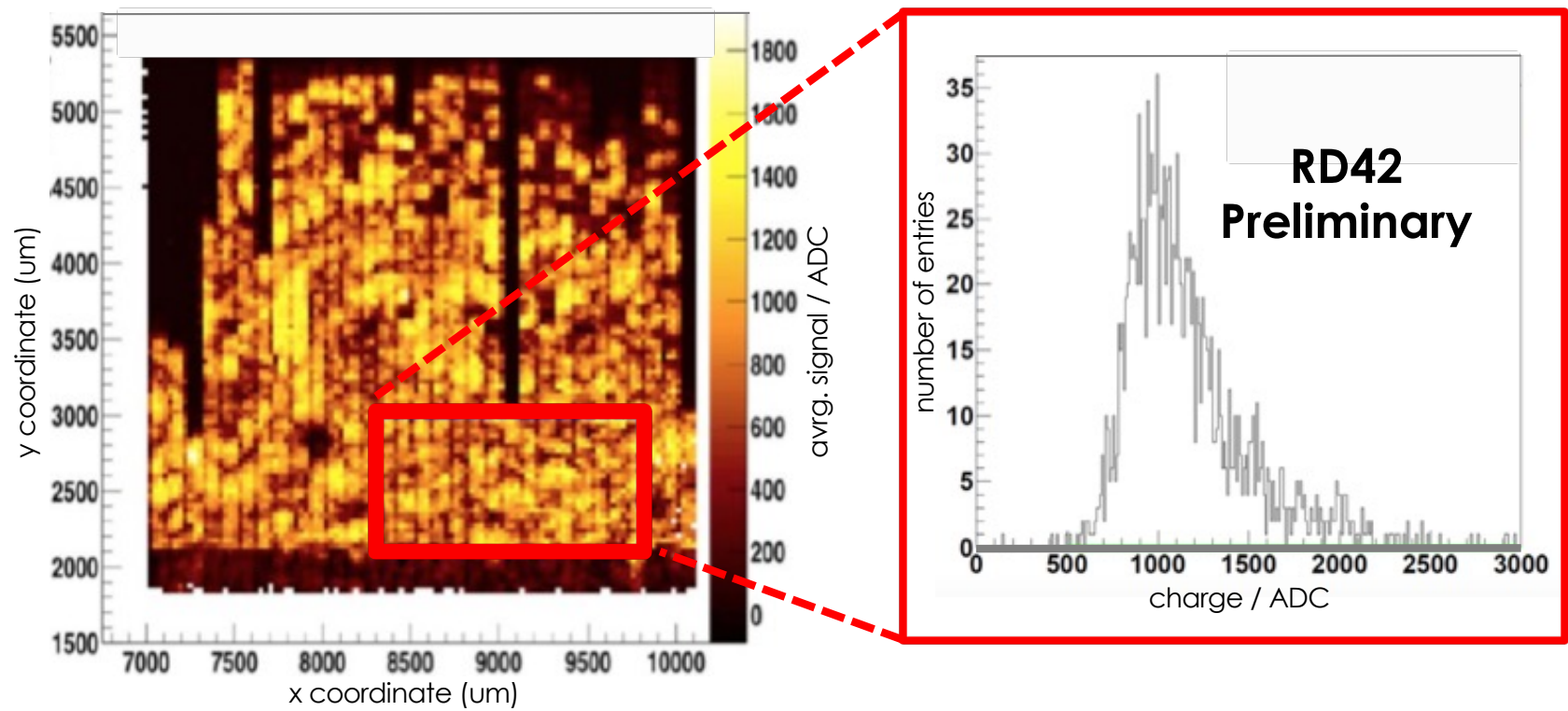


Readout side

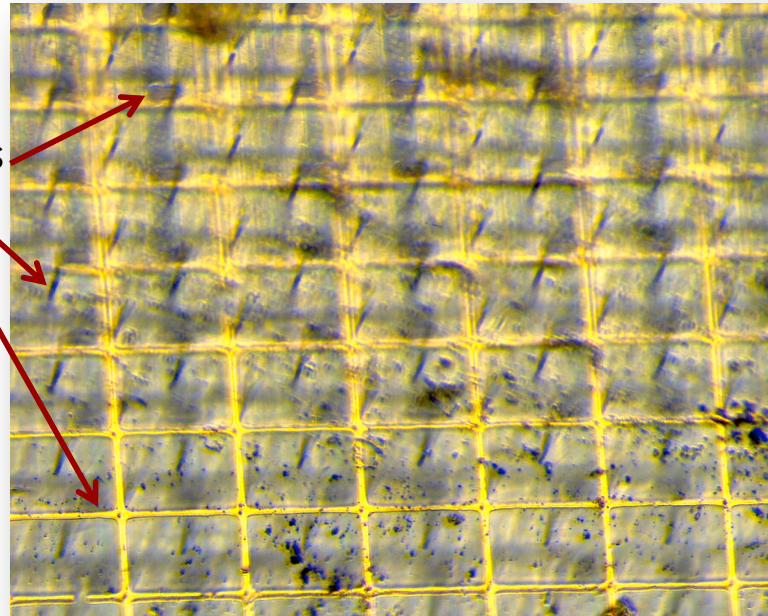


Large area 3D, pCVD, 100x100

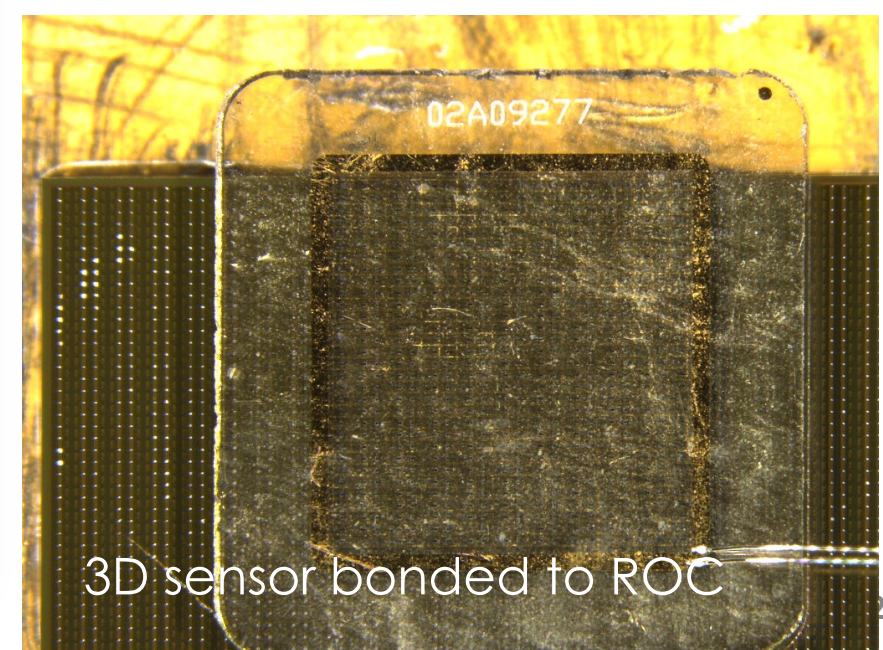
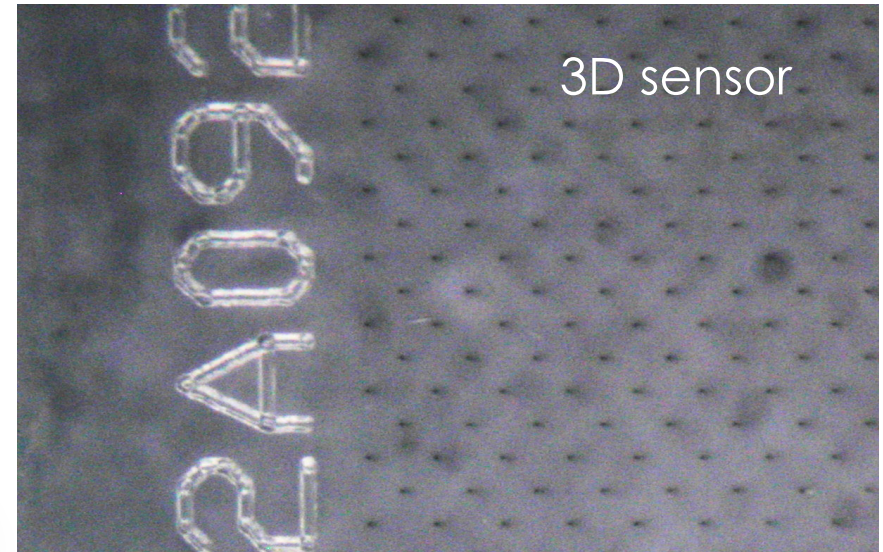
- Largest charge collection to date in pcCVD diamond!
 - >85 % of charge collected in continuous region, about twice as much as planar.



- First assembly with ROC chip produced.
 - Bump bonded in Princeton.
 - Cr-Au on bias side.
 - Ti-W under-bump metal.
 - Indium bumps on sensor.

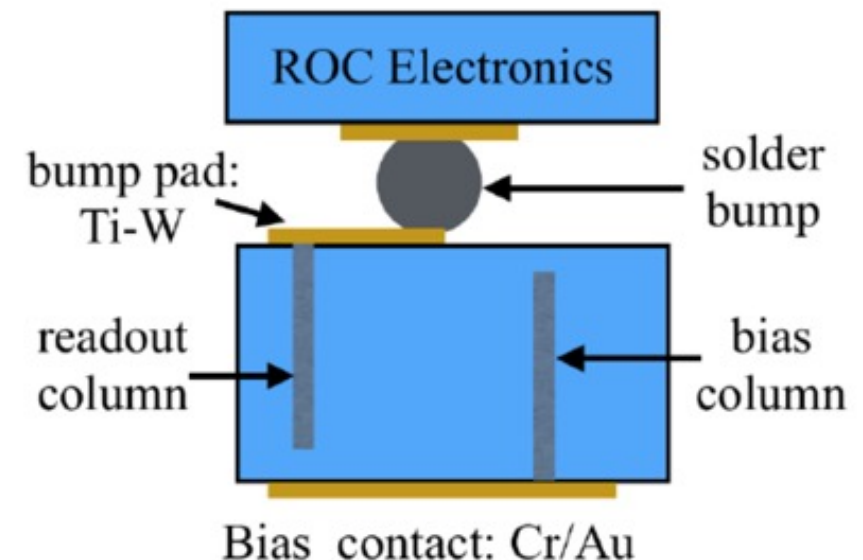
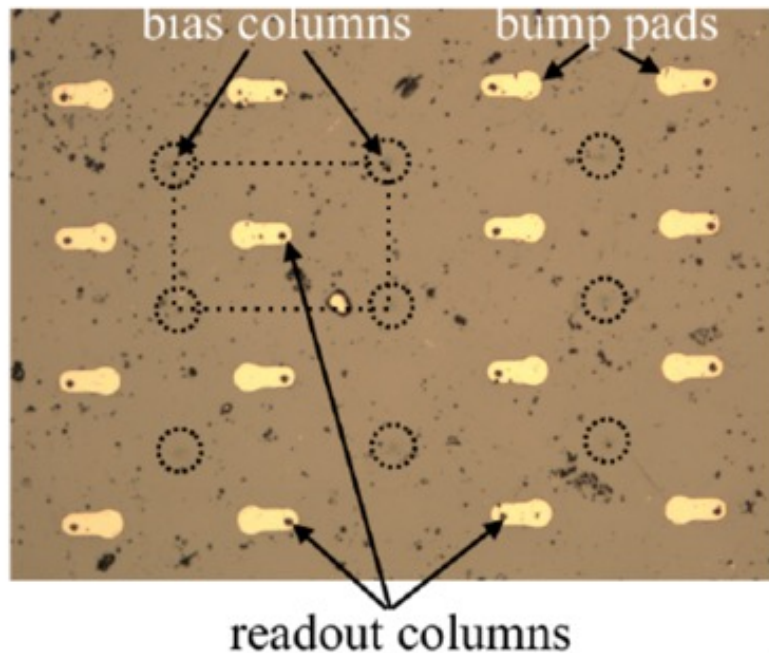


Advanced UK Instrumentation Training 2022



Pixel 3D, pCVD, 100x100

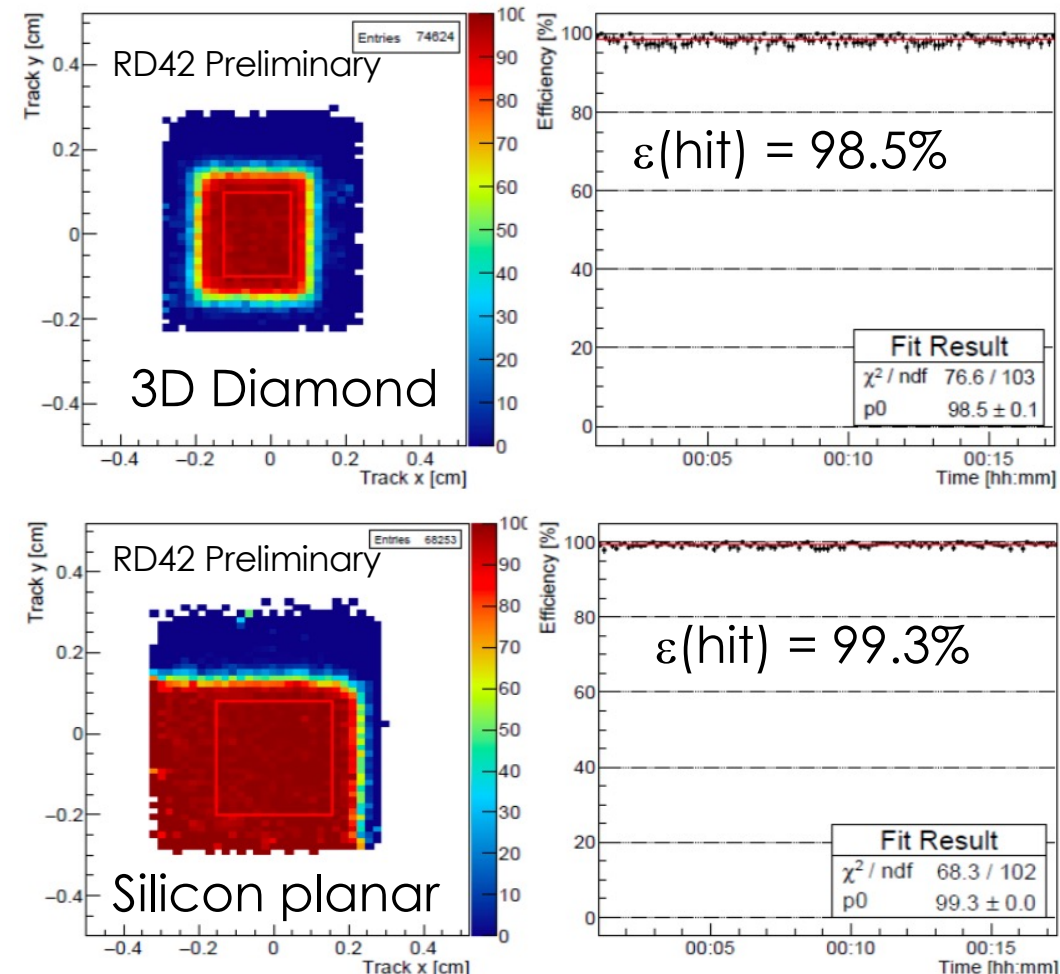
- Production of first pixel device using CMS readout electronics.



- Active region 3x3 mm with cell size ~100x100 μm .

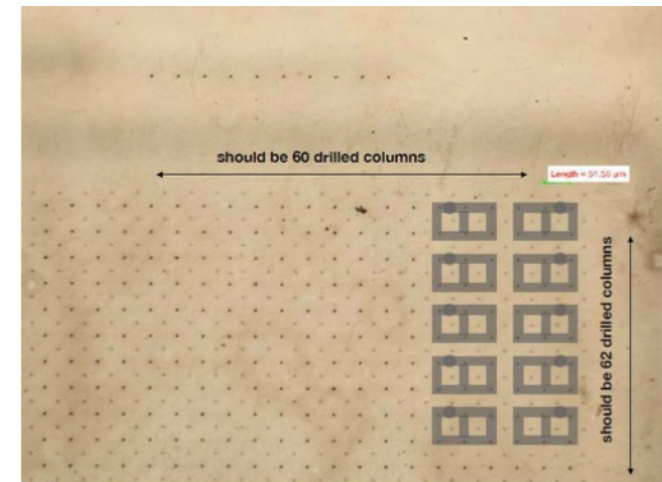
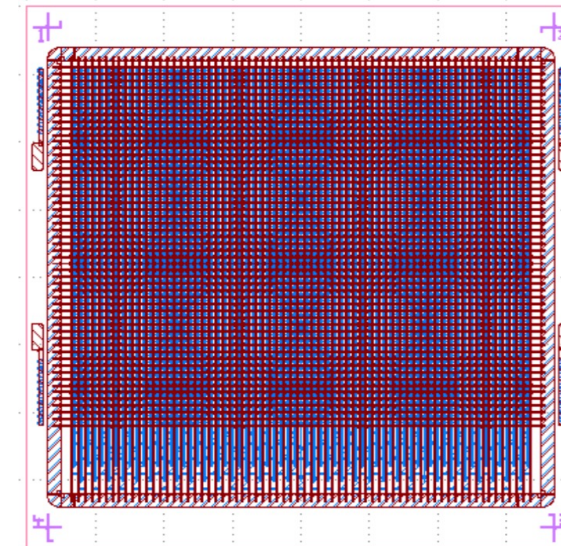
Pixel 3D, pCVD, 100x100

- 3D diamond device and Silicon reference planar device.
- Pixel threshold 1500e.
- Check hit efficiency over time.
- Device works!



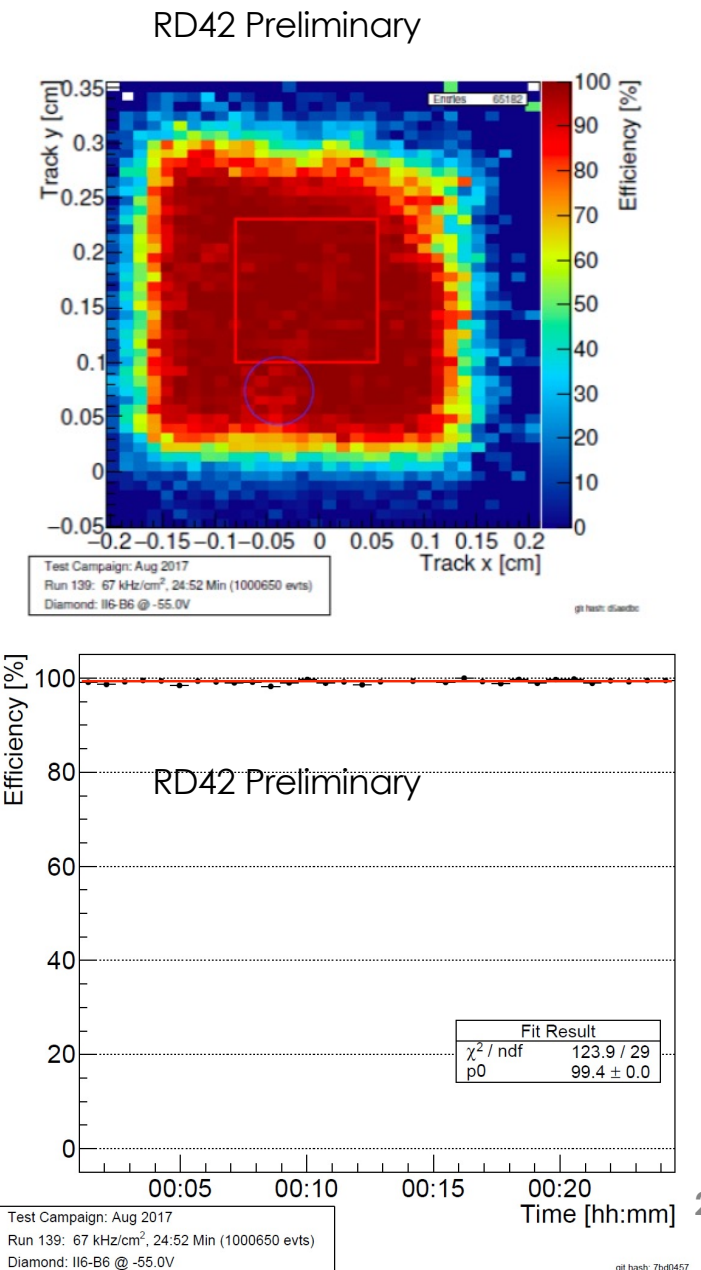
Next generation 3D Diamond

- Produced 3500 Cell pixel prototype, 50x50um cell size.
- Sample production:
 - Oxford (2x cubic cells)
 - Manchester set-up in progress (expected production date end of month.)
 - Bump bonding
 - For ROC (CMS) Princeton.
 - For FE-I4 (ATLAS) IFAE.
- Data taking in August 2017 at PSI.



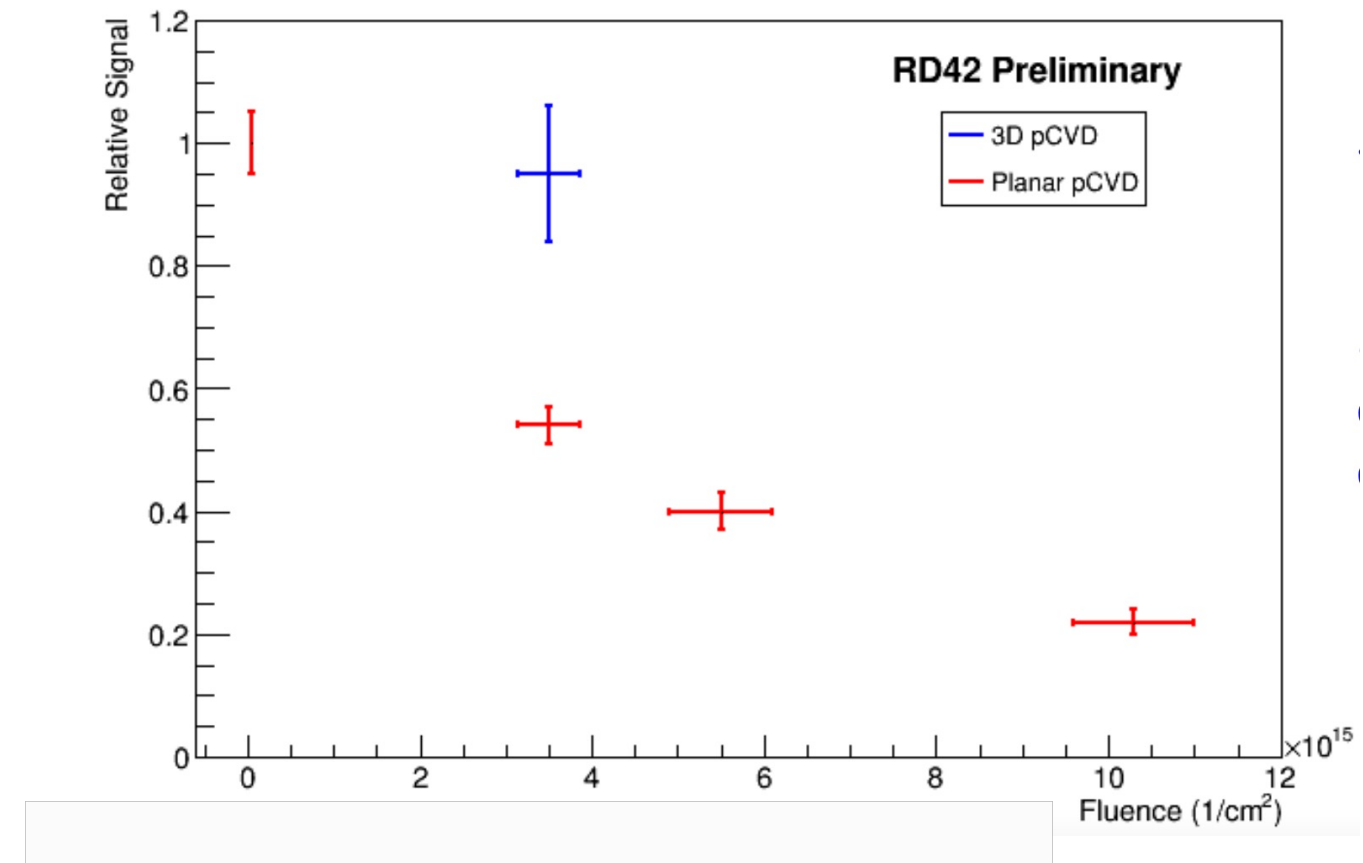
First 50x50 μm cell 3D Diamond (2017)

- Readout with CMS pixel readout.
- Bump bonding issue in upper right edge (Indium bump deposition machine not working properly)
- 6 columns (3x2) ganged together.
- Preliminary hit efficiency **99.2%**
- Preliminary:
Collect **>90%** of charge!
- Rate dependence tested with 10 kHz/cm⁻² and 10 MHz/cm⁻² ->
no dependence observed.



3D diamond radiation tolerance

- Tested a 3D device irradiated to 3.5×10^{15} p/cm² and compare to a planar diamond device at same fluence.
- Signal reduction:
Planar $45 \pm 5\%$
3D $5 \pm 10\%$
- Assuming scaling is similar 3D should operate at 10×10^{15} p/cm²



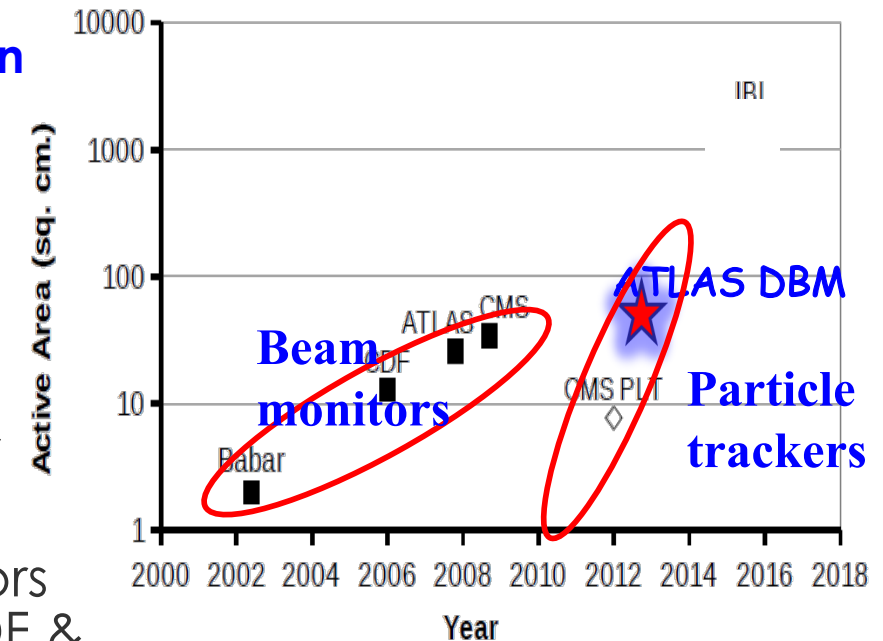
Applications in HEP

Applications in HEP

- Vertex detectors with CVD Diamond are not considered yet as an option for LHC.
- For Beam monitoring CVD Diamond is used at CMS and ATLAS at the LHC.
- BaBar and Belle test already CVD Diamond in their beam monitoring system.

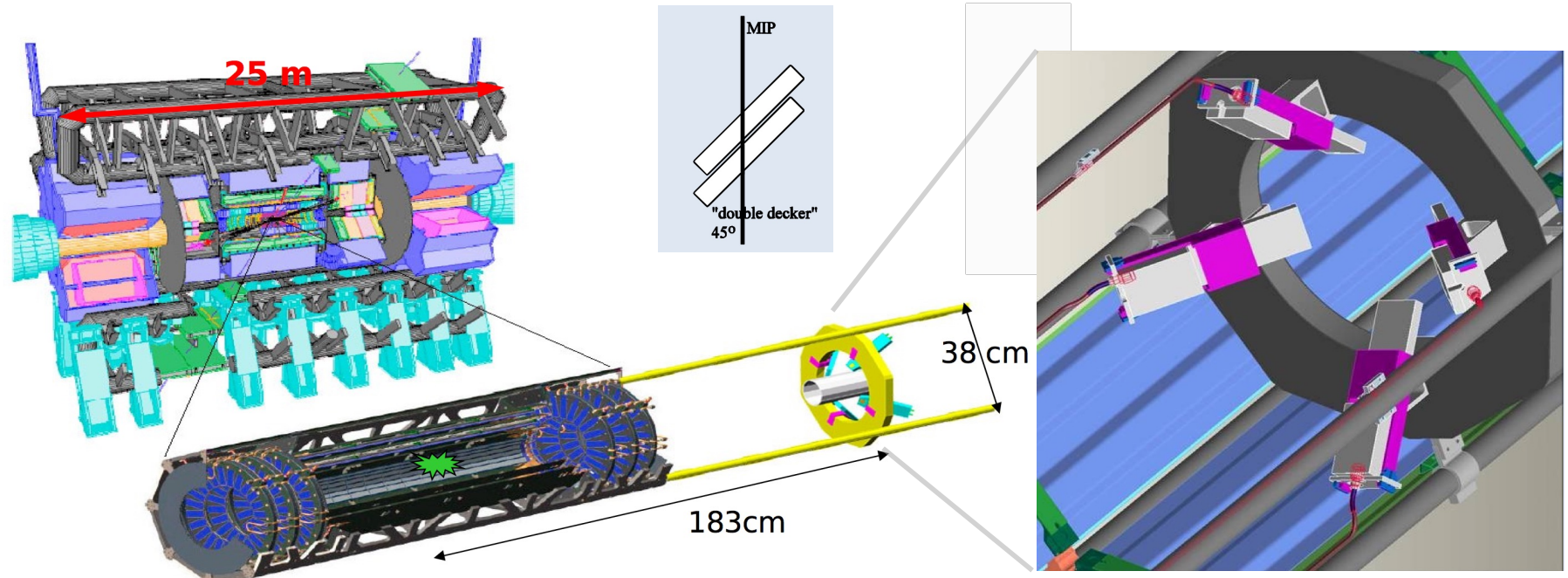
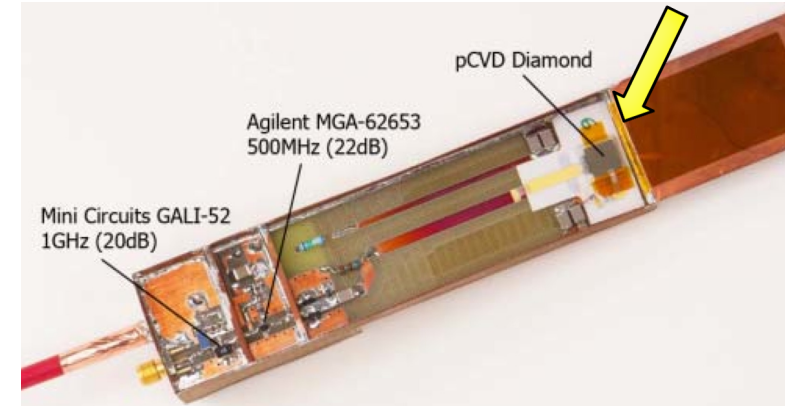
Diamond in current HEP experiments

- Beam monitors to protect experiments against beam losses at the LHC, CERN.
 - For Silicon Vertex systems careful monitoring is crucial.
 - Beam monitors have to be radiation hard.
 - Abort beam when monitors signal dangerous beam conditions.
 - False signals must be avoided.
- During run-1 diamond beam monitors operated in ATLAS, CMS, and LHCb.
- Previously diamond beam monitors were installed in BaBar(SLAC), CDF & D0 (Tevatron).



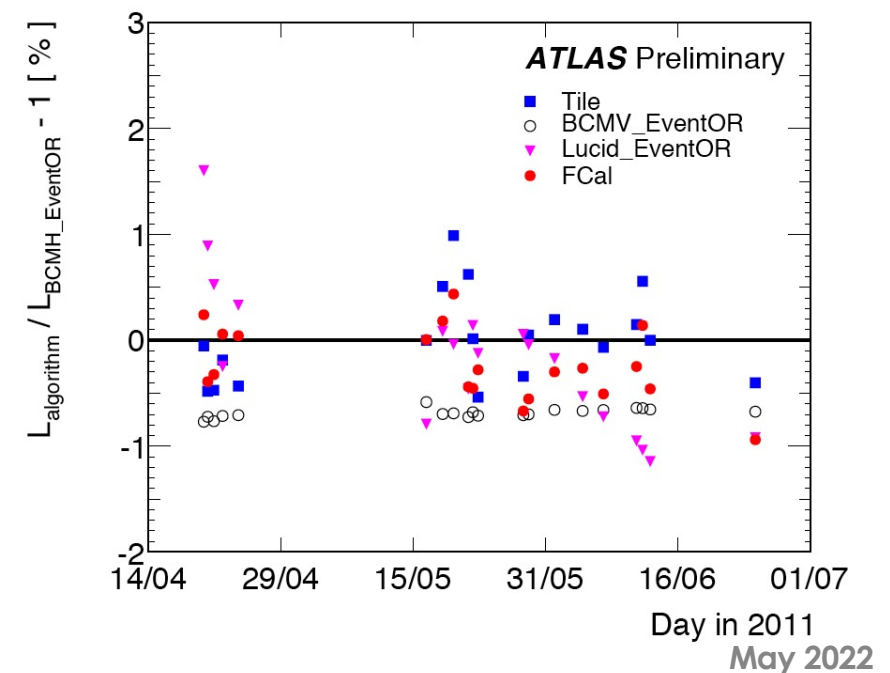
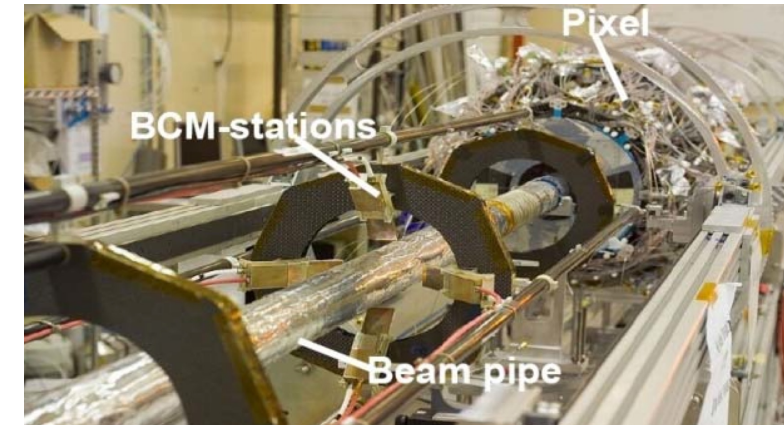
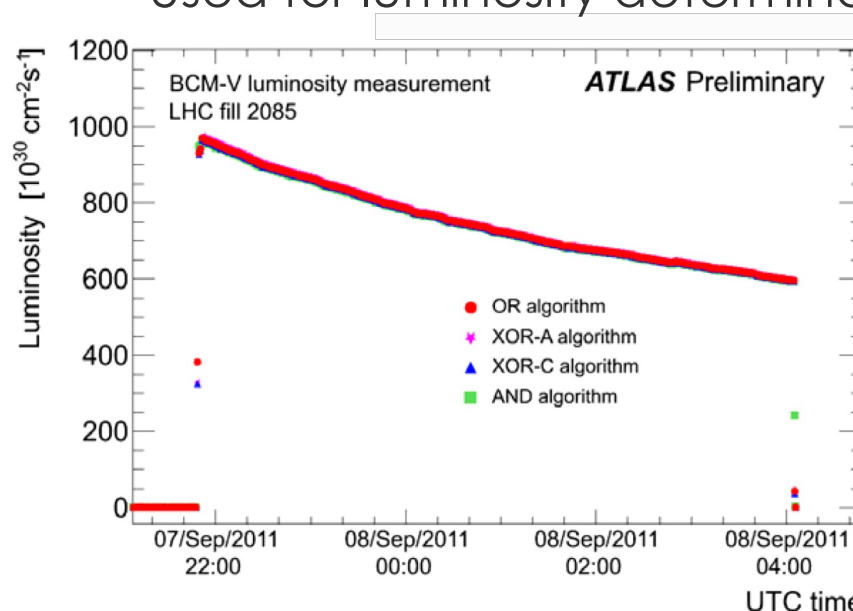
ATLAS beam conditions monitor

- Use 2x polycrystalline CVD diamonds per station (10 x 10 mm).
- 4 stations on each side of the ATLAS pixel detector
 - $z = \pm 183.8 \text{ cm}$ ($\sim 12.5\text{ns}$) and $r \sim 5 \text{ cm}$



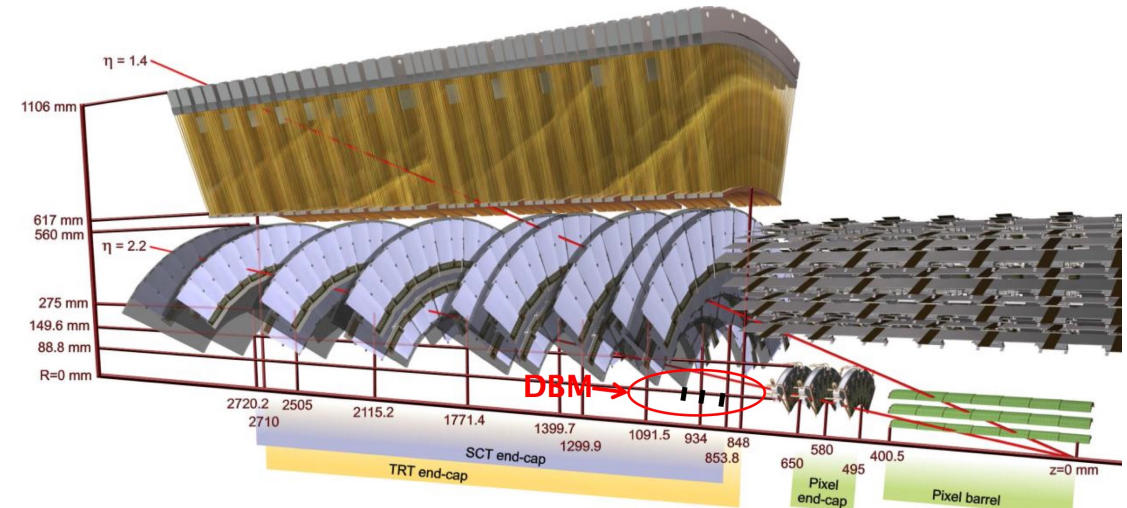
ATLAS beam conditions monitor

- Single particle counting with $\sigma=0.7\text{ns}$.
- Distinguish between collision events and out-of-time background.
- Good stability
 - Used for luminosity determination.



Run 2: ATLAS Diamond Beam Monitor

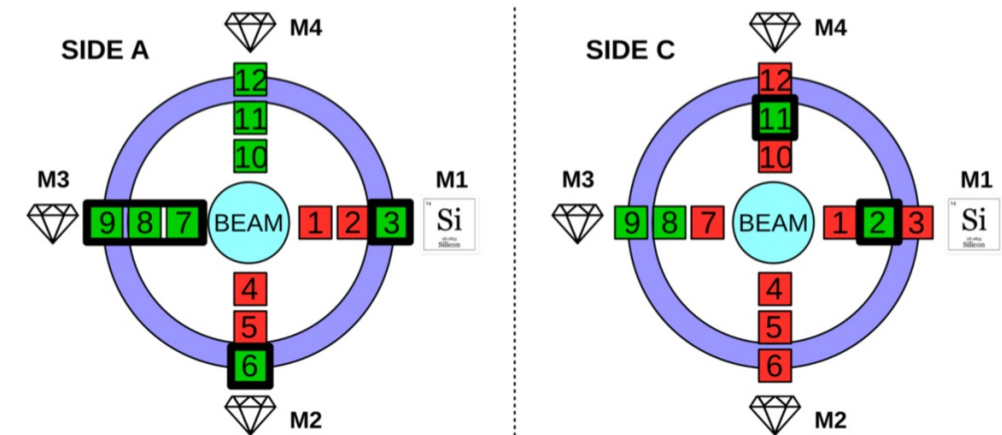
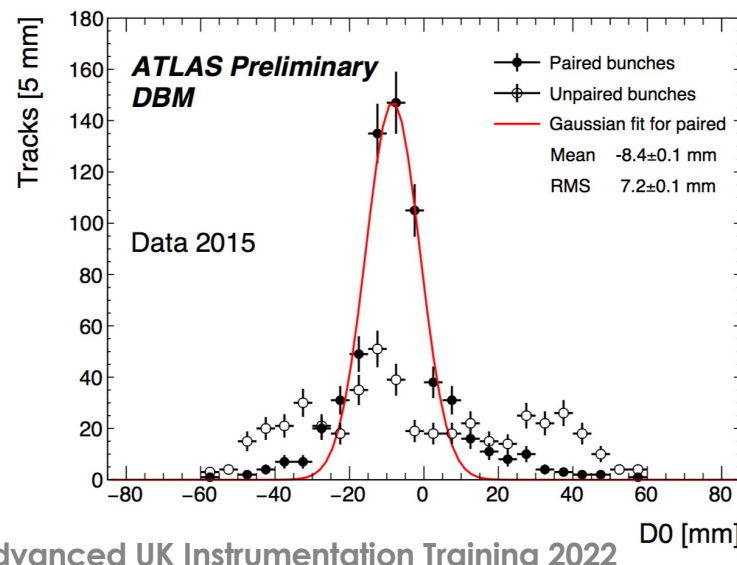
- 8 mini-trackers of 3 planes each using pixel-detectors.
- polycrystalline diamond sensors, 18mm x 21mm, $\delta > 250\mu\text{m}$.
- bump-bonded to FE-I4 pixel read-out chip.
 - 336 x 80 pixels
 - pixel size : $50\mu\text{m} \times 250\mu\text{m}$
- Purpose:
 - Bunch-by-bunch luminosity monitor (aim $< 1\%$ per BC per LB)
 - Bunch-by-bunch beam spot monitor



Run 2:

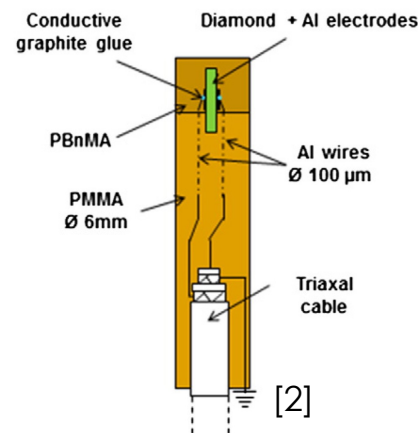
ATLAS Diamond Beam Monitor

- Installed in ATLAS during LS1, but switched off due to unexpected death of Si and Diamond modules.
- DBM recommissioned in 2017/18 with 50% working modules.

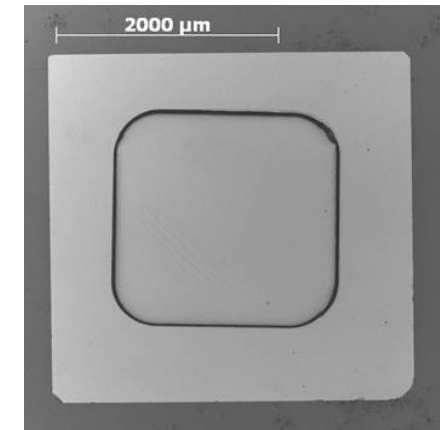


Examples of diamond detectors in related areas

- Synchrotron labs
 - beam position monitor
- Radiation Therapy
 - small field dosimetry
- Heavy Ion (GSI, FAIR)
 - beam diagnostic
 - particle tracking and TOF
 - hadron spectroscopy

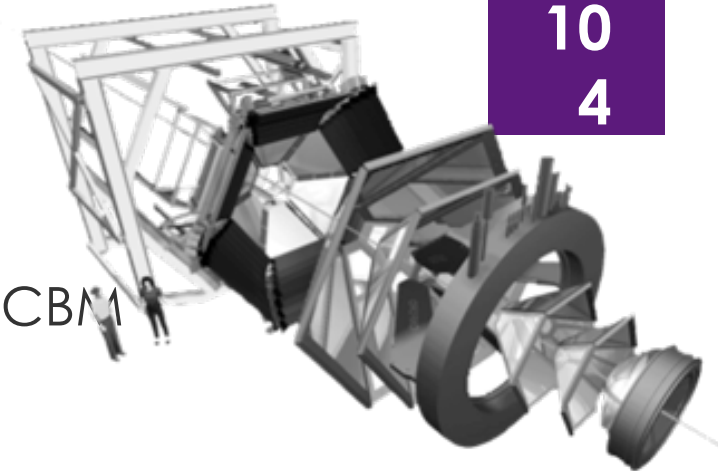


scCVD dosimeter,
0,4 mm³ active vol. [2]

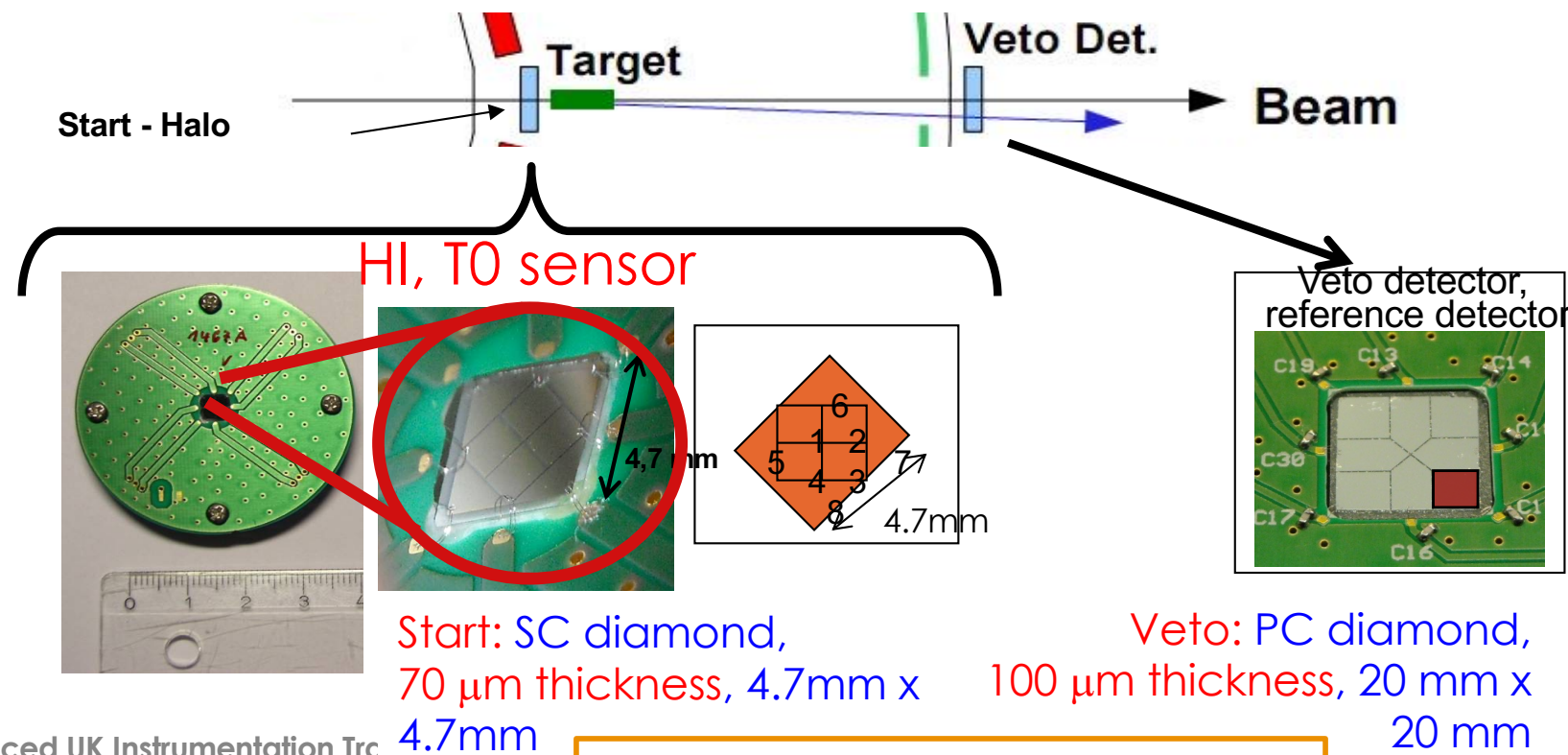


3 µm thick membrane
in 40 µm thick scCVD [1]

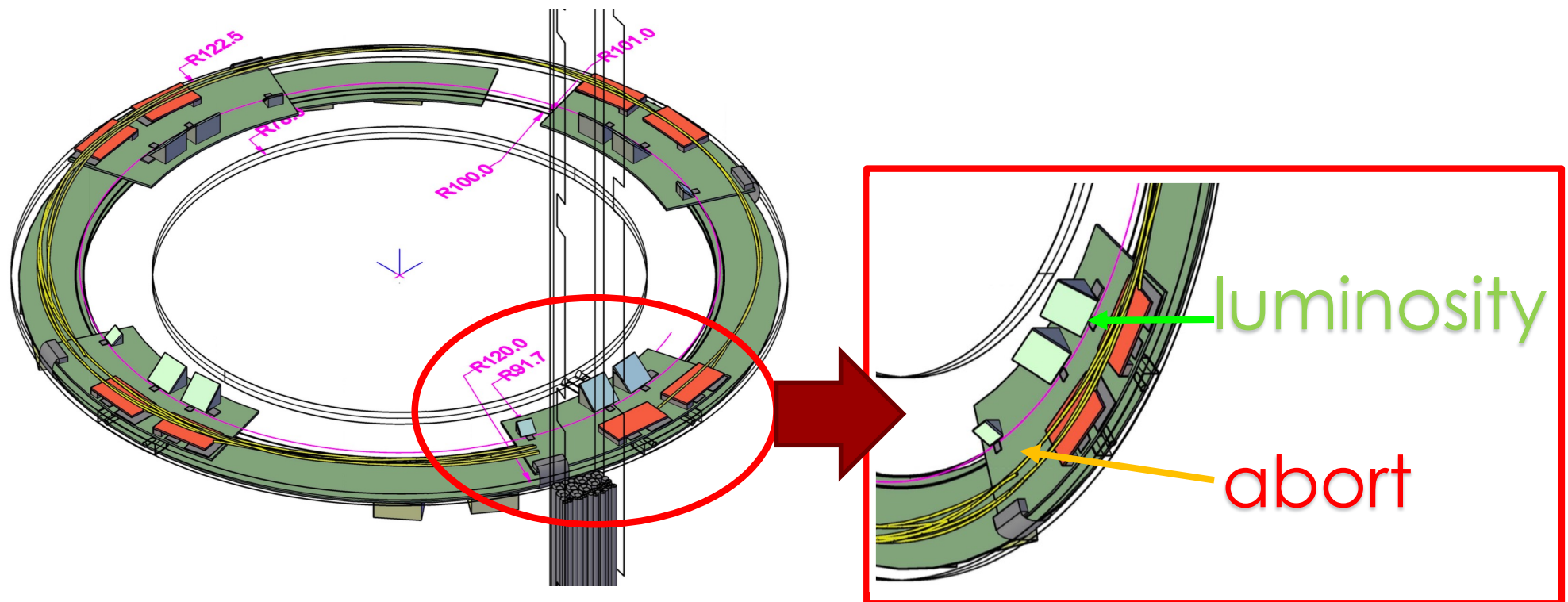
Detectors for Heavy Ion



- In-beam START-VETO detectors for HADES and CBM
 - High beam intensities (10^7 #/s).
 - Protons (MIPS) up to very heavy ions (Au, U)
 - Excellent time resolution (30-100 ps)
 - Radiation hard up to 10^{12} /cm Au ions



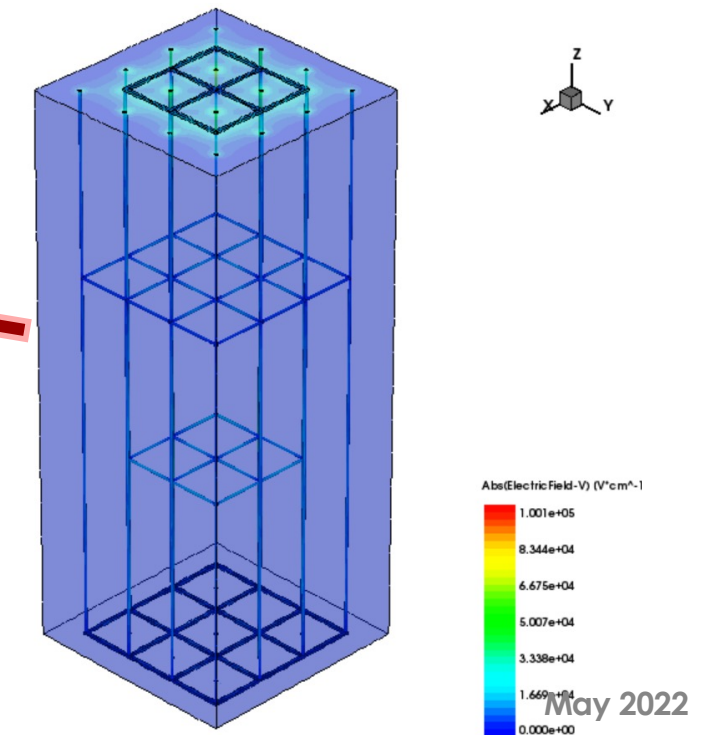
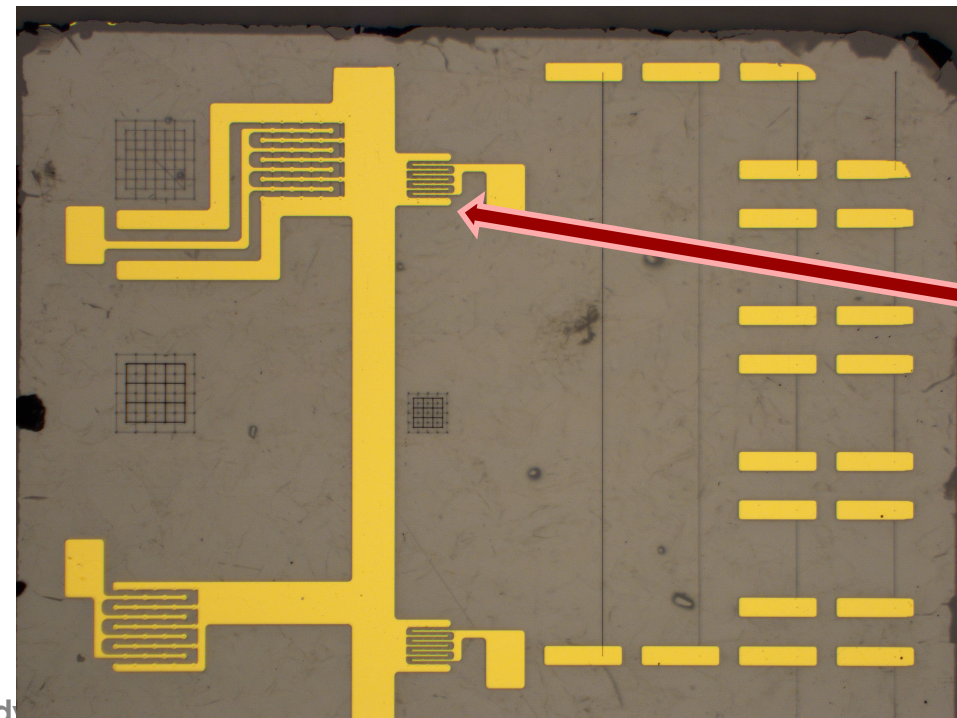
Upgrade for LHC Phase-2: BCM' modules



First BCM' 3D test structure with new “cage” design

10
6

- Fabricated March 2020 (~week of UK Lockdown) first 3D diamond device with horizontal ganging
- Test structure has horizontal wires at depths of 125 and 375 μm in a 500 μm thick substrate (ρ measurement)
- Metallised 3D detector with alternating ganging (~model) read out in current mode in **RD42 Zagreb Testbeam 06-2021, second version tested April 2022**



Summary

- Diamond systems are used as beam and luminosity monitors in current HEP experiments and foreseen for future experiments.
- Radiation hardness and rate dependence has been studied.
- 3D diamond has been demonstrated to work.
- The understanding of diamond as a detector material is advancing.

EXTRA MATERIAL

3D Detector Characterization

- Proton Micro-beam: 4.5 MeV p

Proton micro-beam measurements

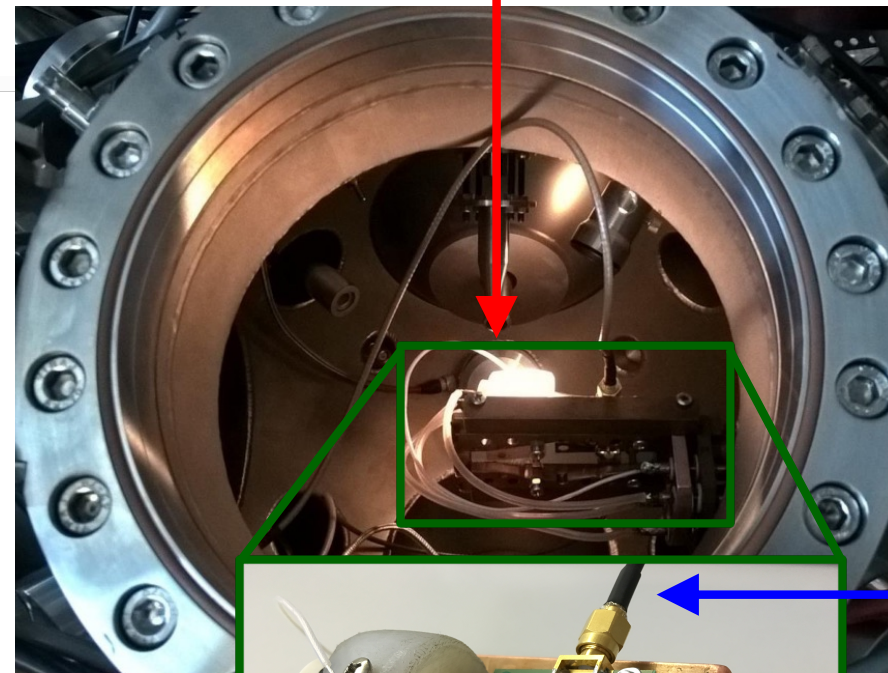


Rudjer Bošković Institute

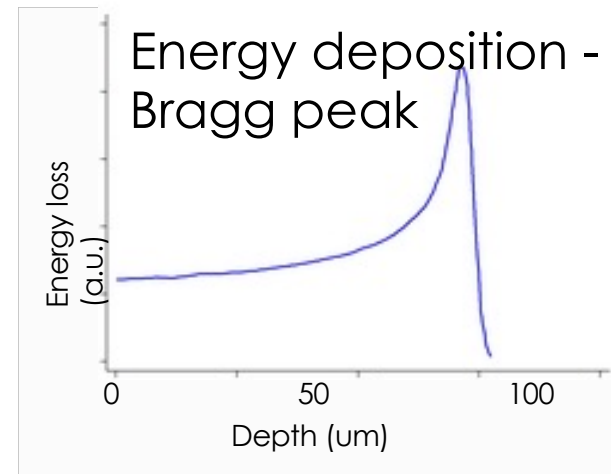
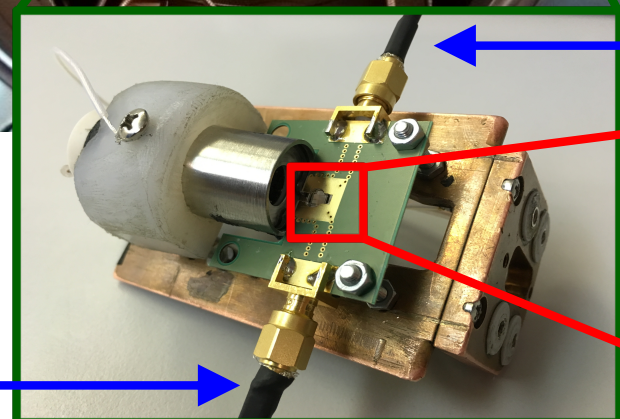


AIDA²⁰²⁰

4.5 MeV
protons



Read-out
channel 2



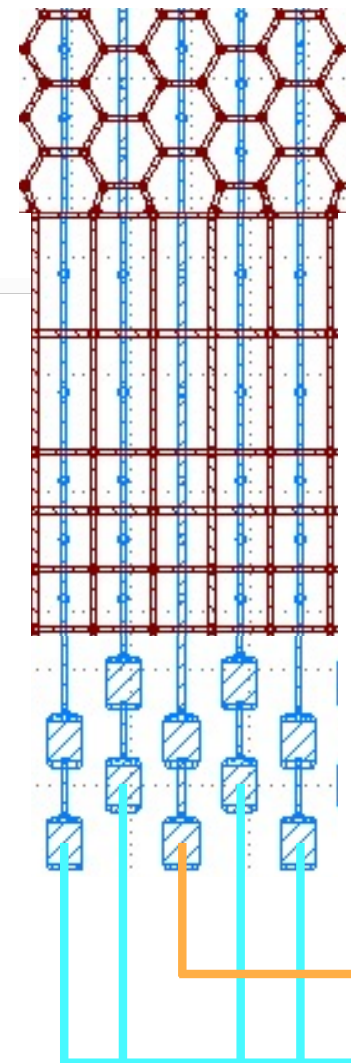
- Single particle beam.
- Rate $\sim 1\text{kHz}$.
- Beam position resolution $< 2\mu\text{m}$.

Read-out
channel 1

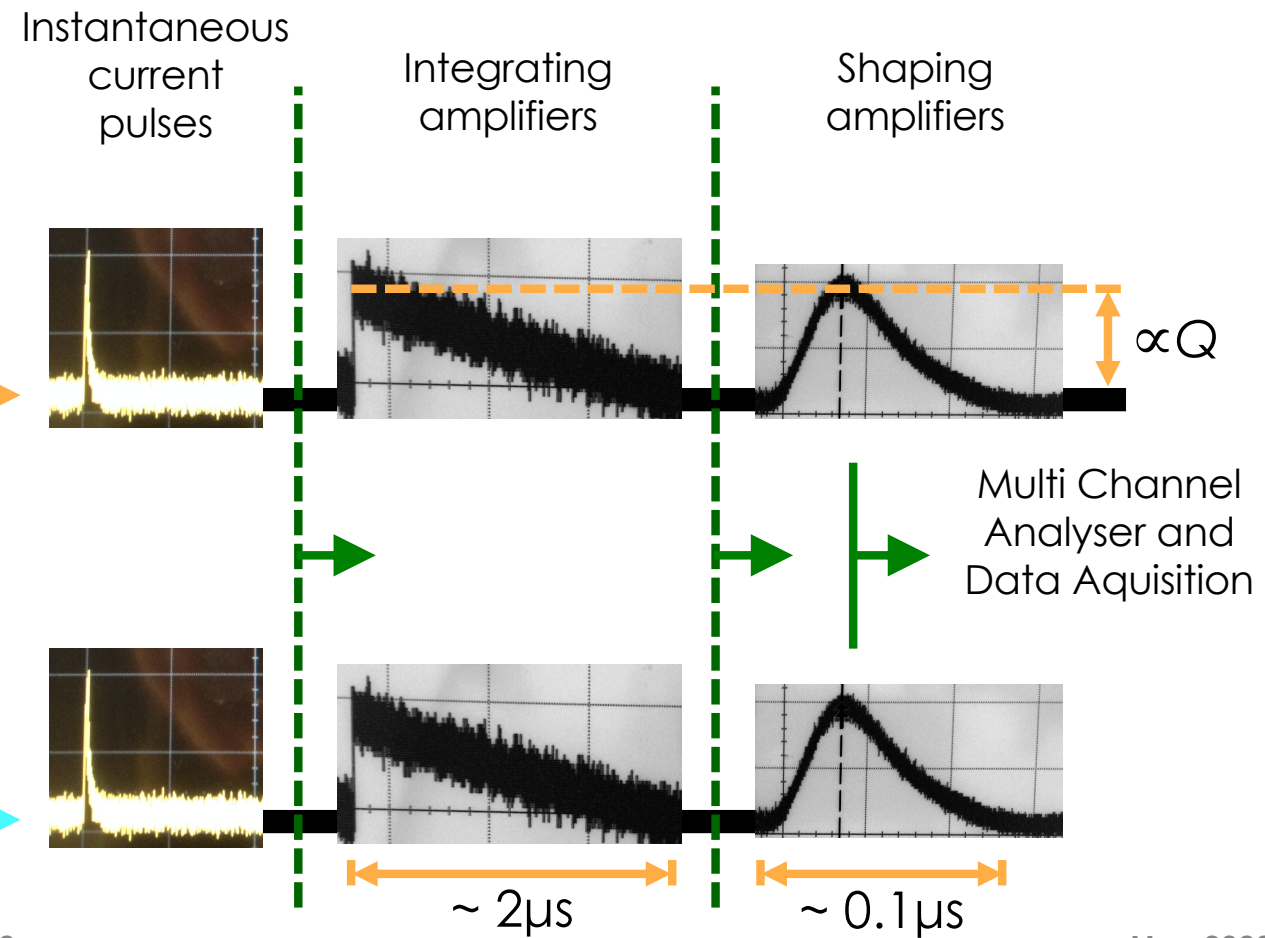
3D diamond
detector

IBIC - setup

I



- Two read-out channels and amplification chains.



Proton micro-beam measurements

4

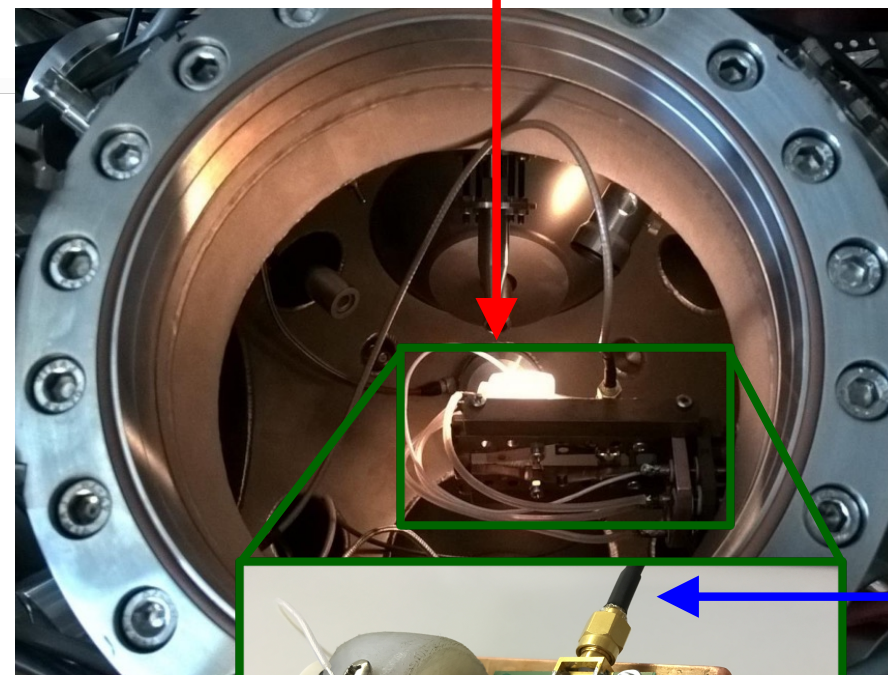


Rudjer Bošković Institute

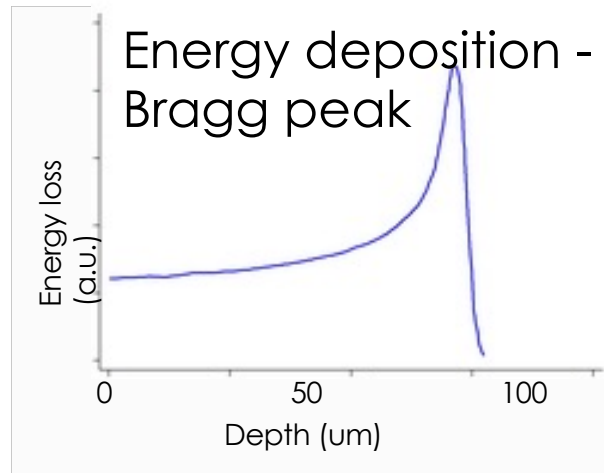
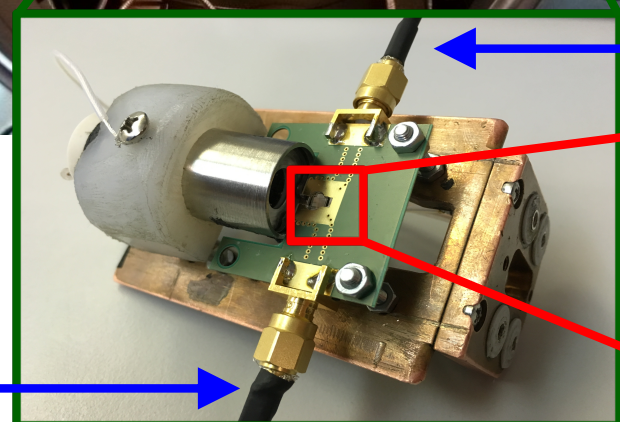


AIDA²⁰²⁰

4.5 MeV
protons



Read-out
channel 2



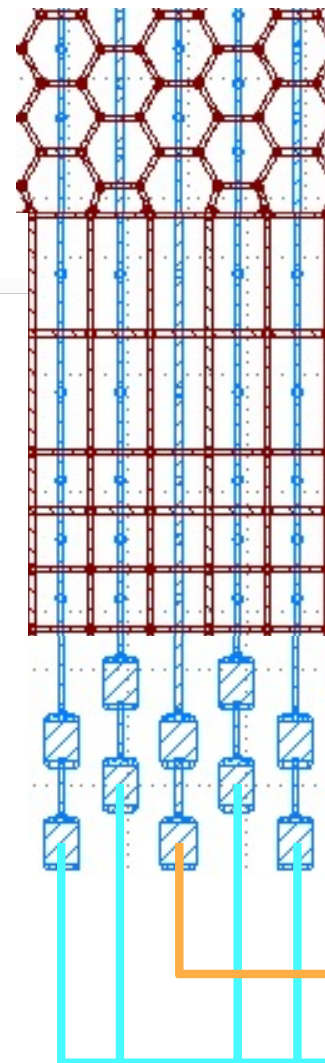
- Single particle beam.
- Rate $\sim 1\text{kHz}$.
- Beam position resolution $< 2\mu\text{m}$.

Read-out
channel 1

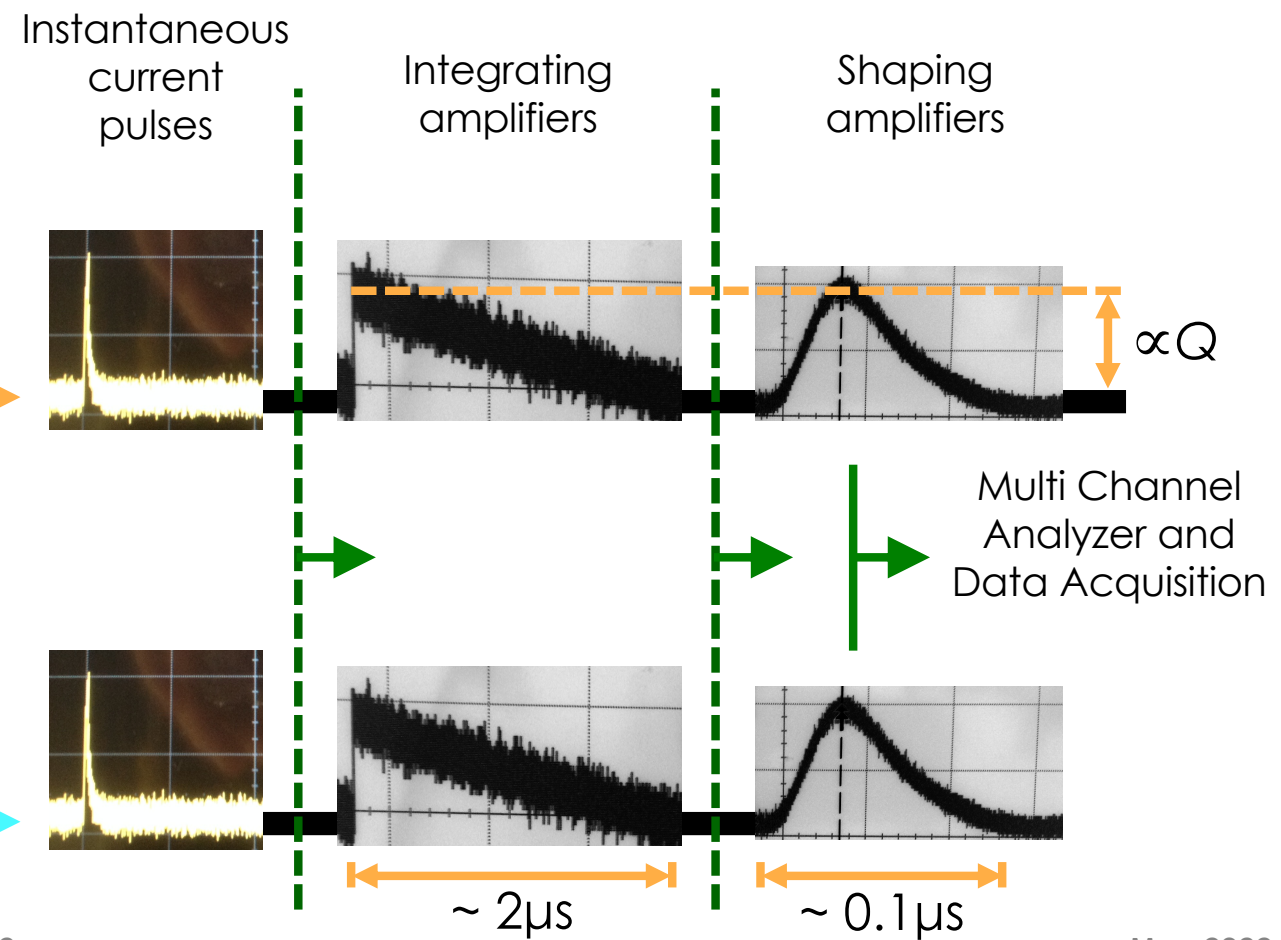
3D diamond
detector

(TR)IBIC

(Time Resolved) Ion Beam Induced Current

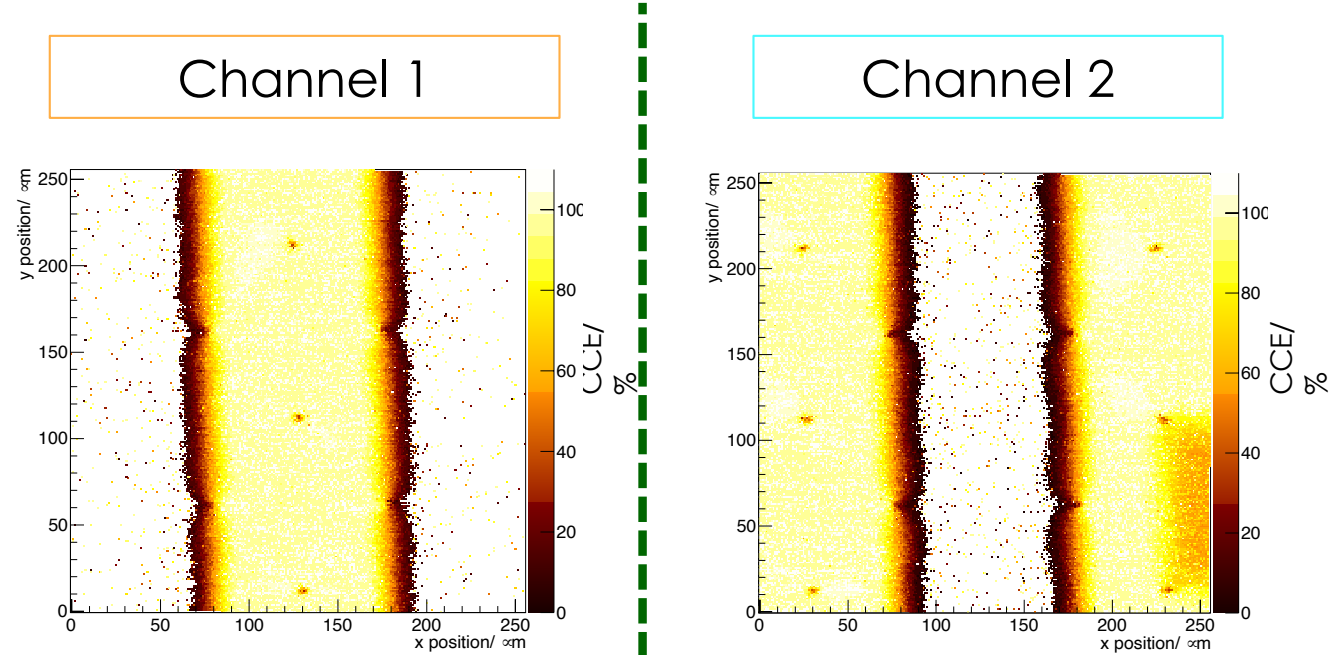
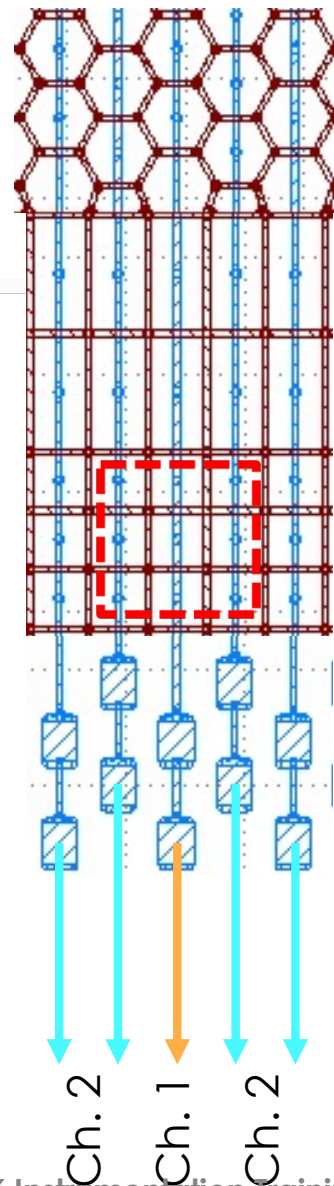


- Two read-out channels and amplification chains.

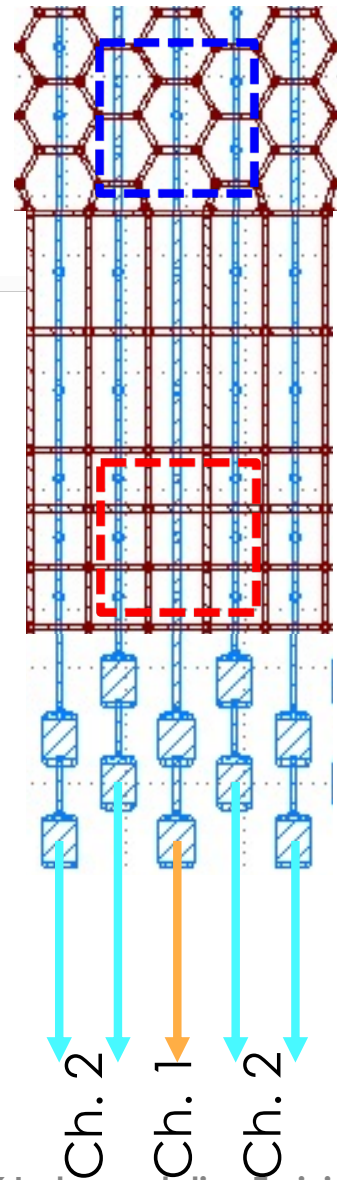


Signal efficiency at +20V

- Electronics chain calibrated with silicon detector.



Charge sharing

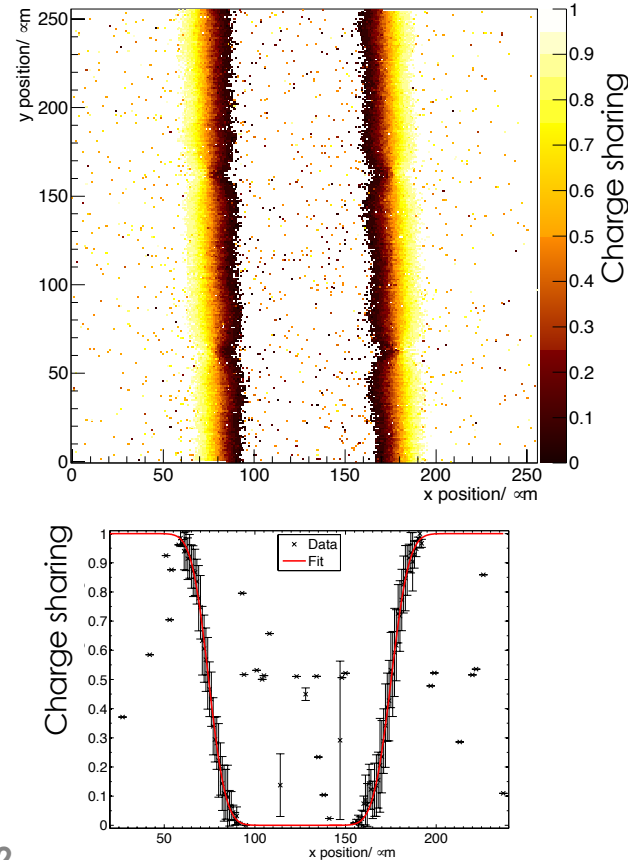


Charge Sharing

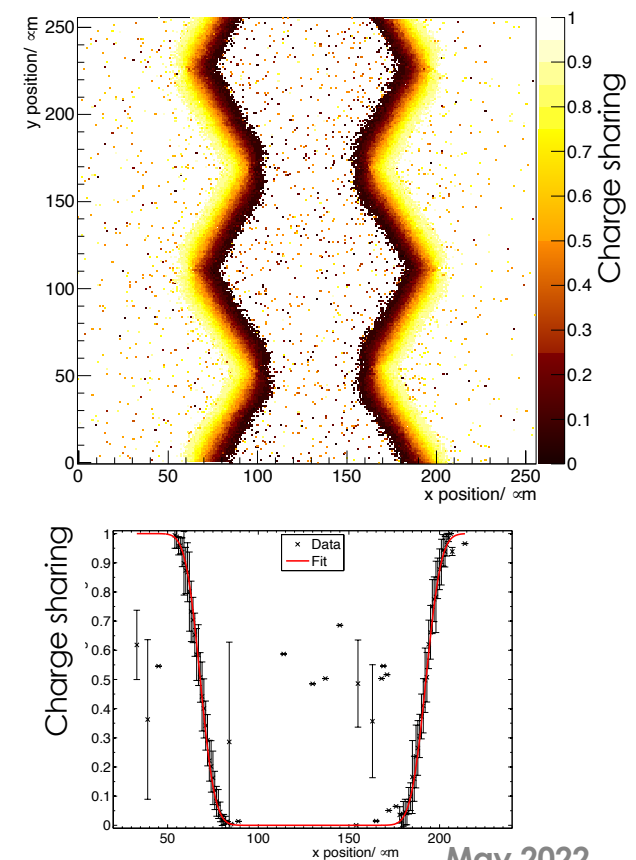
$$\rho = Q_2 / (Q_1 + Q_2)$$

Induced charge on Ch. 2 Induced charge on Ch. 1

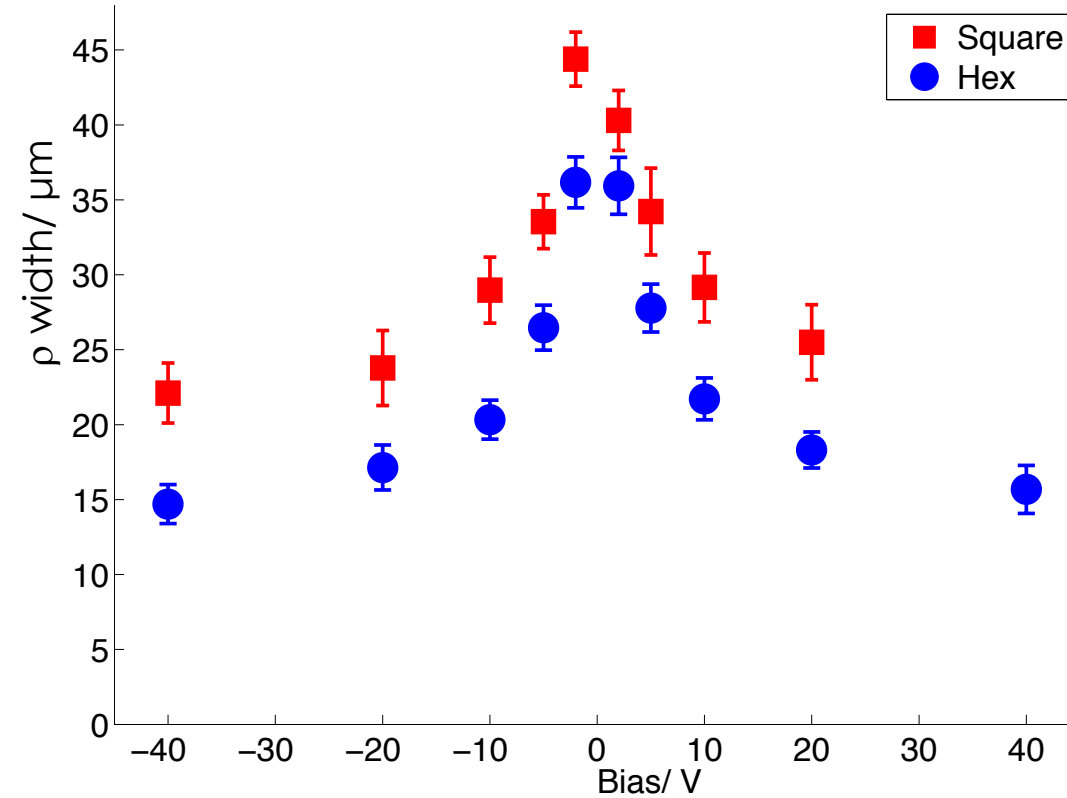
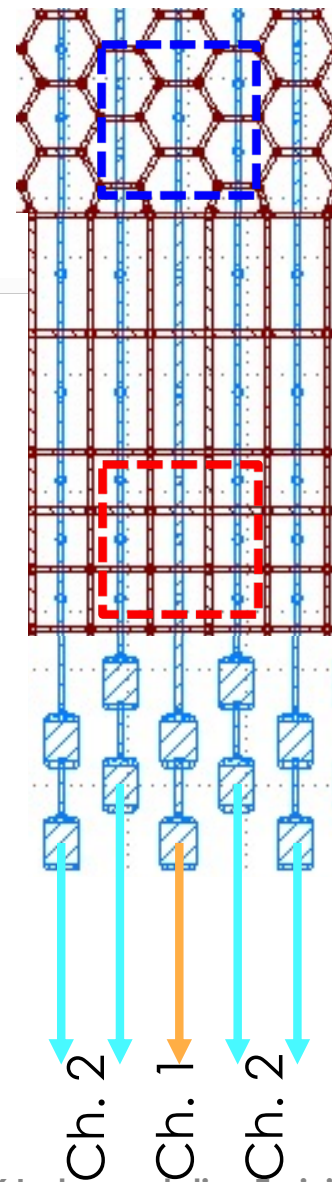
Square



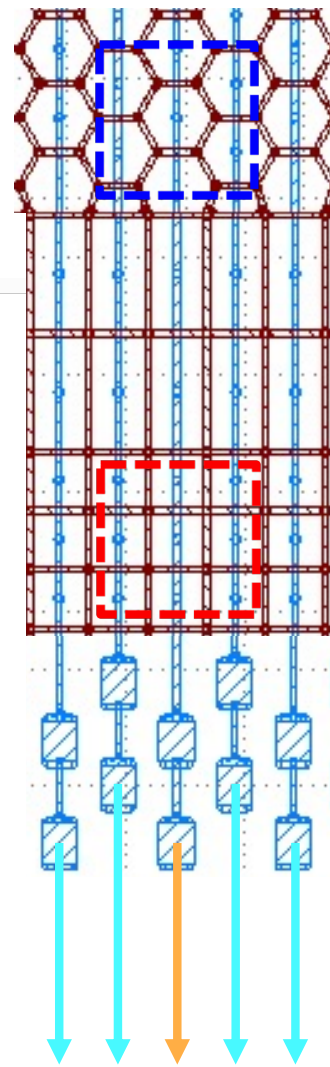
Hexagonal



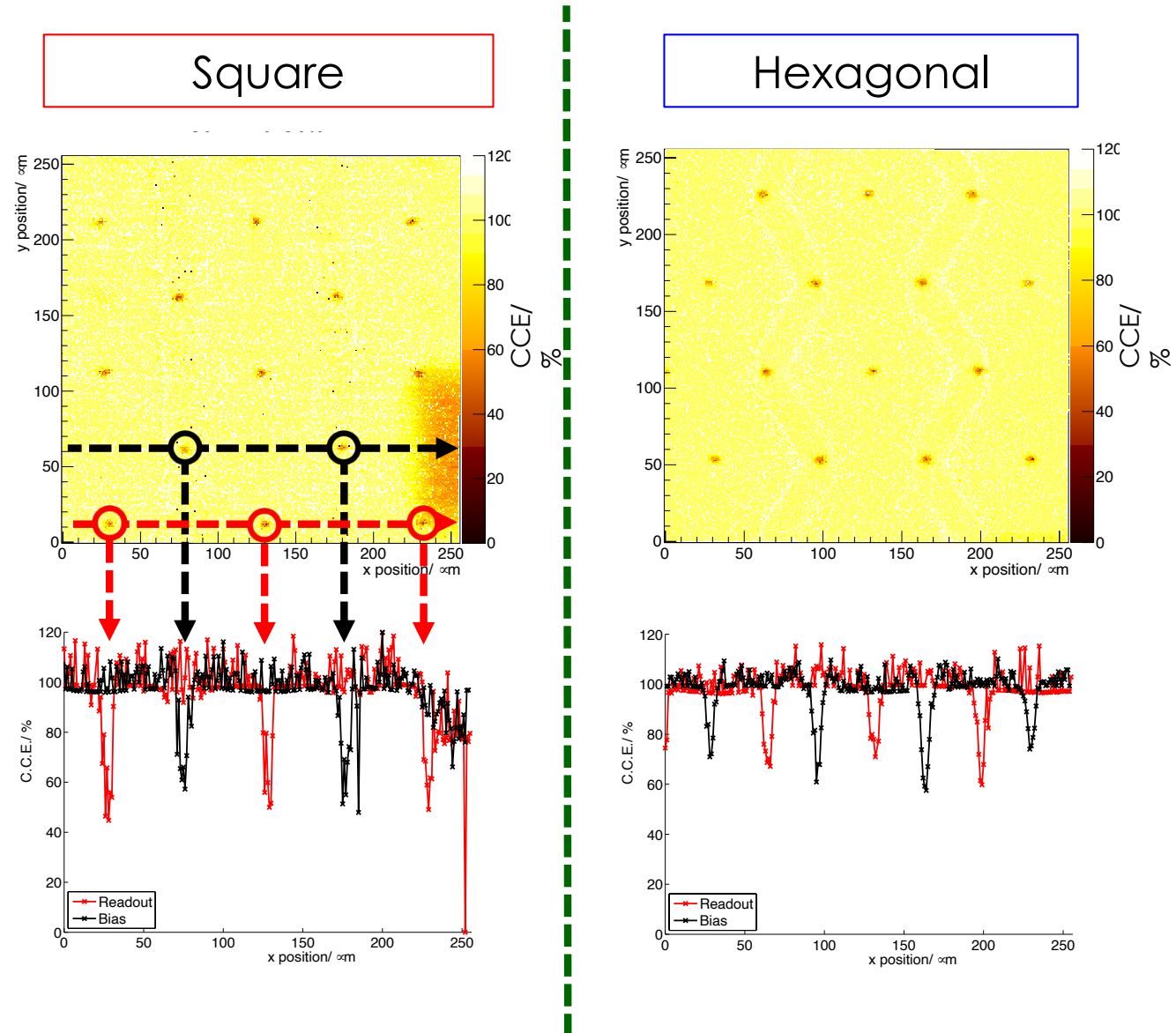
Charge sharing comparison



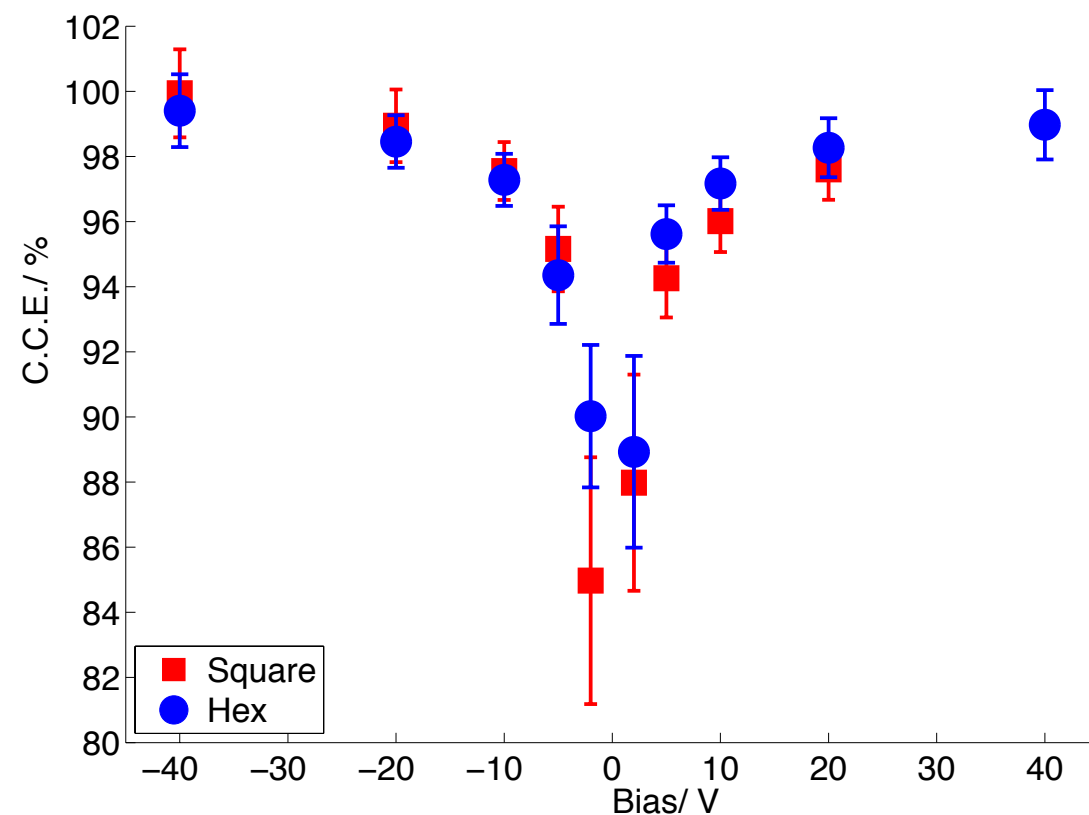
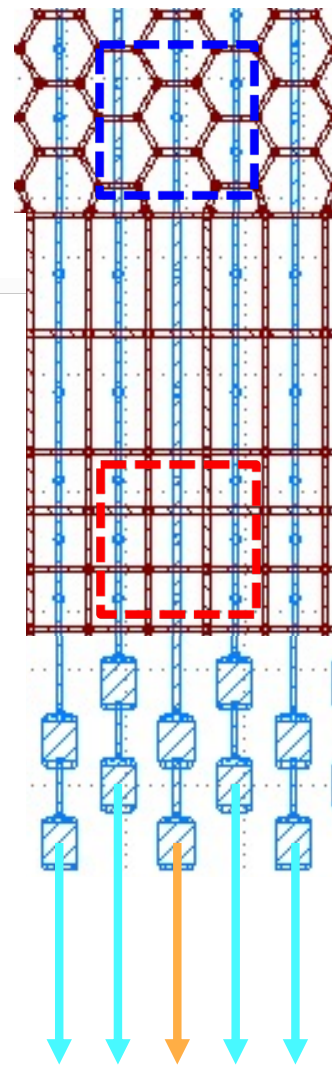
Combined Ch. 1 and Ch. 2 at +20V



Combine



Signal efficiency comparison



Summary IBIC

- Measured the Signal Efficiency versus position.
- Both geometries show > 98% CCE above 20V.
- There is a measured drop in signal due to columns of diameter $\sim 6\mu\text{m}$.
- A small region of charge sharing, $\sim 20\mu\text{m}$, is observed in both geometries.

Time Resolved IBIC (TRIBIC)

$$i = E_w q v$$

Instantaneous current

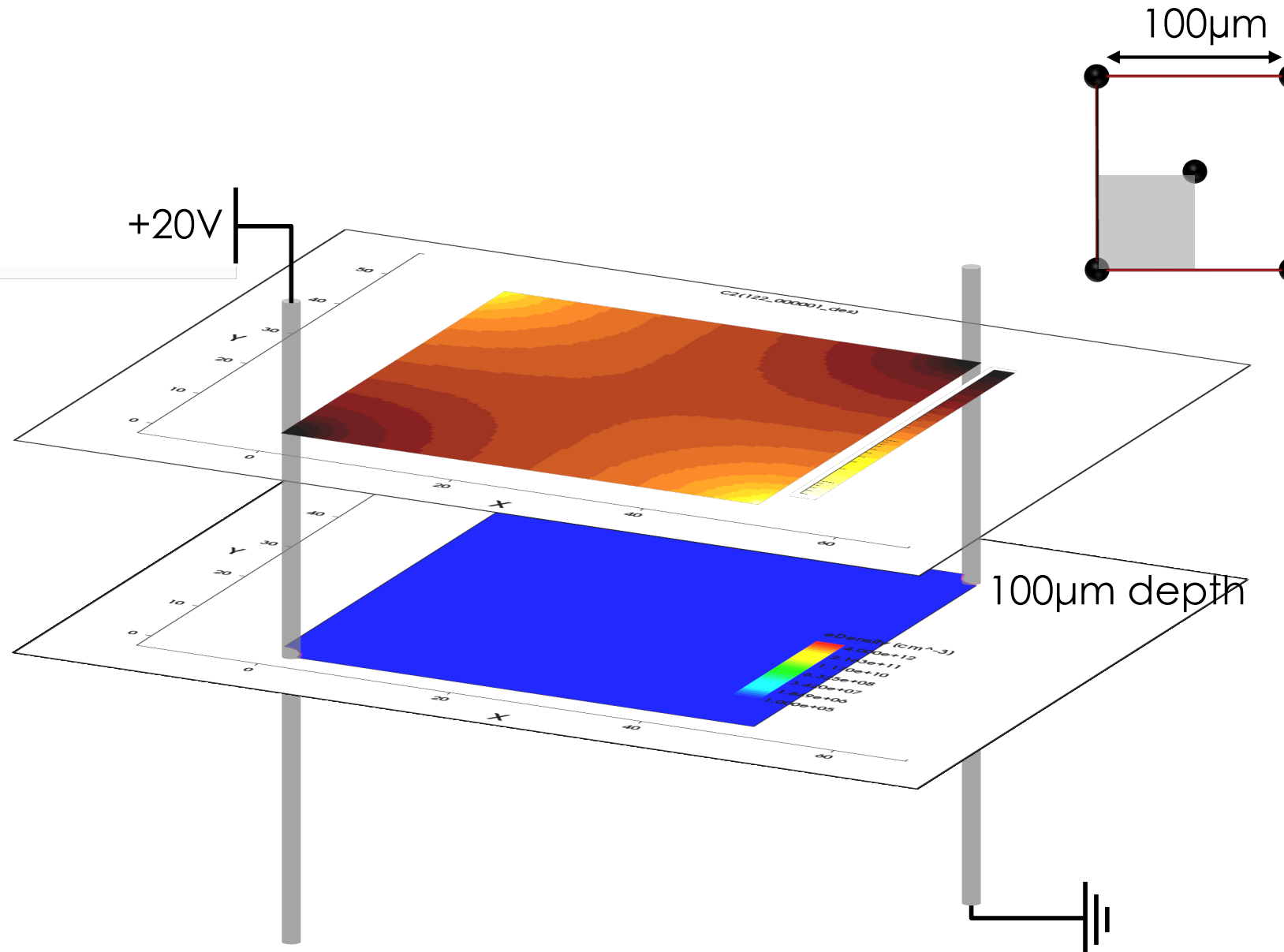
Carrier charge

Weighting field

Carrier velocity

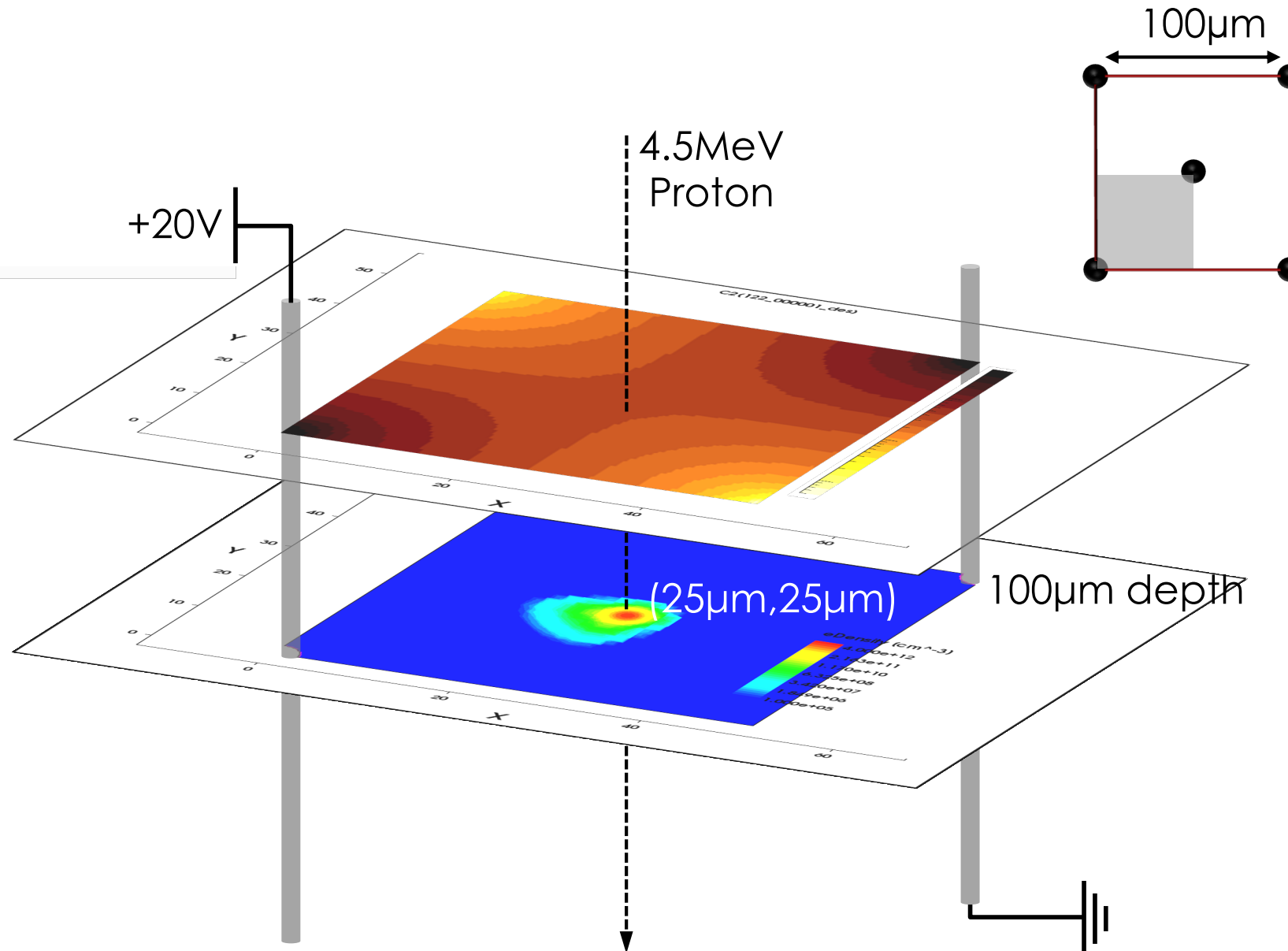
Simulation

12
1



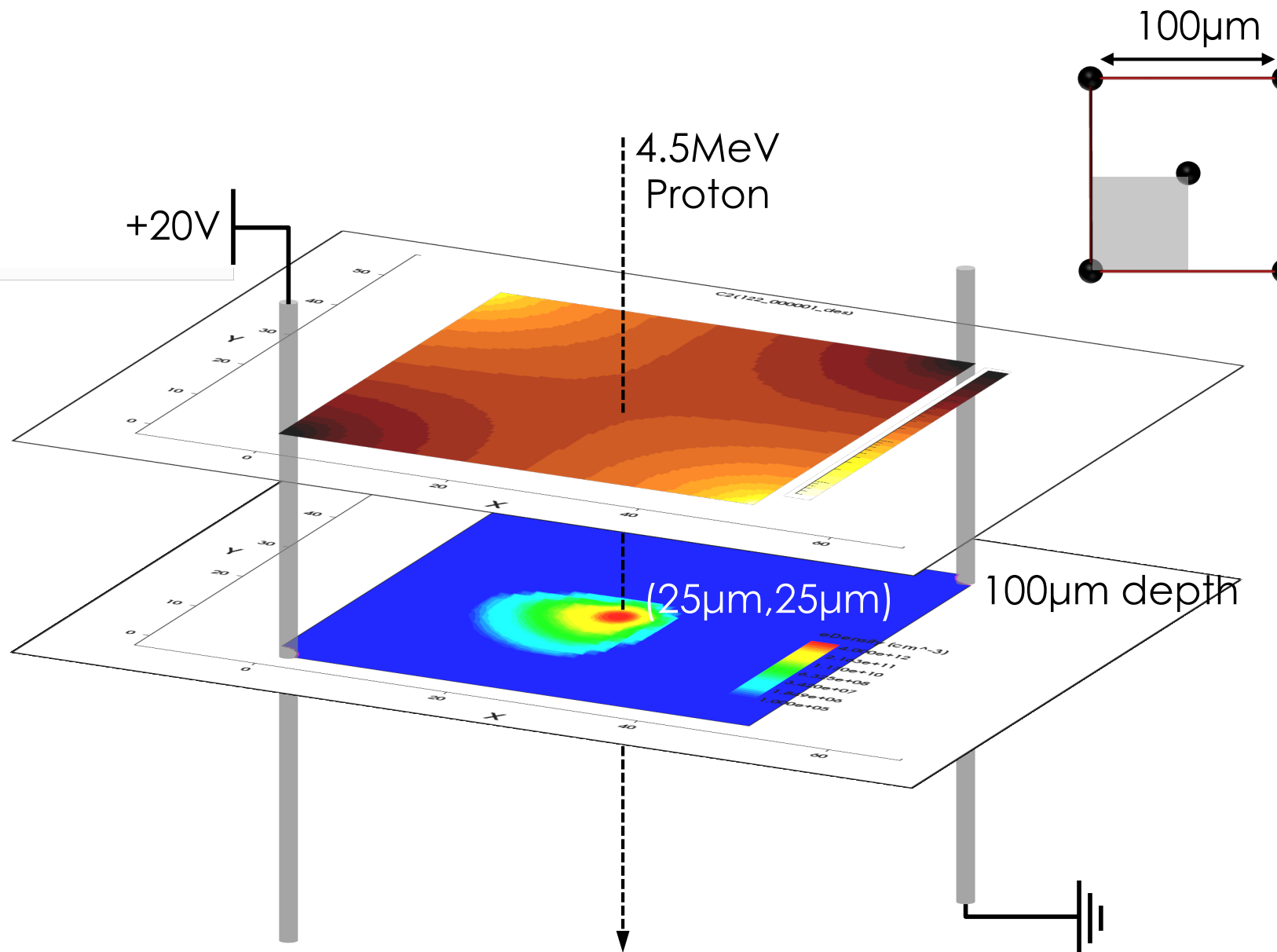
Simulation

12
2



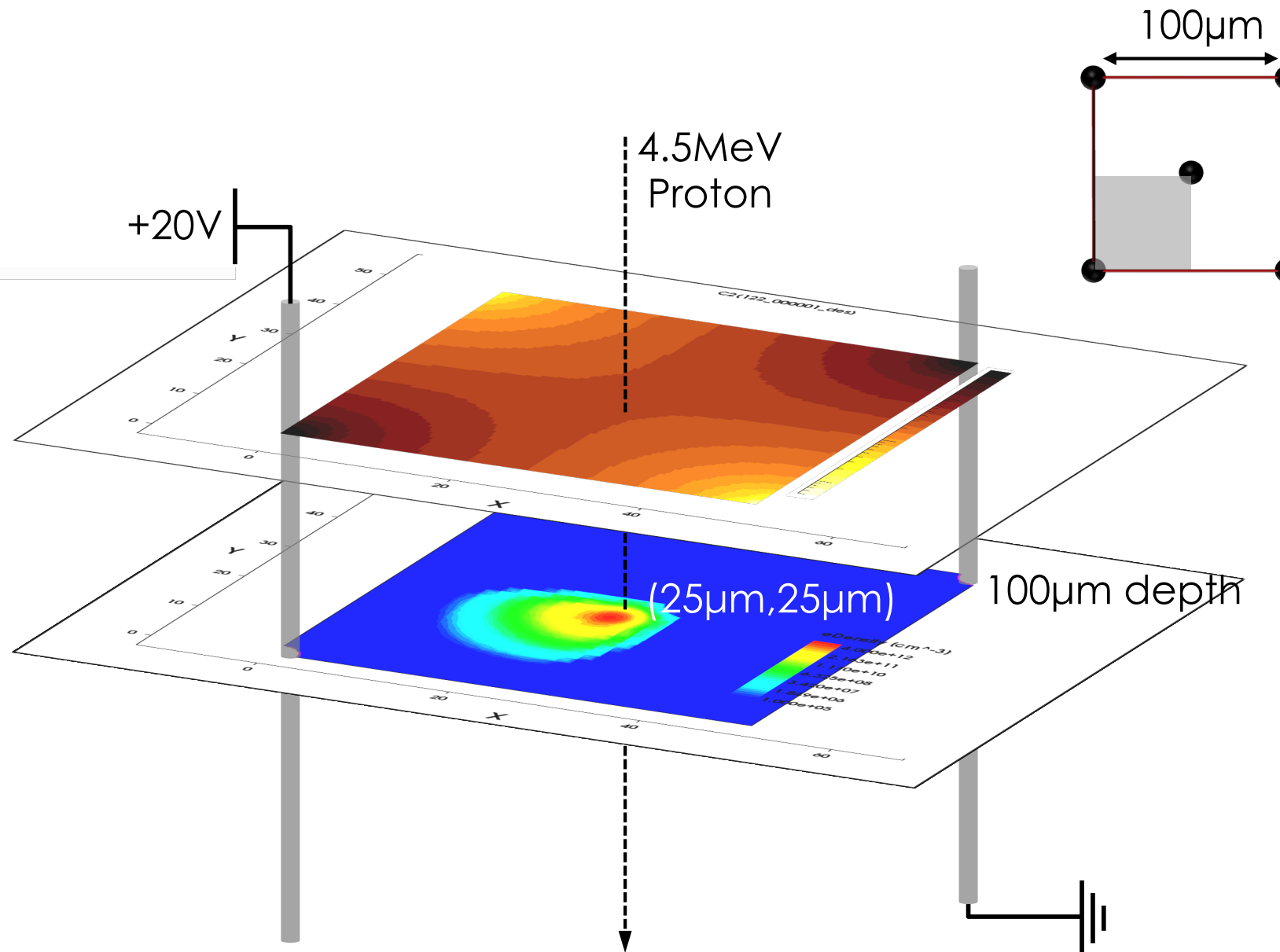
Simulation

12
3



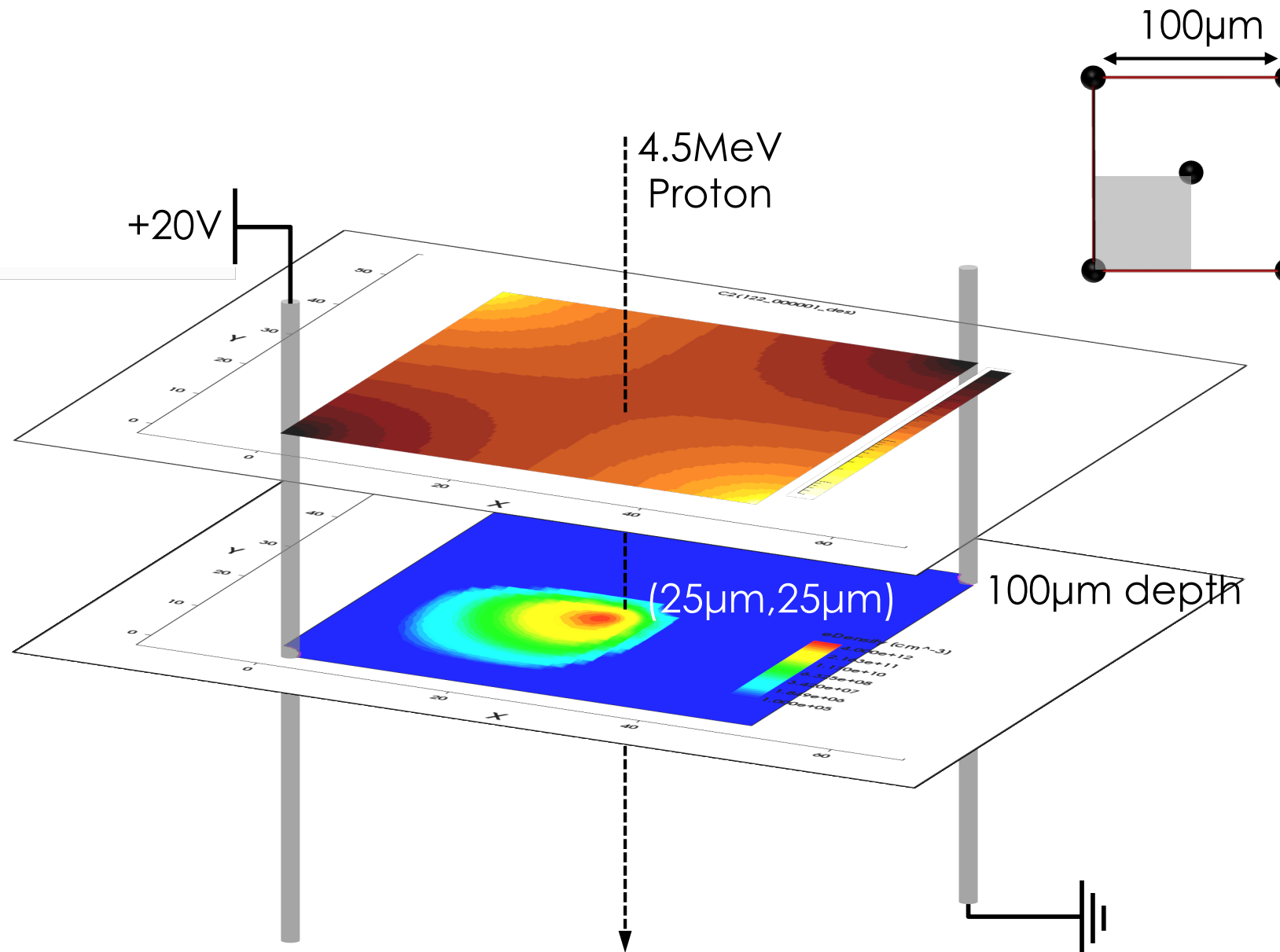
Simulation

12
4



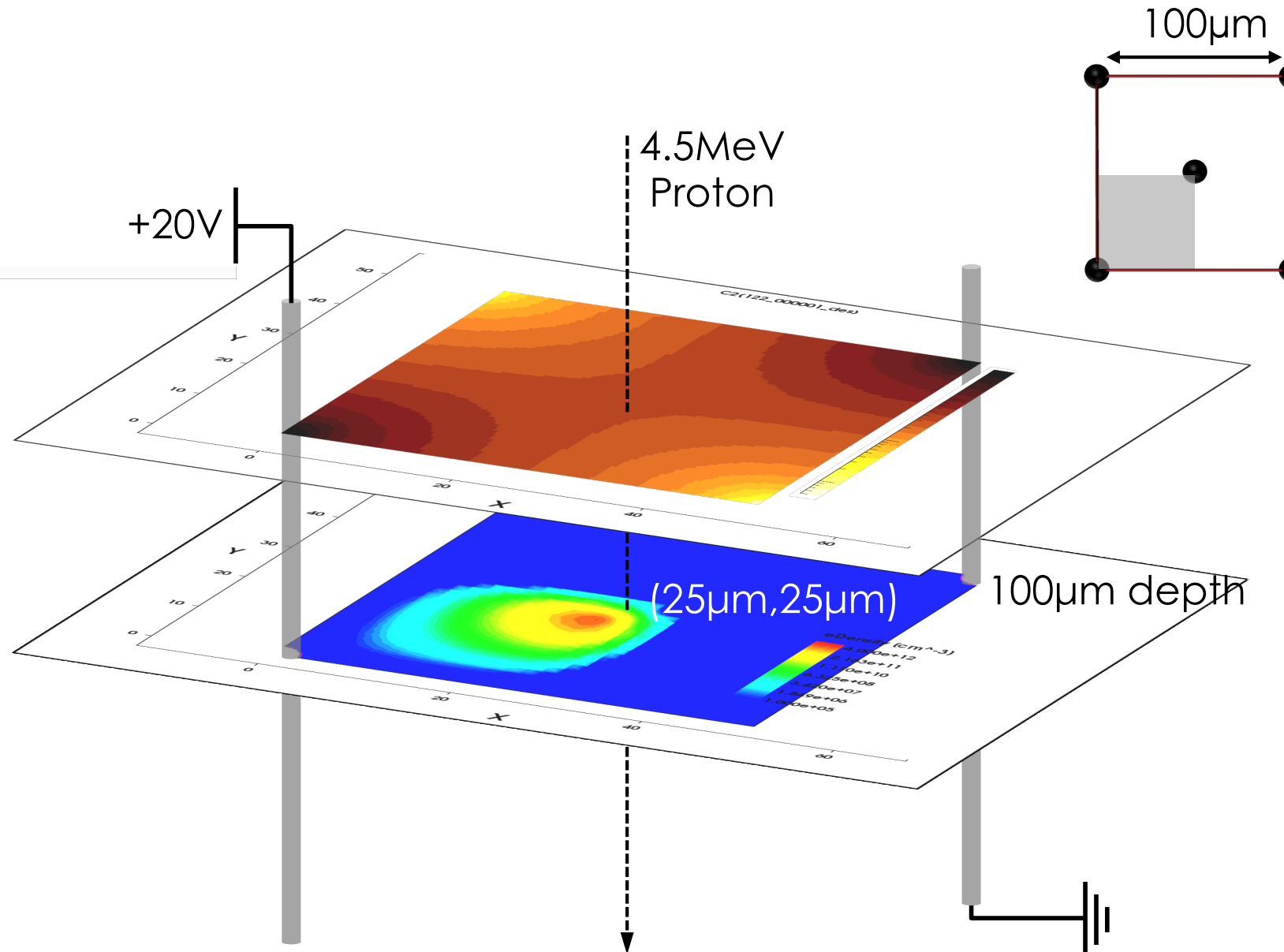
Simulation

12
5



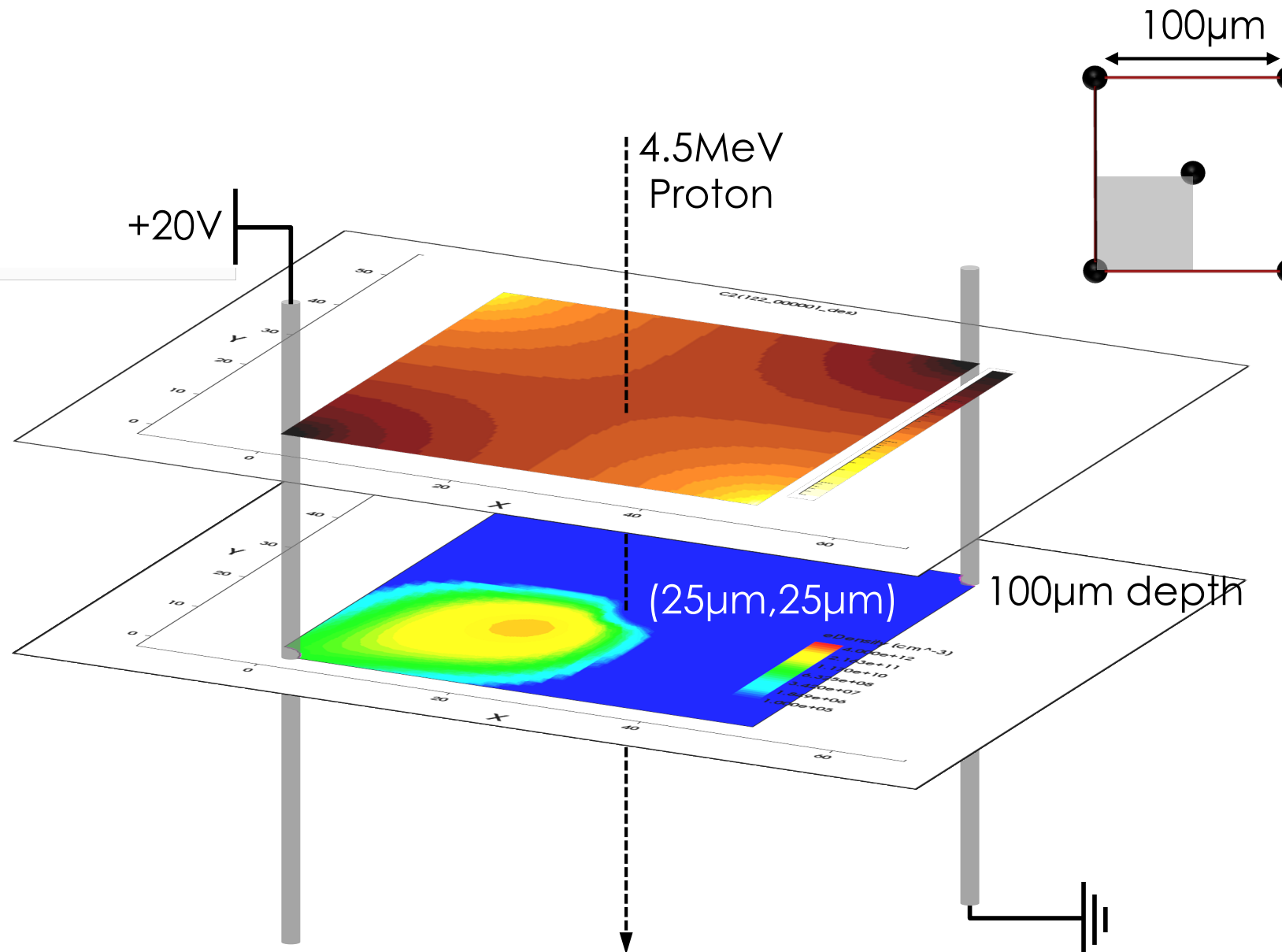
Simulation

12
6



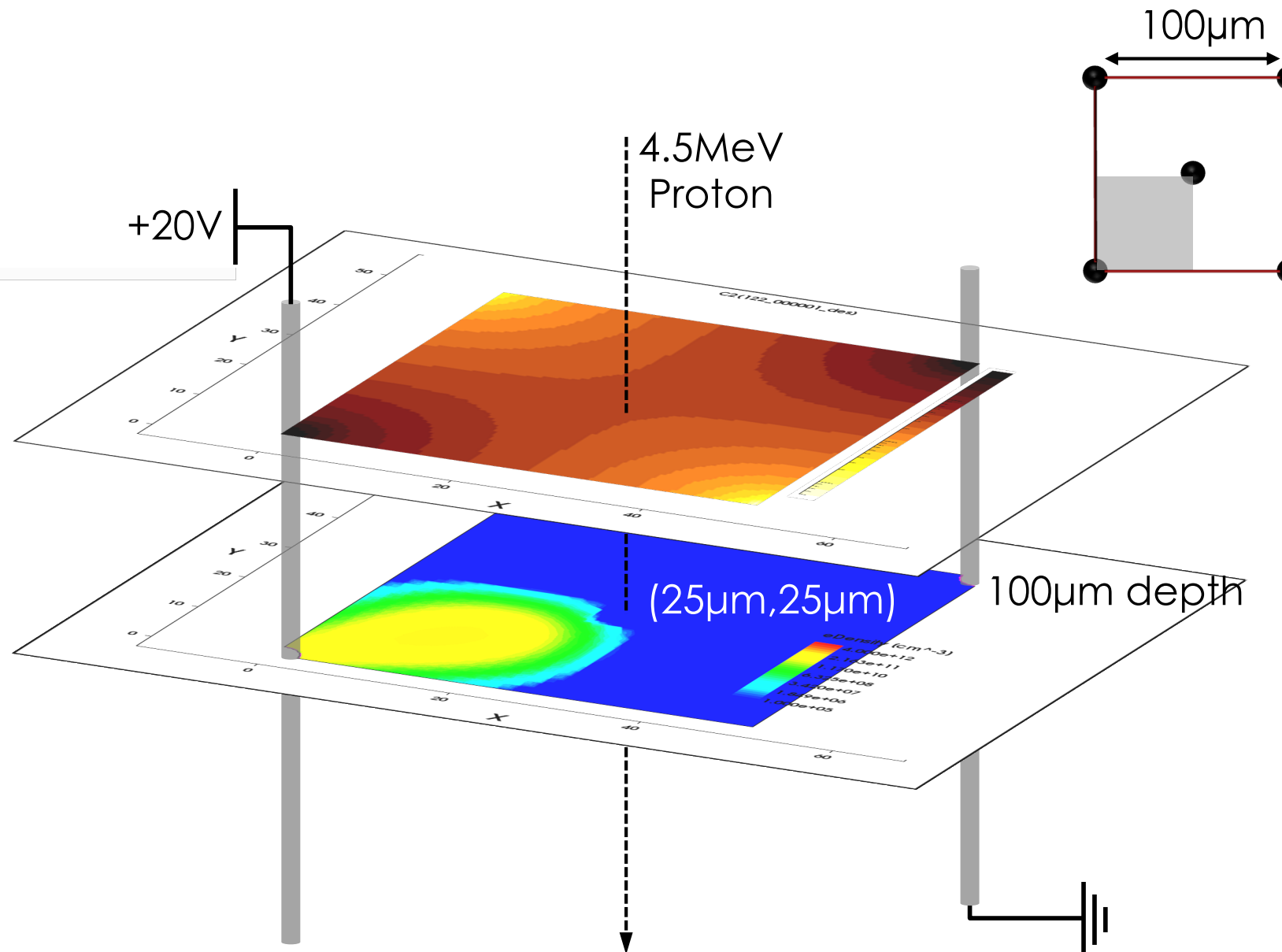
Simulation

12
7



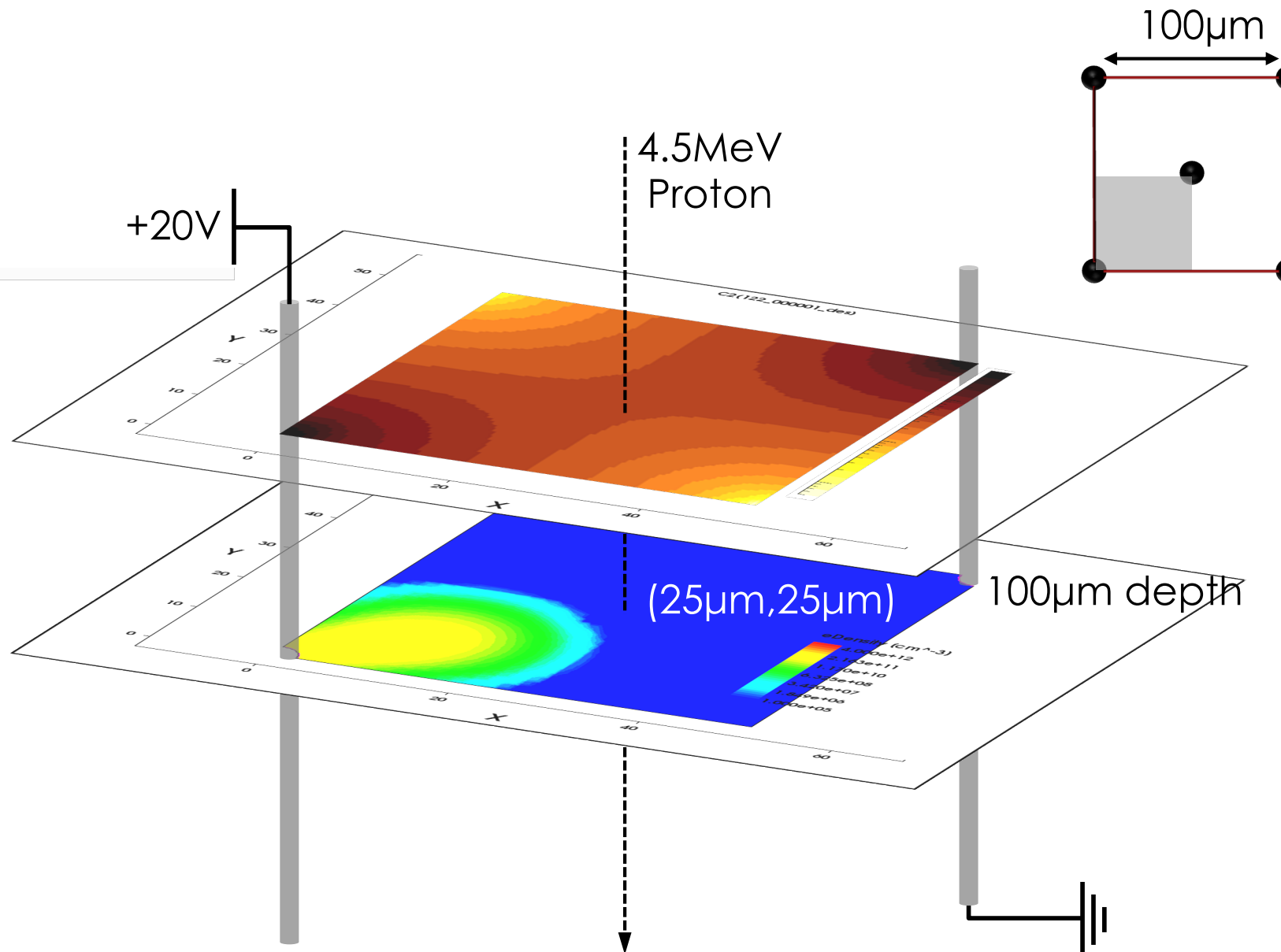
Simulation

12
8



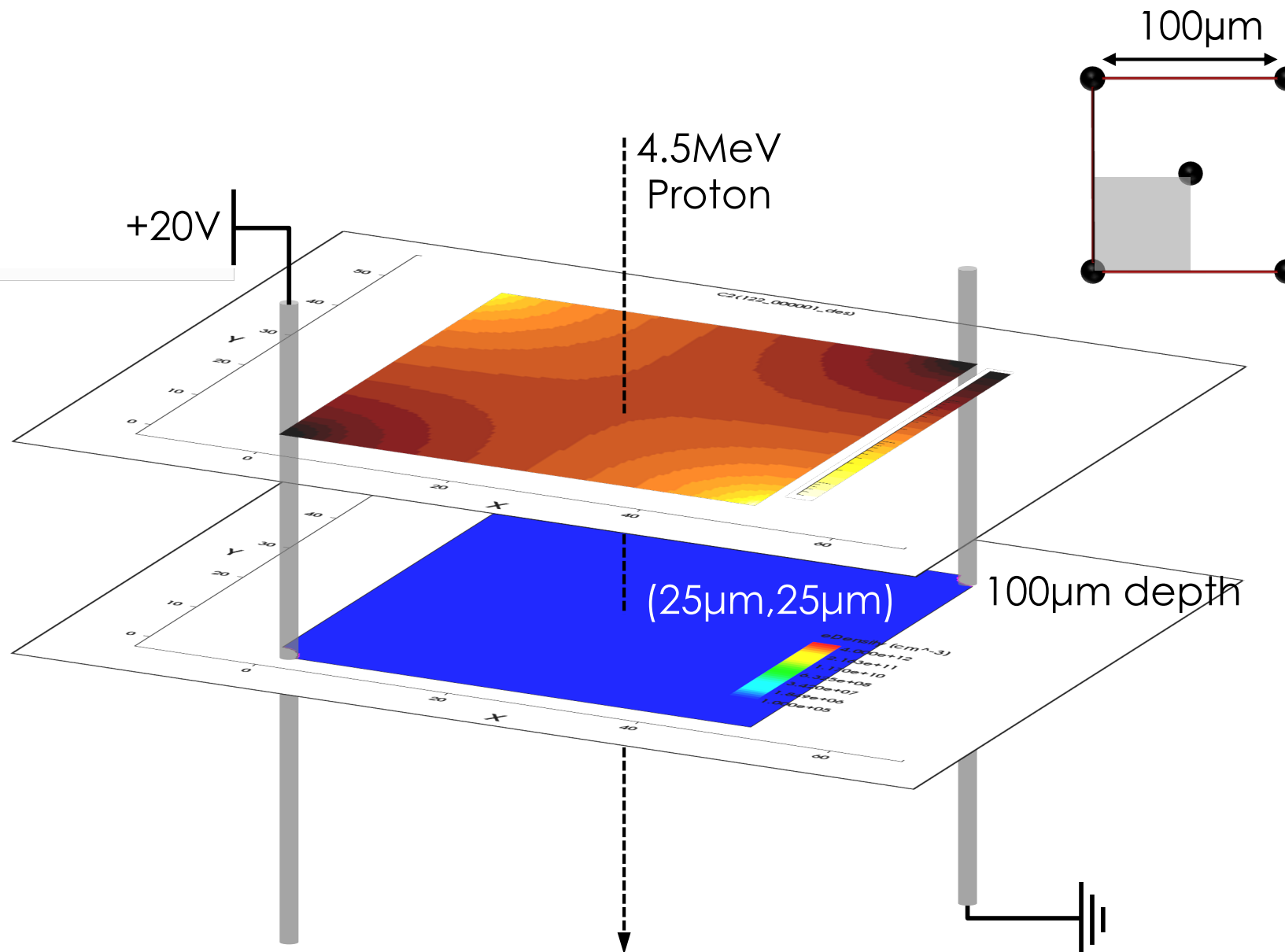
Simulation

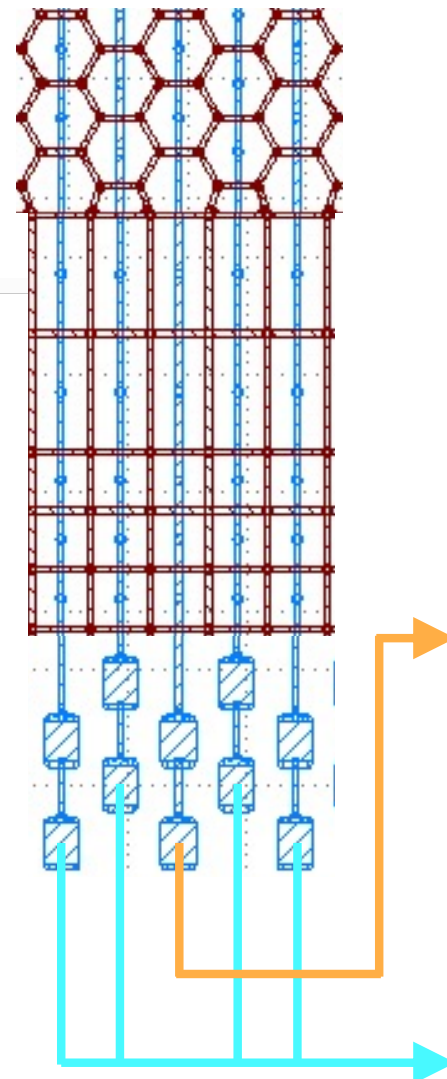
12
9



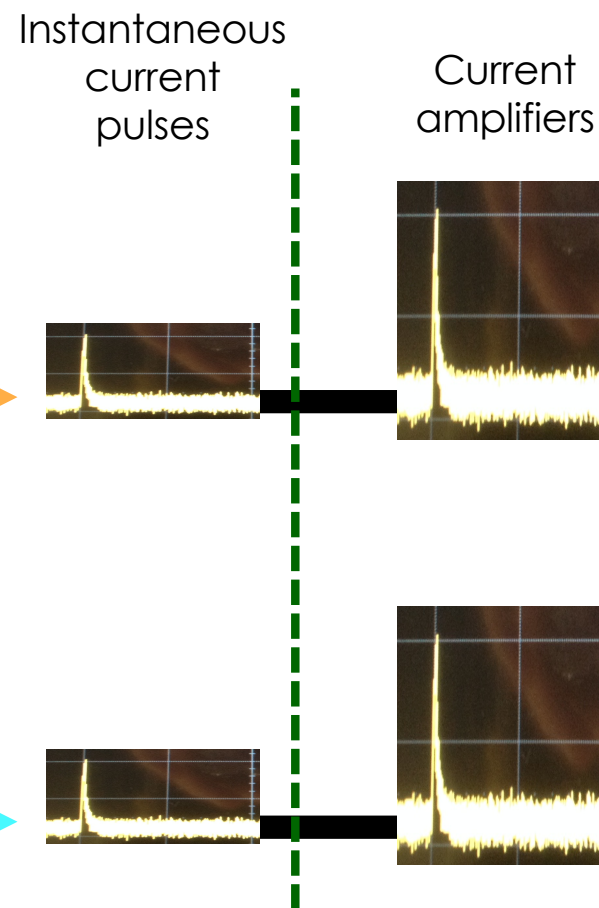
Simulation

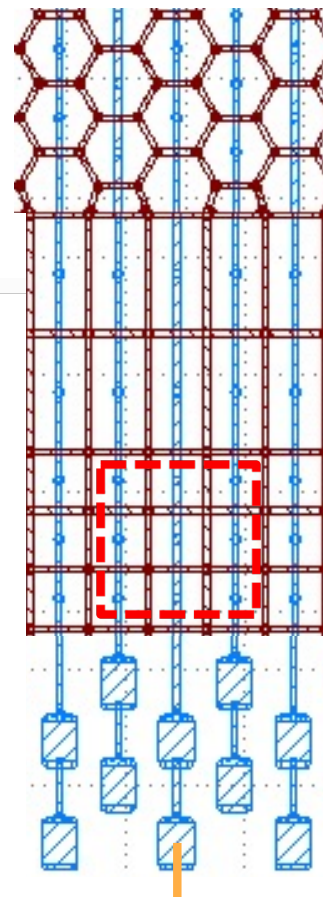
13
0



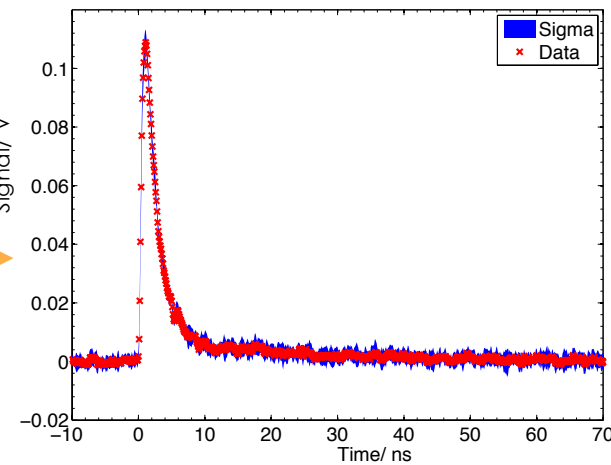


- Two read-out channels and amplification chains.

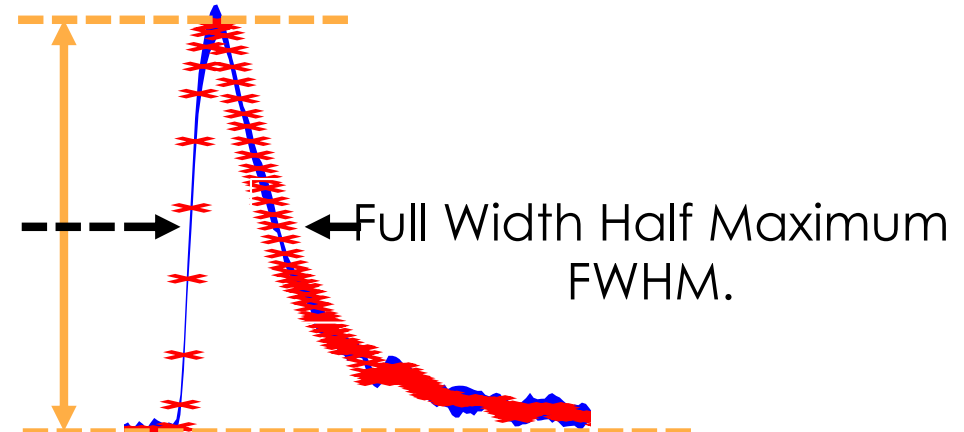
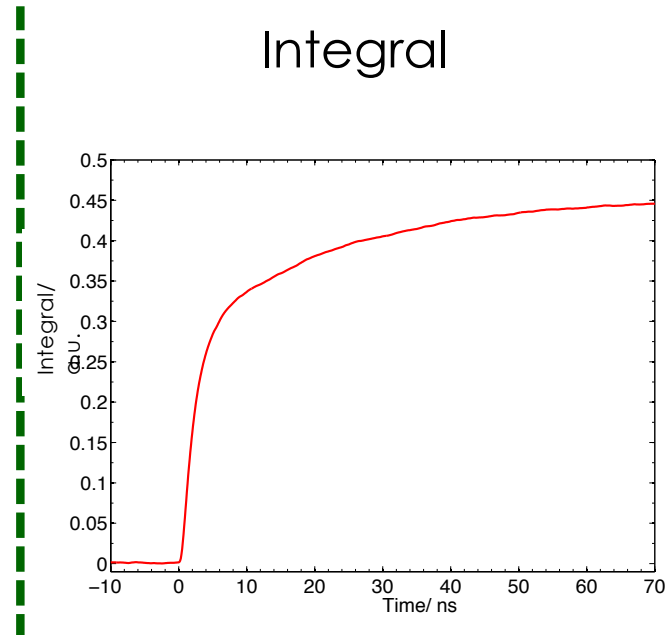




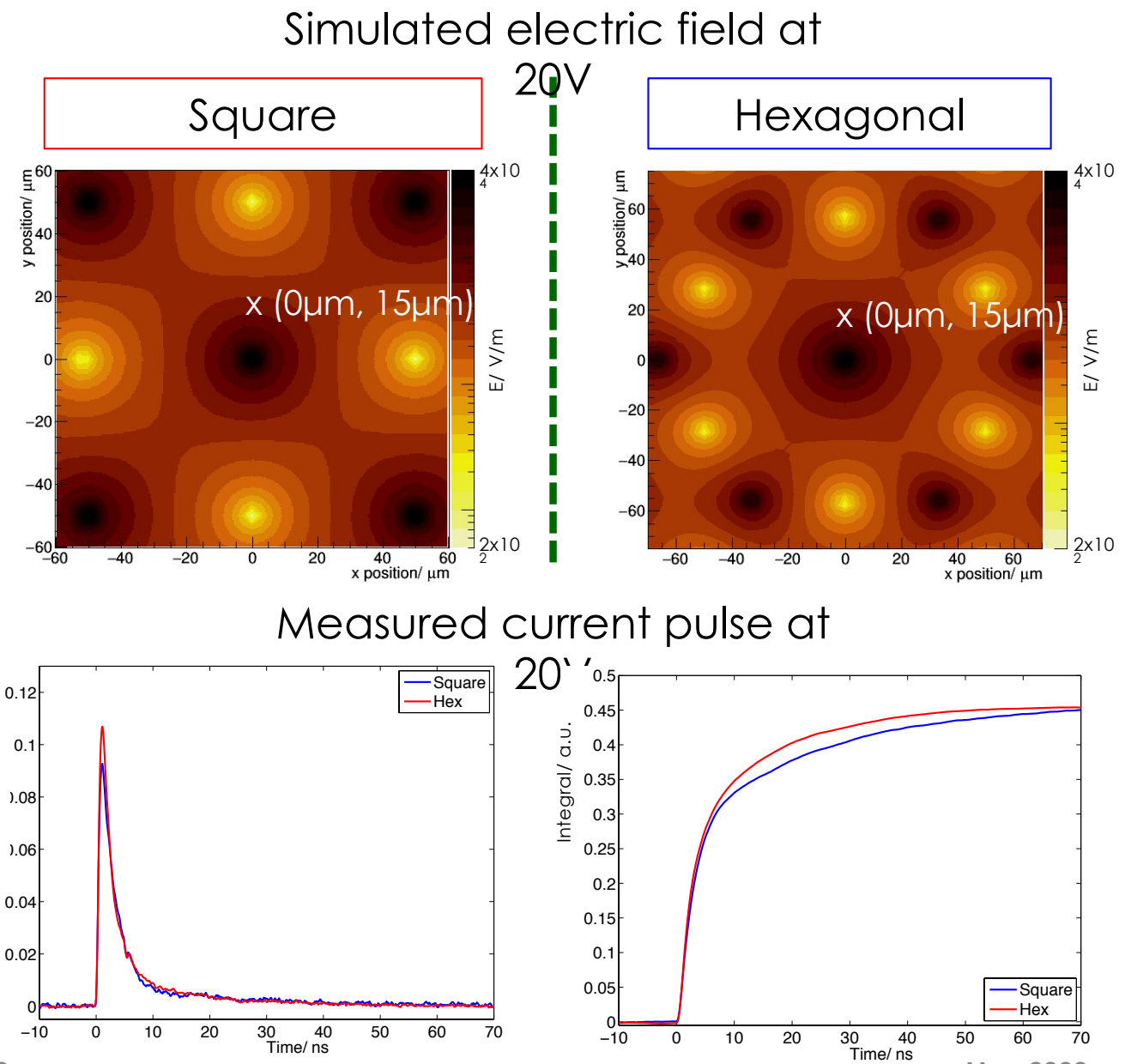
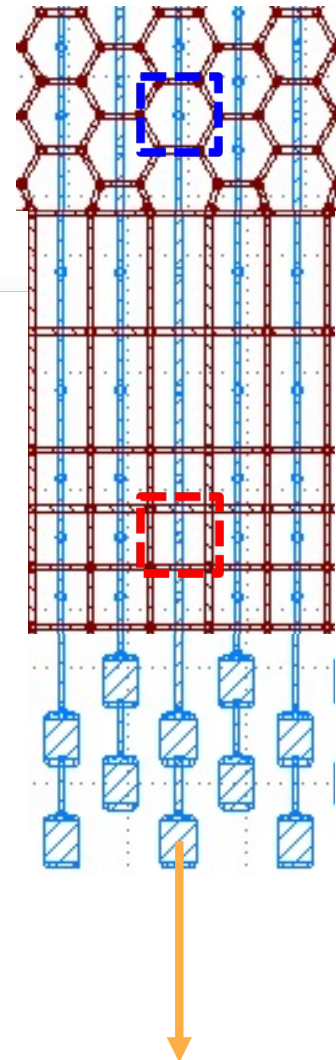
Instantaneous current
pulse



Integral

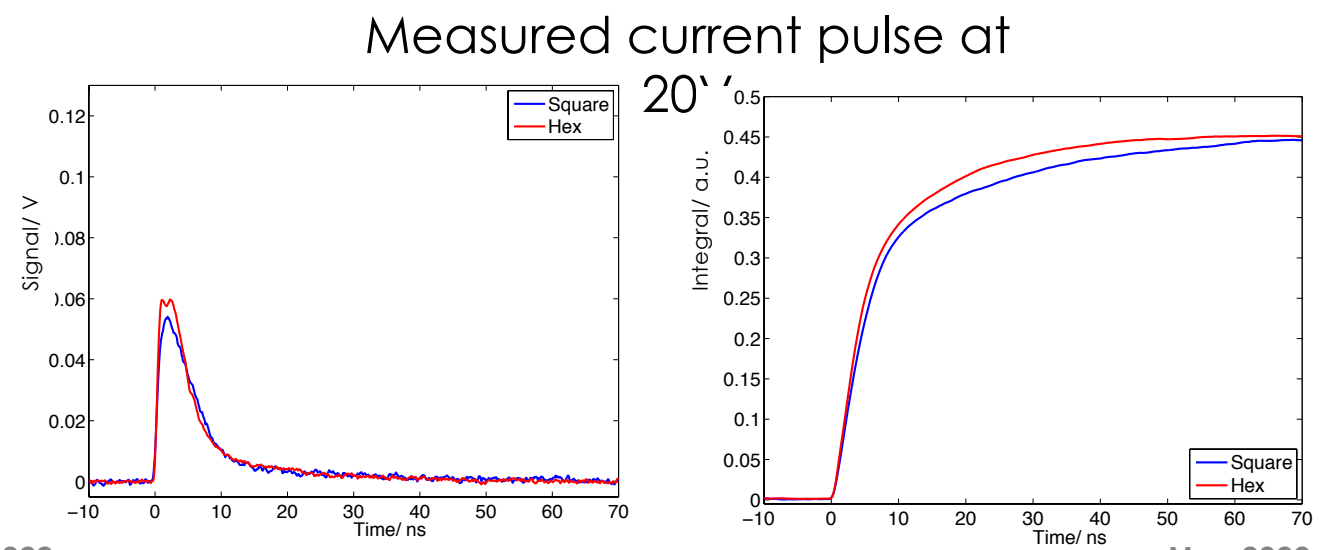
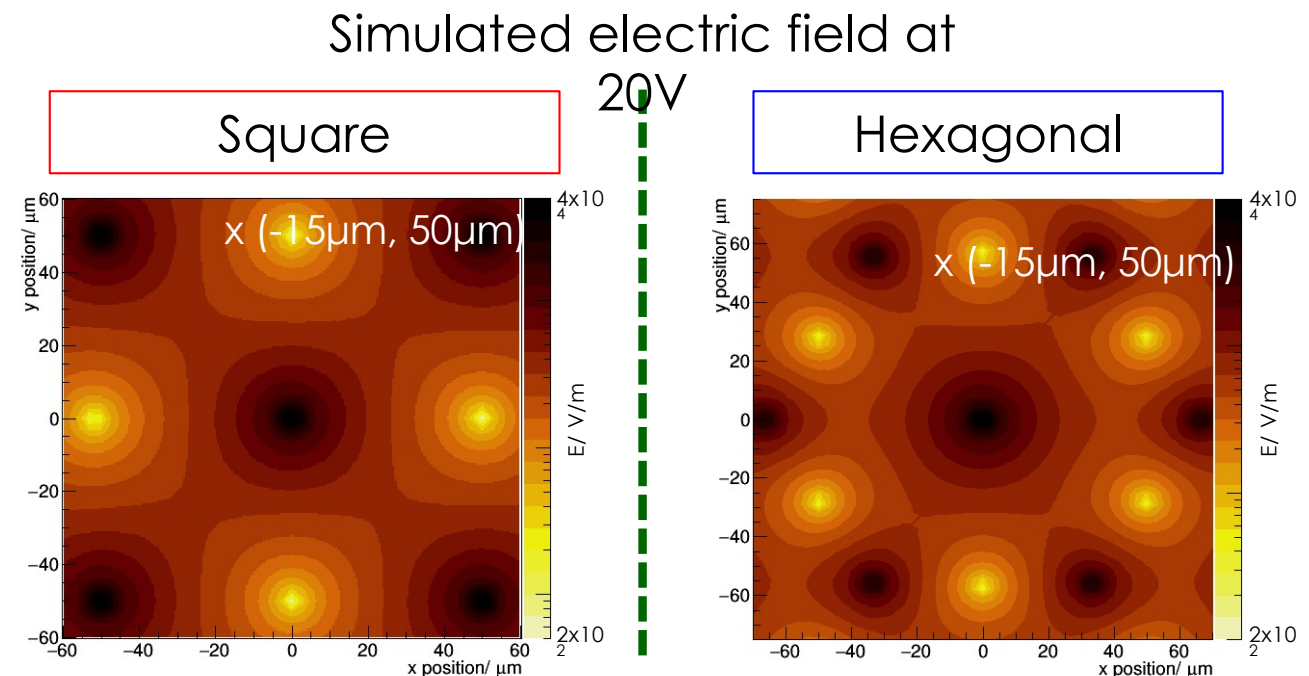
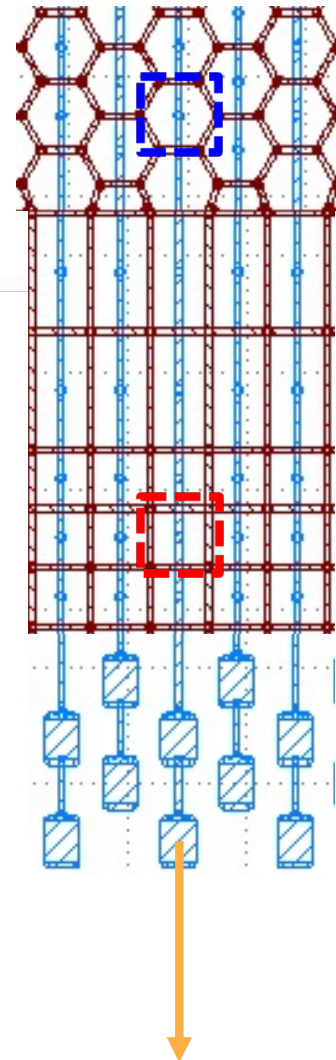


Position dependence – near electrode 3

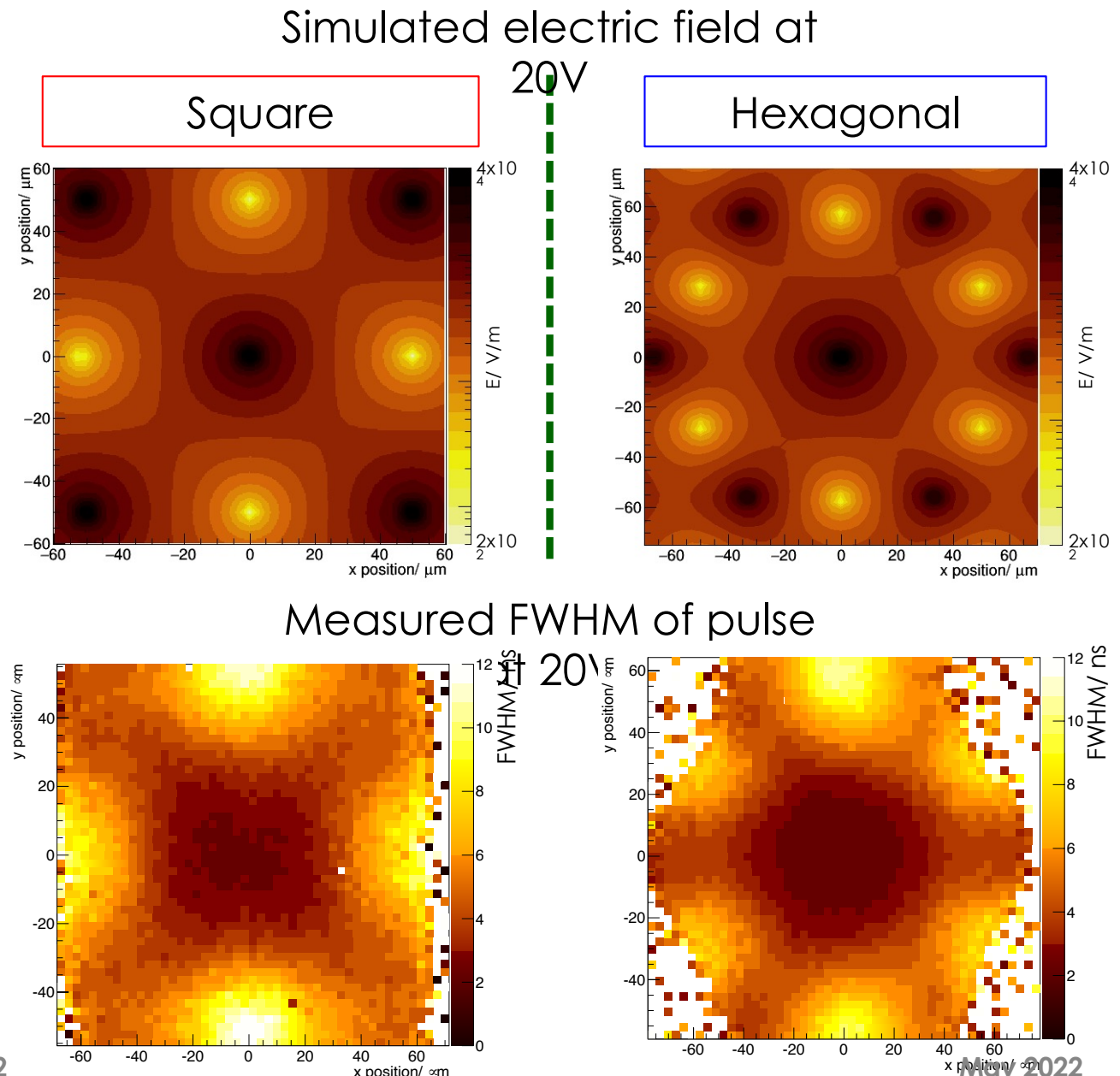
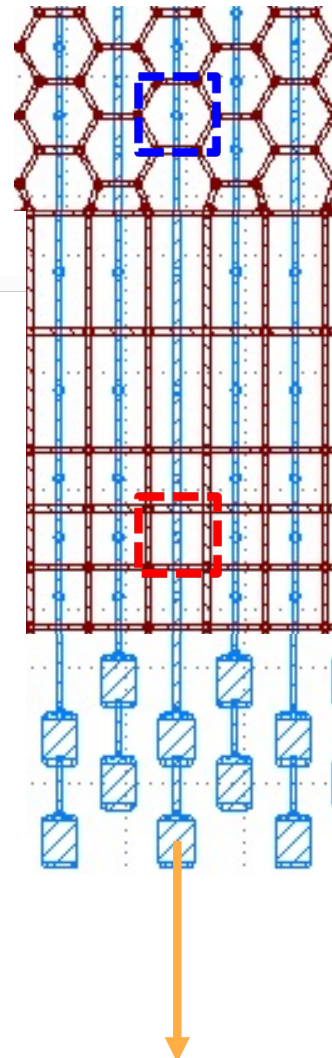


Position dependence – far from electrode

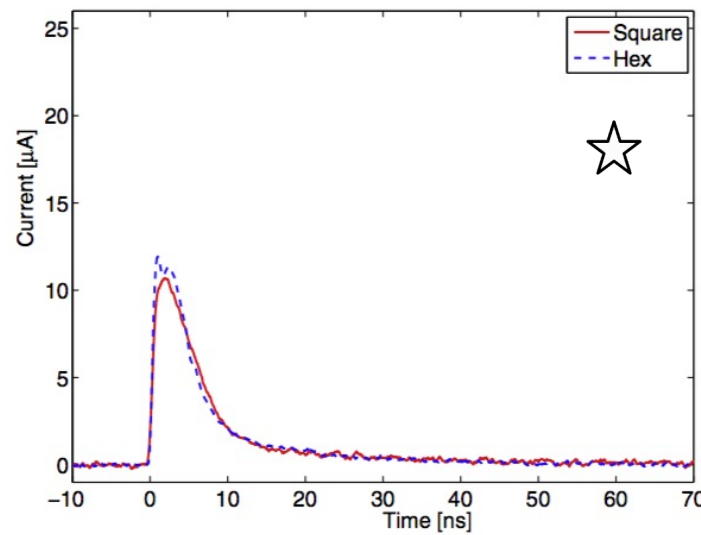
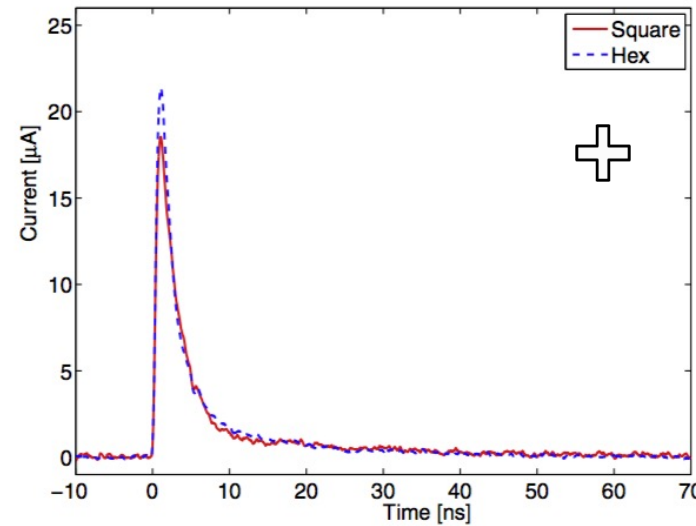
4



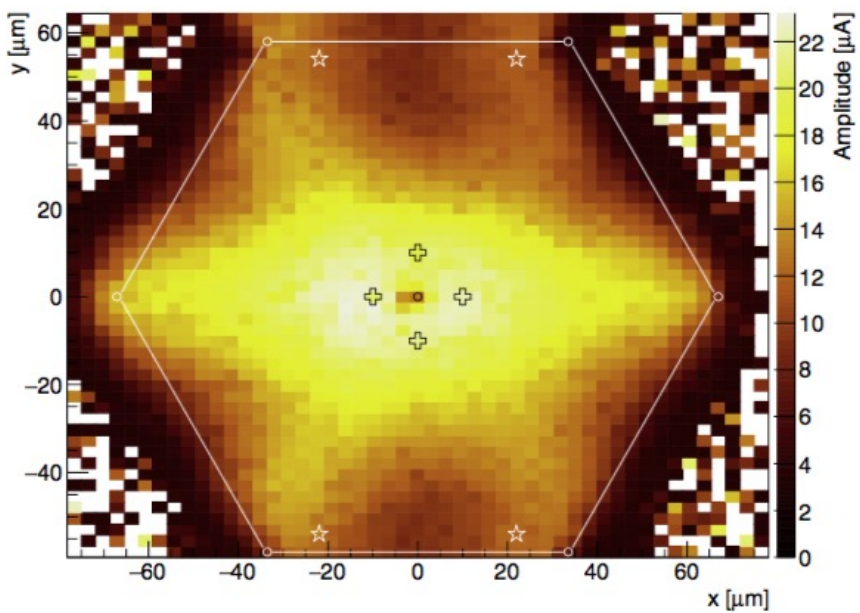
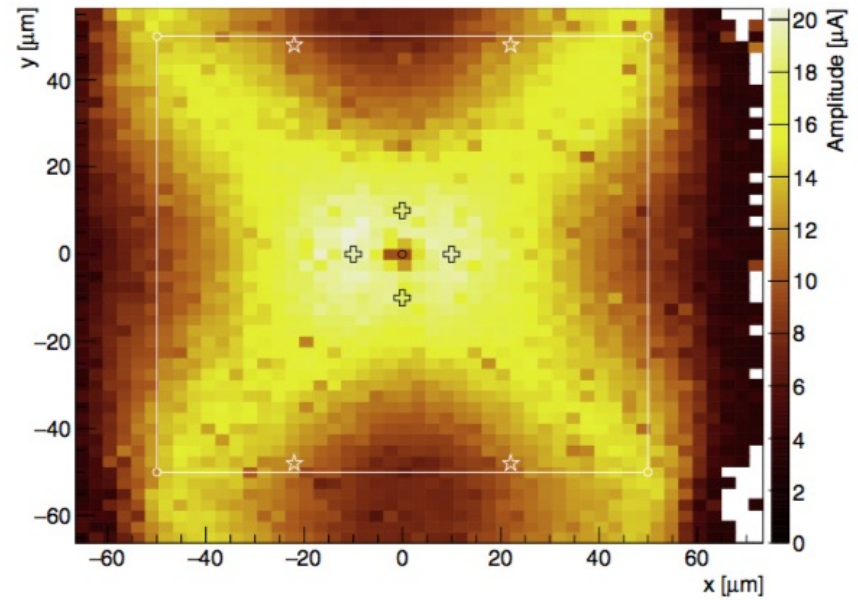
Position dependence - cell



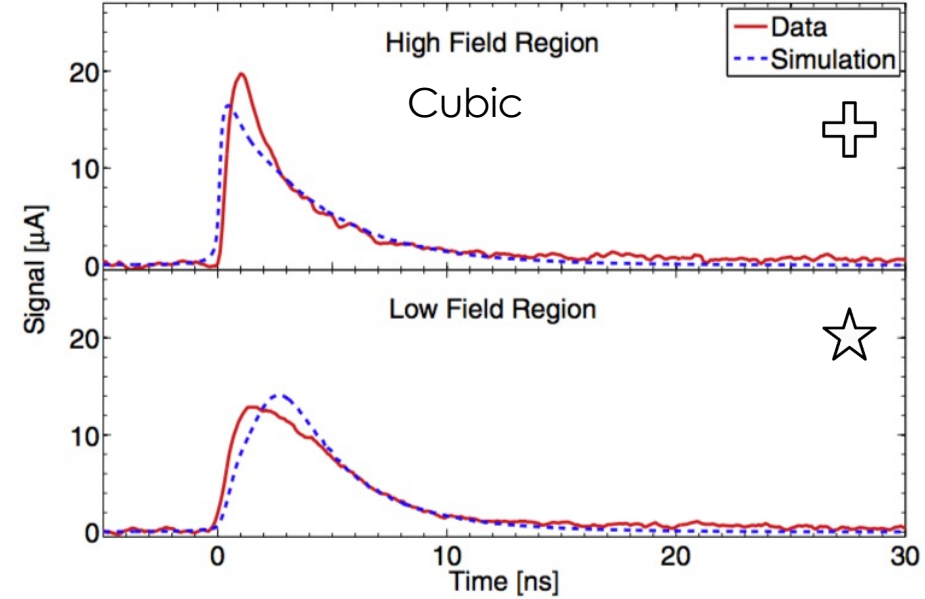
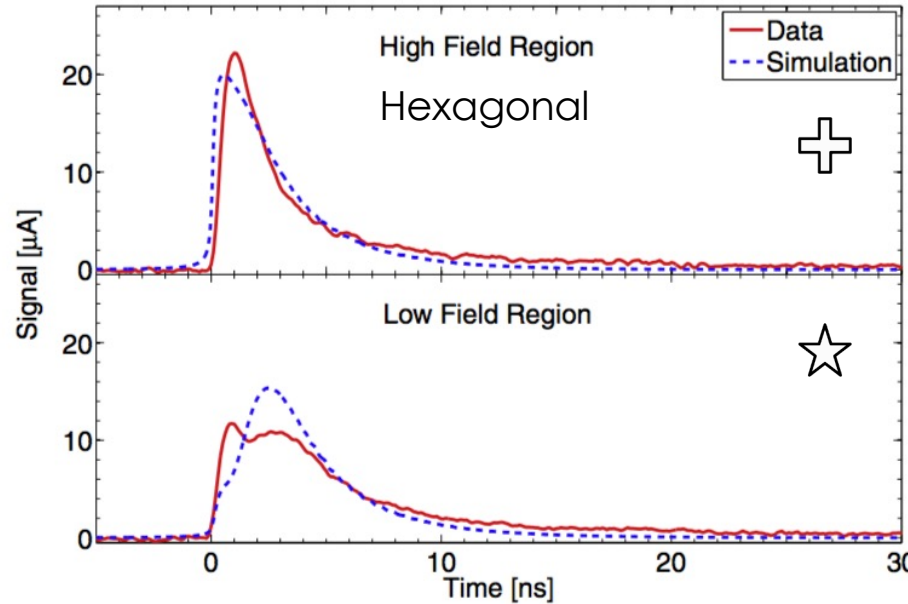
TRIBIC



$U_b = -20\text{V}$



TRIBIC: Results



Comparison with TCAD Simulation model:

- basic features qualitatively reproduced.
- Reasonable agreement, but simplified model.

Summary TRIBIC

- First study of hexagonal and cubic 3D diamond cells with TRIBIC.
 - Hexagonal and cubic cells show expected characteristics.
 - Qualitative agreement with simulations.
- Results shown are preliminary, analysis ongoing.
- Next steps:
 - Quantitatively verify electrical field distribution.
 - Disentangle hole and electron contributions.
 - Radiation hardness studies.

BACKUP

3D Diamond detector for medical dosimetry

Dosimetry application

- Planning of dose distribution delivered dose distribution challenging with narrow field beams.
- Need high spatial resolution of tissue equivalent dose deposited.
- Target numbers:
 - Dose uncertainty <1%
 - Spatial resolution ~0.1mm



Dosimetry application

- **Diamond key properties for dosimetry**

- Tissue equivalence
- Radiation hardness
- Room temperature operation
- bio-compatibility

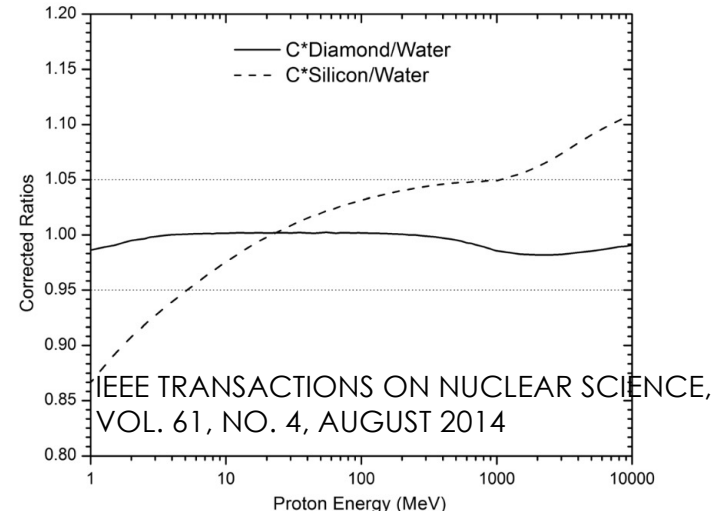
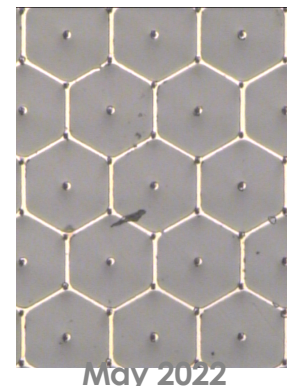
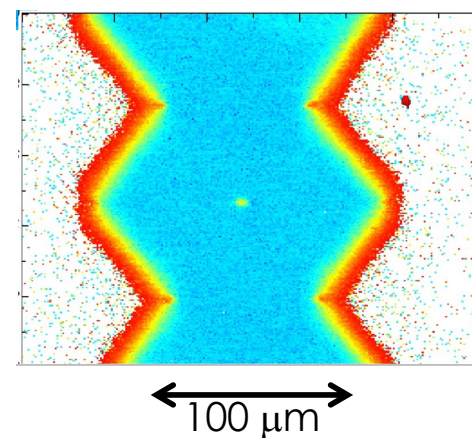
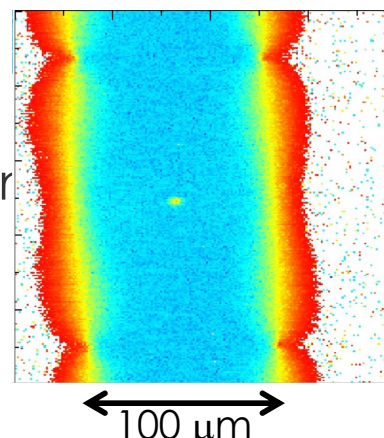


Fig. 14. Comparison of the corrected ratio of stopping powers for protons of diamond and silicon with water.

- **3D Advantage**

- Flexible active volume
- Radiation hardness
- Potential for 3D position information

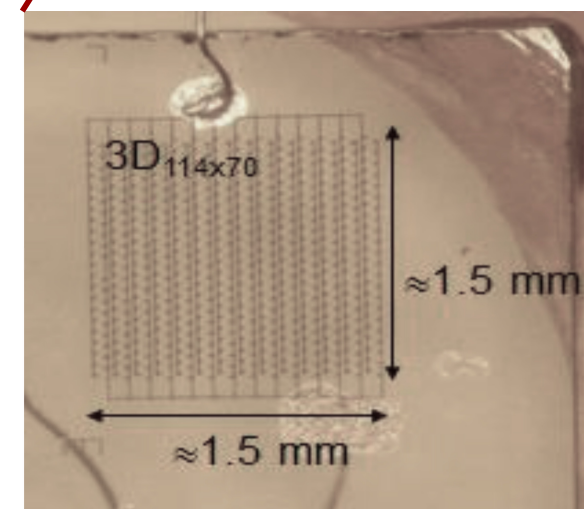
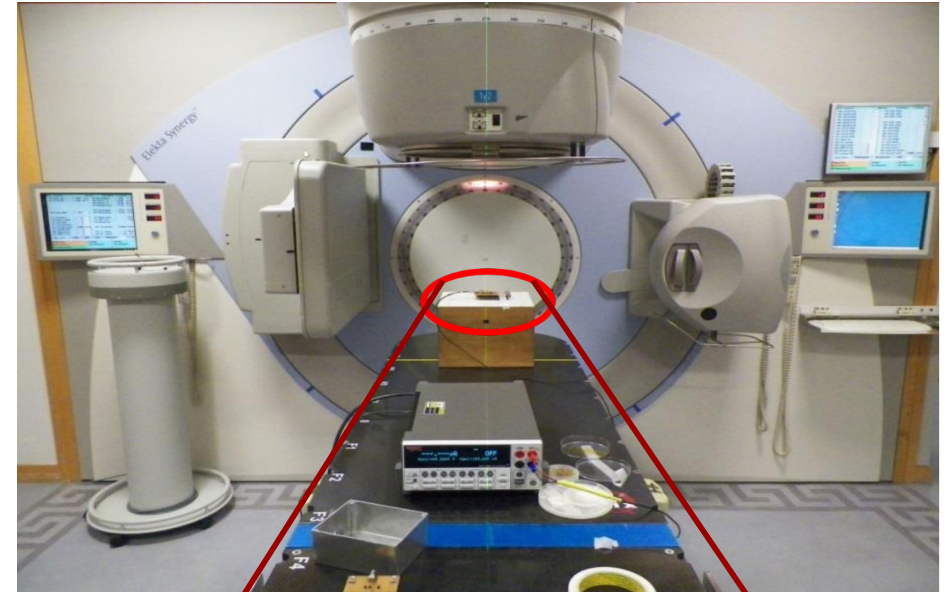


Dosimetry application



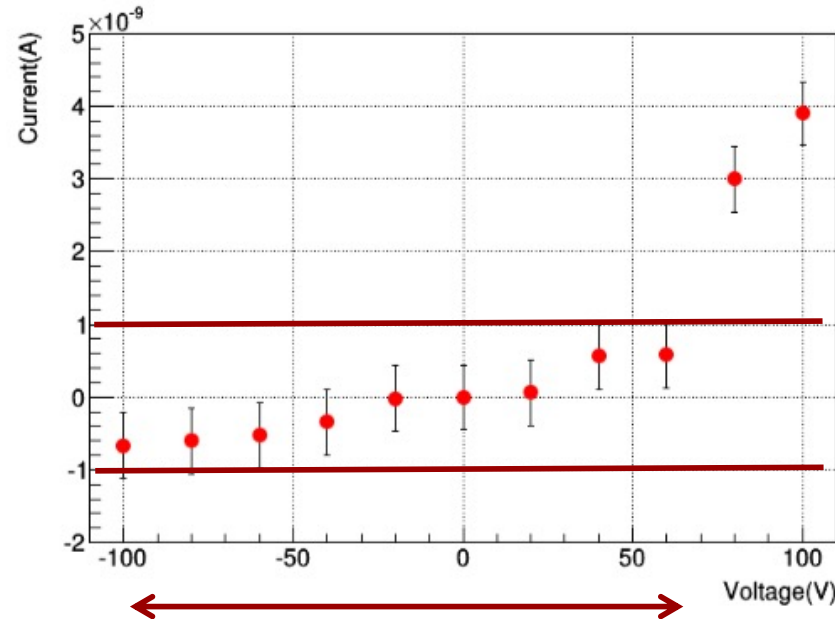
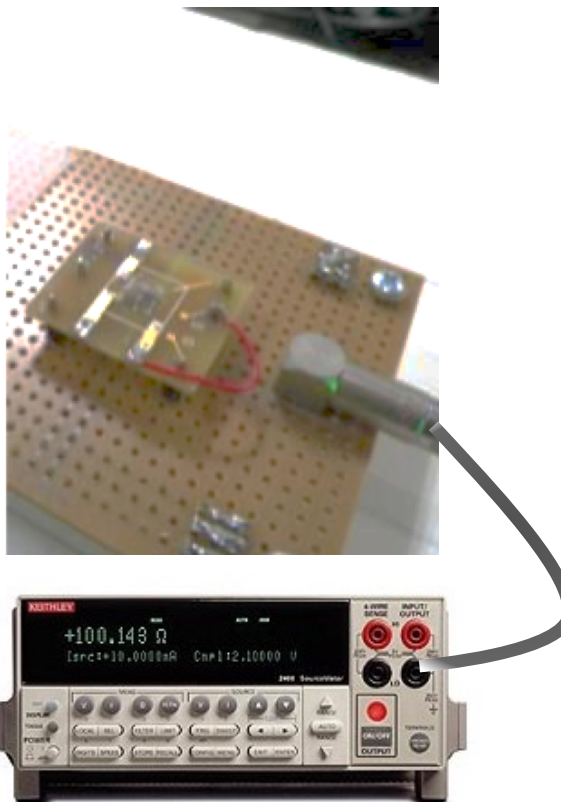
■ The Christie Hospital, Manchester

- medical linear accelerator (Elekta Synergy Sband)
- 6MV and 10MV acceleration.
- 10x10cm radiation field.
- Dose rate dependence.
- Photon beam profile.



Dosimetry application

- Test set-up:

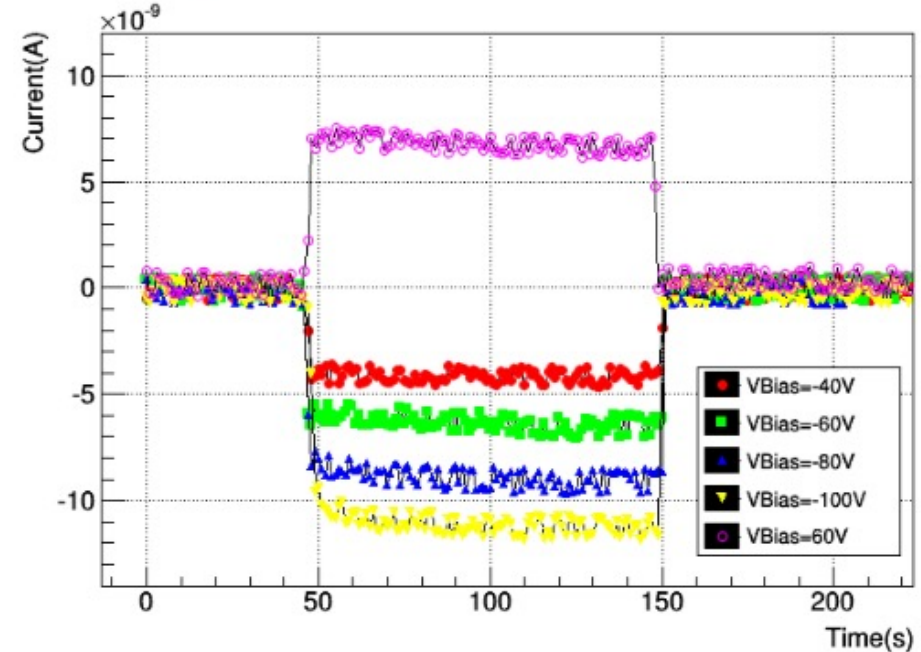


Asymmetric leakage current.
 $I_{\text{leak}} < 1 \text{nA}$ for -100V to +60V

Dosimetry application

First 3D diamond results:

- Pre-irradiated with 5 Gy.
- Clear response to presence to 6MV photons.
- Return to baseline <1s, no significant baseline shift.
- Plateau stability needs further studies.

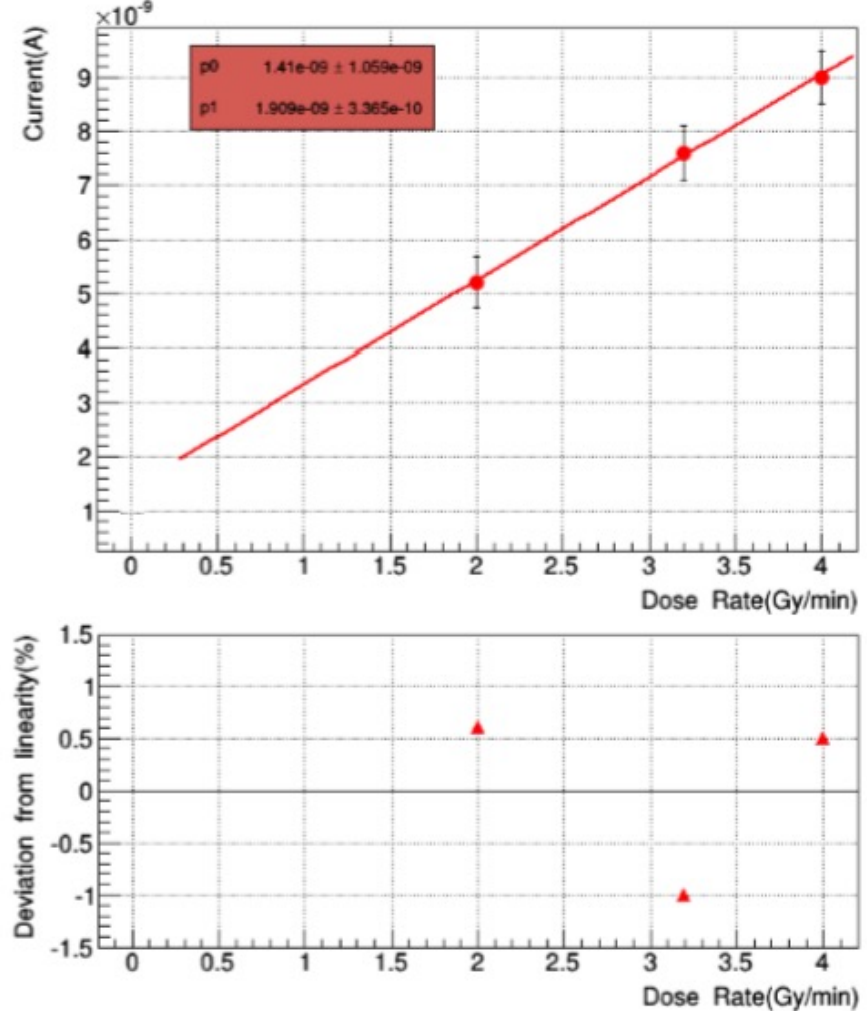


On-off response to 6MV photon beam with 4Gy/min.
Variation of bias voltage.

Dosimetry application

First 3D diamond results:

- Good linearity of ~1% over **dose rate** range of 2-4 Gy/min.

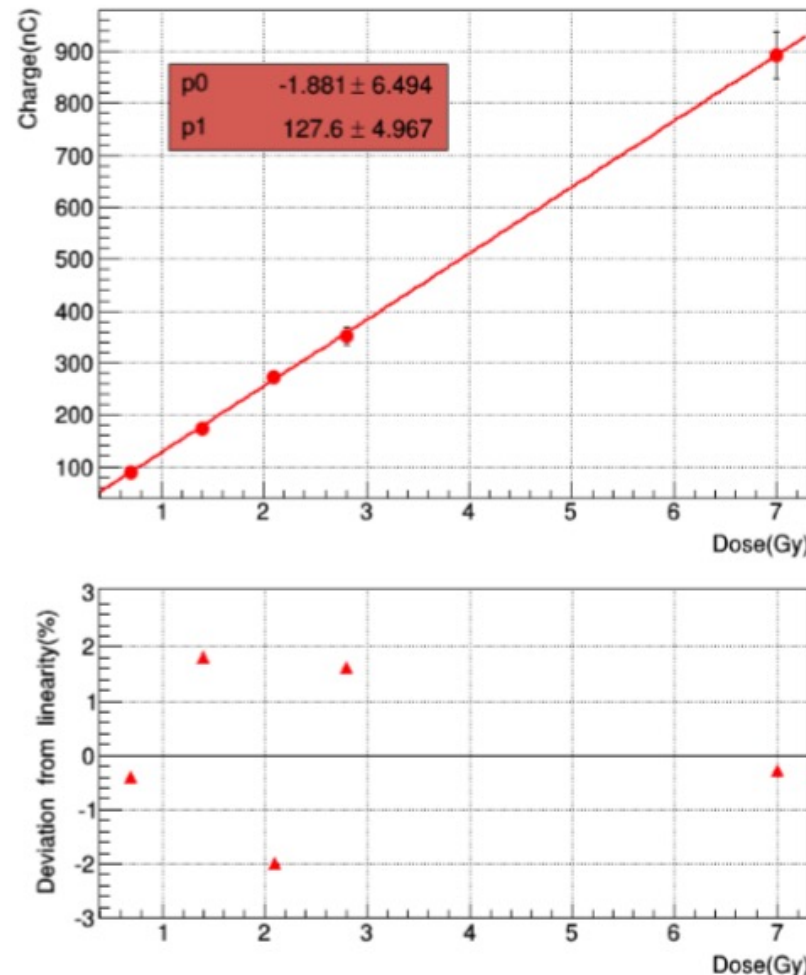


Dose rate linearity for 6MV photons at -80V

Dosimetry application

First 3D diamond results:

- Good linearity of ~1% over dose rate range of 2-4 Gy/min.
- Good linearity of ~2% over **dose range** of 0.5 to 7 Gy.

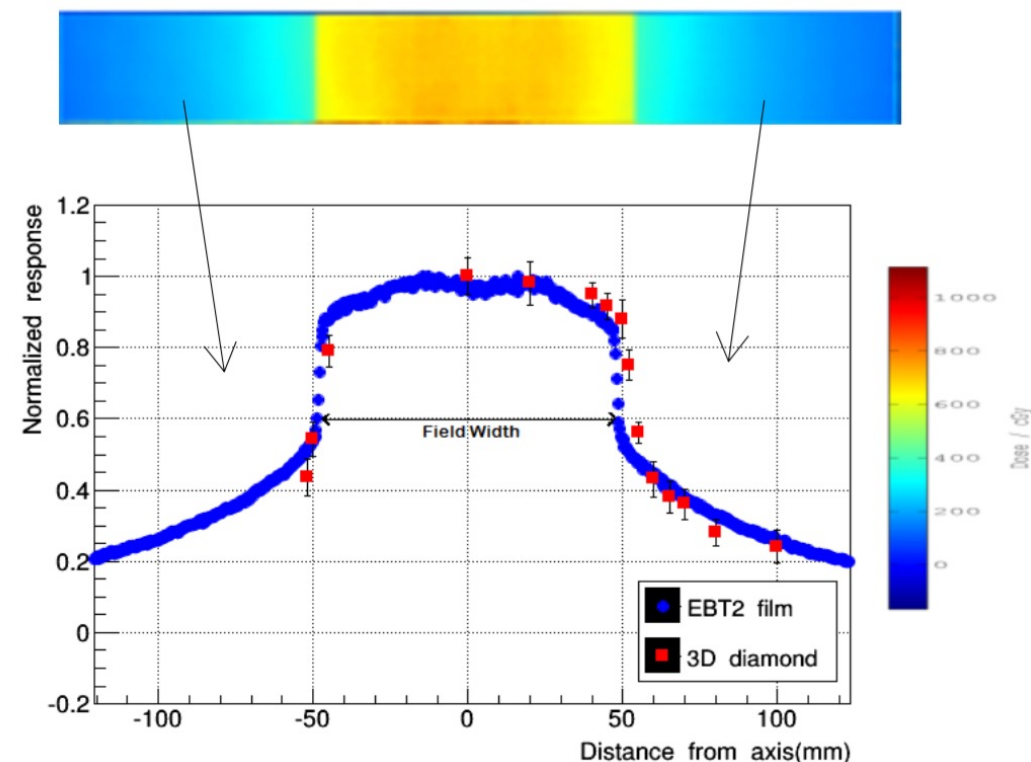


Dose linearity for 6MV photons at -80V

Dosimetry application

First 3D diamond results:

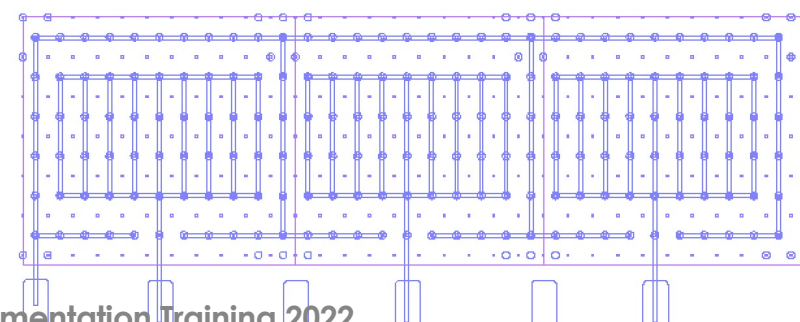
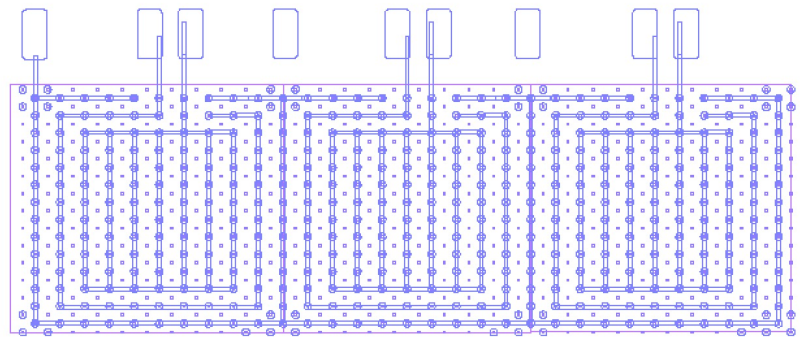
- Good linearity of ~1% over dose rate range of 2-4 Gy/min.
- Good linearity of ~2% over dose range of 0.5 to 7 Gy.
- **Beam width** well reproduced to 1% when compared to GafChromic film measurement.



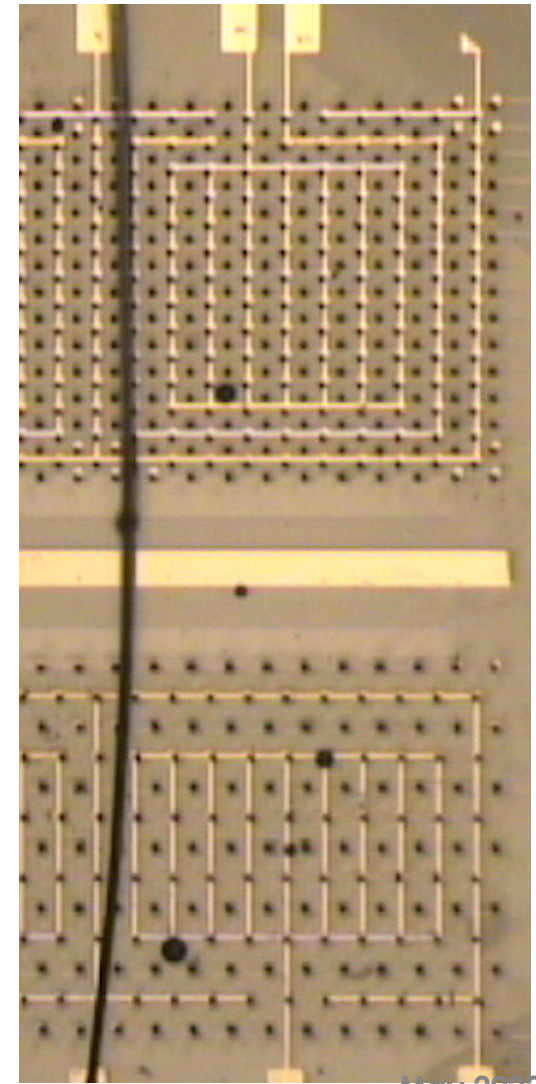
10cm beam profile measured with 3D diamond at -80V, 4Gy/min and film.

Next generation:

- Next generation tests with variable array sizes.



Advanced UK Instrumentation Training 2022



May 2022